

ABSTRACT

Title of dissertation: DEVELOPING HYBRID PHM MODELS FOR PIPELINE PITTING CORROSION, CONSIDERING DIFFERENT TYPES OF UNCERTAINTY AND CHANGE IN OPERATIONAL CONDITIONS

Roohollah Heidary
Doctor of Philosophy, 2019

Dissertation directed by: Professor Katrina M. Groth
Department of Mechanical Engineering

Pipelines are the most efficient and reliable way to transfer oil and gas in large quantities. Pipeline infrastructures represent a high capital investment and, if they fail, a source of environmental hazards and a potential threat to life. Among different pipeline failure mechanisms, pitting corrosion is of most concern because of the high growth rate of pits. In this dissertation two hybrid prognostics and health management (PHM) models are developed to evaluate degradation level of piggable pipelines, due to internal pitting corrosion. These models are able to incorporate multiple sensors data and physics of failure (POF) knowledge of internal pitting corrosion process. This dissertation covers both cases when in some pipeline's segments the pit density is low and in some segments it is high. In addition, it takes into account four types of uncertainty, including epistemic uncertainty, variability in the temporal aspects, spatial heterogeneity, and inspection errors.

For a pipeline segment with a low pit density, a hybrid defect-based algorithm

is developed to estimate probability distribution of maximum depth of each individual pit on that segment. This algorithm considers change in operational condition in internal pitting corrosion degradation modeling for the first time. In this way a two-phase similarity-based data fusion algorithm is developed to fuse POF knowledge, in-line inspection (ILI) and online inspection (OLI) data. In the first phase, a hierarchical Bayesian method based on a non-homogeneous gamma process is used to fuse POF knowledge and in-line inspection (ILI) data on multiple pits, and augmented particle filtering is used to fuse POF knowledge and online inspection (OLI) data of an active reference pit. The results are used to define a similarity index between each ILI pit and the OLI pit. In the second phase, this similarity index is used to generate dummy observations of depth for each ILI pit, based on the inspection data of the OLI pit. Those dummy observations are used in augmented particle filtering to estimate the remaining useful life (RUL) of that segment after the change in operational conditions when there is no new ILI data.

For a pipeline segment with a high pit density, a hybrid population-based algorithm is developed to estimate the probability density function of maximum depth of the pit population on that segment. This algorithm eliminates the need of matching procedure that is computationally expensive and prone to error when the pit density is high. In this algorithm three types of measurement uncertainty including sizing error, probability of detection (POD), and probability of false call (POFC) are taken into account. In addition, initiation of new pits between the last ILI and a prediction time is modeled by using a homogeneous Poisson process. The non-linearity of the pitting corrosion process and the POF knowledge of this process

is modeled by using a non-homogeneous gamma process.

The estimation of these two algorithms are used in a series system to estimate the reliability of a long pipeline with multiple segments, when in some segments the pit density is low and in some segments it is high. The output of this research can be used to find the optimal maintenance action and time for each segment and the optimal next ILI time for the whole pipeline that eventually decreases the cost of unpredicted failures and unnecessary maintenance activities.

DEVELOPING HYBRID PHM MODELS FOR PIPELINE PITTING
CORROSION, CONSIDERING DIFFERENT TYPES OF
UNCERTAINTY AND CHANGES IN OPERATIONAL
CONDITIONS

by

Roohollah Heidary

Dissertation submitted to the Faculty of the Graduate School of the
University of Maryland, College Park in partial fulfillment
of the requirements for the degree of
Doctor of Philosophy
2019

Advisory Committee:

Assistant Professor Katrina M. Groth, Chair/Advisor

Professor Mohammad Modarres

Professor Ali Mosleh

Assistant Professor Mark D. Fuge

Professor Mohamad Al-Sheikhly, Dean's Representative

© Copyright by
Roohollah Heidary
2019

Acknowledgments

Firstly, I would like to express my sincere gratitude to my advisor Professor Katrina M. Groth for the continuous support of my PhD study and related research, for her patience, motivation, and immense knowledge. Her guidance helped me in all the time of research and writing of this dissertation. I really enjoyed our technical discussions and her feedback always guided me to be on the right track. Professor Groth, without your guidance and constant feedback this PhD would not have been achievable and it was a great opportunity for me to work with you.

Many thanks also to Professor Mohammad Modarres for all his supports and advice during my PhD. Since my masters that I started to learn about reliability engineering, it was my dream to work with him as an influential person in this area, and I am so happy that my dream come true.

Many thanks are due to Professor Ali Mosleh, Professor Mohamad Al-Sheikhly, and Professor Mark D. Fuge for agreeing to serve on my dissertation committee and for sparing their invaluable time reviewing the manuscript and critical assessment of my dissertation.

I also thank my peers for all good time that we spent to discuss different ideas and methods, and for all the fun we have had in the last four years. My special thanks to my friend Miead Nikfarjam for teaching me how to play ‘Daf’ and to my friend Elizabeth Domingo for all her support and help.

I also thank my sisters and brother for supporting me spiritually throughout my PhD.

Most importantly, I would like to thank my mother and my father, Maasumeh and Einollah, for their love and support and dedication of their life to our success and happiness. Words cannot express the gratitude I owe them.

Finally, I would like to acknowledge financial support from Khalifa University of Science and Technology: This work is being carried out as a part of the Pipeline System Integrity Management Project, which is supported by the Petroleum Institute, Khalifa University of Science and Technology, Abu Dhabi, UAE.

Dedication

To

Mohammad Reza Shajarian

Table of Contents

Dedication	iv
Table of Contents	v
List of Tables	viii
List of Figures	x
List of Abbreviations	xi
1 Introduction	1
1.1 Background and Motivation	1
1.2 Research objectives and scope	8
1.3 Assumptions	9
1.4 Overview of the research	10
1.5 Organization of this dissertation	12
2 Literature review on PHM approaches, sensor data fusion, and similarity-based RUL estimation	14
2.1 Literature on PHM approaches	14
2.2 Literature review on sensor data fusion	16
2.2.1 Motivation for data fusion	17
2.2.2 Categorization of sensor data fusion techniques based on the data type	18
2.2.3 Sensor data fusion algorithms	21
2.2.4 Bayesian Inference for degradation level estimation	21
2.2.5 Artificial Neural Networks (ANNs)	24
2.2.6 Literature review on similarity-based methods for RUL estimation	29
3 A Review of Data-Driven Oil and Gas Pipeline Pitting Corrosion Growth Models Applicable for Prognostic and Health Management	31
3.1 Abstract	31
3.2 Introduction	32

3.3	Probabilistic data driven models	39
3.3.1	Random-variable based corrosion growth models	40
3.3.1.1	Linear random variable corrosion growth model	40
3.3.1.2	Non-Linear random variable corrosion growth model	41
3.3.2	Stochastic-process based corrosion growth models	44
3.3.2.1	Linear stochastic process corrosion growth model	44
3.3.2.2	Non-Linear stochastic process corrosion growth model	46
3.3.3	Markov process based corrosion growth models	47
3.3.4	Gamma process based corrosion growth models	55
3.4	Discussions	62
3.5	Conclusion	64
4	Development of a hybrid defect-based degradation model for a pipeline segment with low pit density	66
4.1	Abstract	66
4.2	Introduction	68
4.3	Related work, approach, and contributions	70
4.4	Bayesian inference methods	72
4.4.1	Augmented particle filtering (APF)	73
4.4.2	Hierarchical Bayesian method	79
4.5	Proposed framework	83
4.5.1	Phase I: estimating the standard deviation of the white noise of APF process model (PM-SD) and the prior values for degradation model parameters	84
4.5.2	Phase II: Defining a similarity index between pit i and pit M	87
4.5.3	Phase III: Inferring the degradation level of pit i	88
4.6	Demonstration of the proposed framework	89
4.6.1	Performing phase I of the proposed framework	89
4.6.1.1	Synthetic data generation procedure	90
4.6.2	Performing phase II of the proposed framework	95
4.6.3	Performing phase III of the proposed framework	97
4.7	Results	97
4.8	Conclusion	105
5	Development of a hybrid population-based degradation model for a pipeline segment with high pit density	109
5.1	abstract	109
5.2	Introduction	111
5.3	Assumptions and methods	115
5.3.1	Assumptions	115
5.3.2	Homogeneous Poisson Process (HPP)	117
5.3.3	Non-homogeneous gamma process	118
5.3.4	Hierarchical Bayesian	120
5.4	Developed algorithm	123
5.4.1	General structure of the developed algorithm	124

5.4.2	Phase I: Using the first ILI dataset	124
5.4.3	Phase II: Incorporating additional data sets	127
5.4.4	Phase III: Prognostics	133
5.5	Demonstration of the developed algorithm	135
5.5.1	Case study data	136
5.5.2	Phases of the algorithm for the case study	138
5.5.2.1	Phase I for the case study	138
5.5.2.2	Phase II for the case study	140
5.5.2.3	Prognostics phase for the case study	144
5.5.2.4	Discussion	145
5.6	Conclusion	148
6	Development of a methodology to estimate the reliability and RUL of a pipeline with multiple segments of varying pit density	150
6.1	Introduction	150
6.2	Pipeline failure modes and reliability analysis	151
6.3	RUL estimation	156
6.4	Case study	158
6.5	Summary	162
7	Summary, contributions, and suggested future work	164
7.1	Summary	164
7.2	Technical contributions	166
7.3	Work Products	169
7.4	Limitations	170
7.5	Future work	171
	References	173

List of Tables

1.1	Usage of potential information and data sources in the available pitting corrosion degradation model in the literature and this dissertation	11
2.1	Example features that can be extracted from sensor data [46]	20
3.1	Evaluation of different commonly used probabilistic data-driven pitting corrosion growth models in oil and gas pipelines	62
4.1	Pseudo code for APF	80
4.2	Best fit distribution of the operational parameters [14] and modified values for moderate corrosion rate category	90
4.3	Parametric estimate for power model development [14]	91
4.4	Pseudo code for synthetic data generation	93
4.5	Constant (a) and proportional (b) biased error and scattering error of inspection tools [13]	94
4.6	Comparing the results in case of no change in operational conditions	100
4.7	Comparing the results in case of considering change in operational conditions	102
5.1	Nomenclature	110
5.2	Nomenclature (Cont.)	111
5.3	Operational parameters considered in the underlying generic model for data simulation [14]	136
5.4	Assumed values for input data simulation	138
5.5	Number of existing and reported pits at each time interval	138
5.6	Estimated hyper-parameters at t_1	139
5.7	Updated hyper-parameters at t_2	141
5.8	Updated hyper-parameters at t_3	143
5.9	Comparing hyper-parameters	145
5.10	Comparing No. of pits	145
5.11	SKLD and χ^2 measures	148
6.1	Criteria for occurrence of different health states (failure modes or safe operation). f_1, f_2, f_3 refer to limit state functions defined in Equations 6.3-6.6.	154

6.2	Pseudo code to calculate the reliability of a pipeline	156
6.3	Probabilistic characteristics of the random variables	159
6.4	Probability of occurrence of different health states for Segment S1 and S2, 50 years after operation	161

List of Figures

1.1	PHM steps [6]	4
1.2	An example of a smart pig (in-line inspection device) [ieccetech.org]	6
1.3	Summary of the proposed PHM degradation models for internal pitting corrosion of oil and gas pipelines	12
2.1	Specimens used to generate ground truth data [53]	27
2.2	Sketch of the four studied conditions: a) non-defect; b) lack of penetration (LP); c) external corrosion (EC); d) internal corrosion(IN) [53]	27
3.1	An example of pitting corrosion on X70 carbon steel surface in a corrosive environment (magnification scale: 200X) [63]	33
3.2	Hierarchical levels of uncertainty in degrading systems (modified) [16]	36
3.3	Breakdown of probabilistic data-driven based models for internal localized corrosion in pipelines	39
3.4	Linear stochastic process model [30]	45
3.5	Non-Linear stochastic process model [30]	46
3.6	Hierarchical Bayes framework for heterogeneous degradation, modified from [83]	57
4.1	Hierarchical Bayesian model based on a non-homogeneous gamma process modified from the approach that is proposed in [16]	83
4.2	Flowchart of the proposed framework	85
4.3	A realization of simulated actual maximum pit depth	87
4.4	Generated synthetic data for an OLI and an ILI pit	95
4.5	Estimated model parameters for the reference pit by using APF for a random seed number	98
4.6	Estimated maximum depth of the reference pit by APF	99
4.7	Estimated maximum depth of pit No.29 by this framework and Maes model, without change in operational conditions	101
4.8	Estimated maximum depth of pit No.53 by this framework and Maes model, without change in operational conditions	102
4.9	Estimated maximum depth of pit No.50 by this framework and Maes model with change in operational conditions	103

4.10	Estimated maximum depth of pit No. 31 by this framework and Maes model with change in operational conditions	104
5.1	General HB model for each category of pits at each ILI time based on their initiation time	122
5.2	Modified general HB model for each category of pits at each ILI time based on their initiation time	123
5.3	General structure of the developed algorithm	125
5.4	Modified HB model for ILL_1	126
5.5	Estimating number of the pits that were initiated before ILL_1 that are expected to have been detected at ILL_2	130
5.6	Modified HB model for ILL_2	132
5.7	PMF of the reported and true calls measurements at ILL_1	139
5.8	Simulated and estimated PMF of pits' actual depth at $t_1(X_1)$	140
5.9	Simulated and estimated PMF of pits' actual depth at $t_2(X_2)$	142
5.10	Simulated and estimated PMF of pits' actual depth at $t_3(X_3)$	143
5.11	Simulated and estimated PMF of pits' actual depth at $t_4(X_4)$	144
6.1	RUL estimation for small leak failure mode	157
6.2	Probability of occurrence of each health state for Segment S1	160
6.3	PMF of operating, burst, and rupture pressure for Segment S1, 50 years after operation	160
6.4	PMF of operating, burst, and rupture pressure for Segment S2, 50 years after operation	162

List of Abbreviations

APF	Augmented particle filtering
EMPD	Estimated maximum pit depth
HB-NHGP	Hierarchical Bayesian based on a non-homogeneous gamma process
ILI	In-line inspection
KLD	Kullback–Leibler divergence
MFL	Magnetic flux leakage
OLI	Online inspection
PF	Particle filtering
PHM	Prognostics and health management
POD	Probability of detection
POF	Physics of Failure
POFC	Probability of false call
PWT	Pipe wall thickness
RMSE	Root mean squared error
RUL	Remaining useful life
SKLD	Symmetric Kullback–Leibler divergence
UT	Ultrasonic testing

Chapter 1: Introduction

1.1 Background and Motivation

Pipelines are the most efficient and reliable way to transport oil and gas products in large quantities. However, failure of the pipelines could cause an environmental hazard, a potential threat to life, and/or impose a huge cost; hence, their integrity management becomes very critical [1]. In order to have a comprehensive pipeline integrity management, it is necessary to consider all pipeline failure mechanisms and modes. In oil and gas pipelines, corrosion is one of the main ones and among different corrosion failure mechanisms, pitting corrosion is more critical because of the high rate at which pits can grow [2, 3]. According to the data in the literature, 57.7% of oil and gas pipeline failures in Alberta, Canada between 1980 and 2005, and 15% of all transmission pipeline failures between 1994 and 2004 in the US were due to internal corrosion [4]. In addition, 90% of corrosion failures of transmission pipelines in the US, between 1970 and 1984, were due to localized pitting corrosion [4]. Therefore, in terms of the failure mechanism, the main focus of this dissertation is on internal pitting corrosion.

The most efficient approach to managing the integrity of pipelines due to internal pitting corrosion is to develop a hybrid PHM model. In recent years, PHM

approaches have emerged and became an essential requirement to improve reliability, maintainability, safety, and affordability of a component or system [5]. Generally, PHM approaches have three main steps; observation, analysis and action (Figure 1.1) [6]. Along the way, developing a proper degradation model in the analysis step plays a critical role to make a bridge between the observations (i.e., collected condition-based data of the system) and the actions (i.e., decision making to mitigate the consequences of the potential failures). Underestimating the degradation level leads to unpredicted failures and overestimating the degradation level leads to unnecessary maintenance activities. Most PHM approaches rely on either POF or data-driven degradation models [7].

POF-based degradation models have advantages in long-term damage behavior prediction. However, when the degradation process is complex (e.g., pitting corrosion), it is difficult to estimate and validate the parameters of the POF-based degradation models because usually they are developed based on many approximations and simplifying assumptions [8]. On the other hand, data-driven models use information from measured data collected via sensors to evaluate the degradation process and predict the future state without using any particular physical model [8]. The accuracy of data-driven models is highly dependent on the amount of available condition monitoring data [6]. For complex systems, in many applications data-driven models are more practical than the POF-based models. However, since they have no or less physical meaning, they are less sensitive to real system behavior [6].

Pitting corrosion is a complex stochastic process, which is not well understood yet [9] and the geometry of the pipelines (i.e., long length, diameter, curvature)

makes it infeasible to have enough data about the health condition of the pipeline in all locations. Therefore, neither a POF-based model [10, 11] nor a data-driven model alone can capture and model the complexity of this process. The optimal solution is to develop a hybrid PHM degradation model to combine the advantages of both POF-based and data-driven based models and minimize their disadvantages. Therefore the focus of this dissertation is on developing hybrid pitting corrosion degradation models. It is worth noting that this research is a sub-project of a comprehensive pipeline integrity management project that includes three main thrust areas. In Thrust area I, the focus is on data gathering and monitoring technologies. In Thrust area II, the focus is on physics of failure aspects of pipelines corrosion process and failure mechanism sciences. And in Thrust area III, the focus is on predictive models and system-level integrity management. This research as a sub-project of Thrust area III, is mostly focusing on the data-driven aspect of a hybrid degradation pitting corrosion model, however, the POF aspect of the corrosion process is also taken into account. The POF aspect of different corrosion failure mechanisms (i.e., uniform corrosion, pitting corrosion, and microbial induced corrosion) is more emphasized by Thrust area II of this pipeline integrity management project.

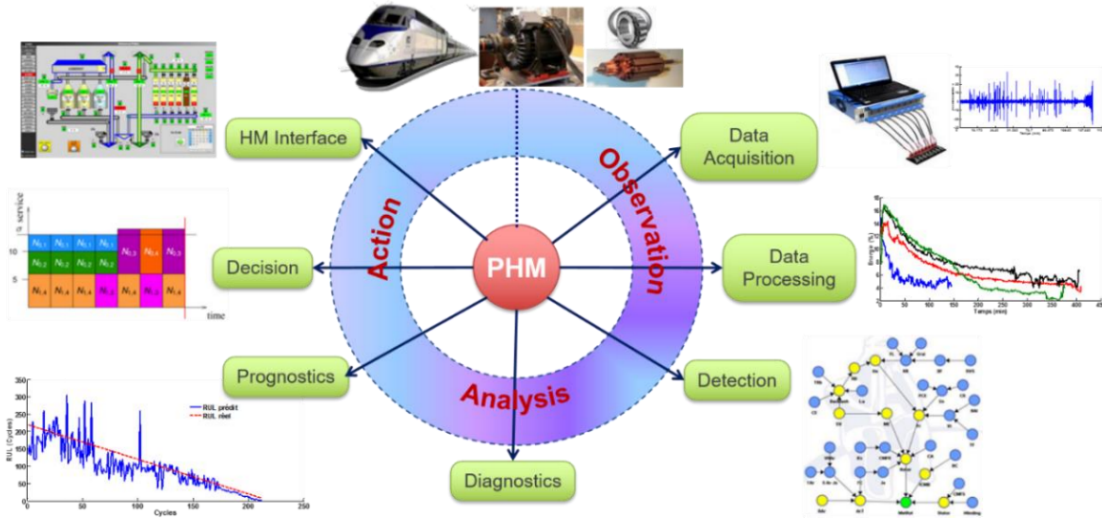


Figure 1.1: PHM steps [6]

Despite significant research efforts that have been made to develop a hybrid PHM model, there is still a high uncertainty in those degradation models and their corresponding predictions [2, 12–14]. With respect to the POF aspect of those models, the localized corrosion mechanism (e.g., pitting corrosion) is still not well understood [9] because of many hydrodynamic, (electro) chemical and metallurgical parameter combinations that affect localized corrosion initiation and growth [9]. Some of those parameters are pH value in the water phase, the water chemistry, the protective scale, the CO_2 partial pressure, the amount of H_2S , the effect of oil wetting, the metal alloy composition, the temperature, the multiphase flow, and flow rate, the variation in material properties and of the pipeline geometry [15]. There are some challenges with respect to the data-driven aspect of a hybrid pitting corrosion degradation model for pipelines because of the special geometry of the pipeline which is a long asset that cannot be monitored online in all locations. Some of those challenges are measurement error, probability of not detecting some of the

existing pits, false positive detection, having a small number of off-line inspection data points for each detected defect, and matching uncertainty (i.e., uncertainty in matching the location of the pits identified by sequential ILIs due to different technologies, vendors, accuracy, etc.). Developing a hybrid model that assimilates all available knowledge and data is desirable.

The next challenge that has been ignored in the available models in the literature is to consider potential change in operational conditions in a pipeline's degradation level estimation. The available models are developed based on this assumption that the distributions of the operational parameters are constant during pipeline life-cycle [13, 16–18]. This assumption is valid only for those pipelines that are designed and used for a specific content and this usage does not change during the pipeline life-cycle. However, in practice, even for the above-mentioned pipelines, the nature of the oil and gas field might change over time. In addition, some pipelines are designed to transport a specific product, but the usage change after some years of operation to transport another product. Also, in some occasions flow reversal happens in a pipeline [19–21]. Therefore, considering change in operational conditions is a potential area to improve the performance of the pipelines' pitting corrosion degradation models.

Generally, pipelines can be categorized as piggable and non-piggable. A pipeline is considered piggable when there is no limitations which prevent using commercial smart pigs to inspect them (because of e.g., small diameter, sharp curvature, unavailability of pig trap). According to [1], approximately 50% of existing pipelines worldwide are detectable by in-line inspection (ILI) instruments, a term referred to



Figure 1.2: An example of a smart pig (in-line inspection device) [iecetech.org]

literature as piggable. Smart pigs (Figure 1.2) are the common tools that are used to inspect oil and gas pipeline. The three common types of sensors that are used in smart pigs for nondestructive evaluation and testing of oil and gas pipelines are magnetic flux leakage (MFL), ultrasonic testing (UT), and eddy current [22, 23].

Two approaches have been developed in the literature for degradation level estimation of piggable pipelines: defect-based (pit-based) and population-based (segment-based) estimation. The first approach is developed for the scenario when the density of the existing pits is low (e.g., 62 pits in 80 km of natural gas pipelines in Alberta, Canada [13]). In this approach the features (e.g., pit depth, length) from at least two ILIs have to be matched with respect to their location in the pipeline [24]. This approach is more accurate and more common [18], because the results of sequential in-line inspections for each specific pit are used to evaluate the degradation level and RUL at each corroded location. The second approach has been

developed to address another scenario when the density of the existing pits is high and the matching procedure is time consuming and prone to error [18]. Zhang and Zhou [13] considered measurement error of ILI data of an aged pipeline by using a hierarchical Bayesian model in a defect-based approach. They also considered POD in simulation of degradation for a new pipeline. Maes et al. [16] developed a degradation model by using a hierarchical Bayesian model and considered FP and ME in a defect-based approach. Dann and Maes [18], developed a population-based degradation model and considered POD, FP, and ME in their model. They used KL divergence method to estimate the parameters of the degradation model and predict the degradation level in the future. To the best knowledge of the author, a hybrid (POF and data-driven) population-based approach based on a hierarchical Bayesian, that consider POD, FP, and ME, is not reported in the literature.

The final task in the analysis step of a PHM analysis (Figure 1.1) is to correlate the estimated degradation level to a reliability metric (e.g., probability of occurrence of potential failure modes, RUL, MTTF) to be used in the action (i.e., decision making) step (Figure 1.1). There are three potential failure modes for oil and gas pipelines due to internal pitting corrosion: small leak, large leak, and rupture. Small leak happens when the pipeline degradation level exceeds the pipe wall thickness (PWT) (in practice 80% of PWT). Large leak and rupture happen because of the plastic breakdown of the pipe wall due to internal pressure even if the pit depth is less than the PWT. These two failure modes are referred to as burst. When an axial propagation is predicated to take place, the failure mode is categorized as rupture and when no unstable axial propagation is expected to happen, the

failure mode is categorized as large leak [25]. These two failure modes happen when the failure pressure of the degraded pipeline is less than the operational pressure. The most commonly used and well-known models that have been developed to estimate the failure pressure of a corroded pipeline are ASME B31G (ASME 1991), RSTRENG [26], PCORRC [27], Fitnet FSS [28]. These models are developed based on fracture mechanic principals. Pandey [29] used RSTRENG, Bazan and Beck [30], Zhang and Zhou [13], and Valor et al. [25] used PCORRC to calculate the burst pressure and RSTRENG to calculate rupture pressure. In all these models, the burst and rupture pressure are functions of some static random variables (i.e., pipeline geometry (thickness and diameter), pipeline material properties) and some dynamic random variables (i.e., pipeline degradation level, and operational pressure). A probabilistic hybrid reliability analysis model (defect-based and population-based) that considers variation of those static and dynamic random variables in calculating probability of occurrence of the potential failure modes is not addressed in the literature and it is desirable to be developed to help pipeline engineers and asset managers to prioritize pipeline repairs and/or replacements based on their estimated probability of failure.

1.2 Research objectives and scope

There are four main objectives of this research to the development of hybrid PHM models for internal pitting corrosion of oil and gas pipelines.

Objective 1: Compile and assess different pitting corrosion rate models and model-

ing techniques applicable for oil and gas pipelines.

Objective 2: Develop a hybrid defect-based degradation model for a segment of a pipeline when the pit density is low, considering change in operational conditions.

Objective 3: Develop a hybrid population-based degradation model for a segment of a pipeline when the pit density is high, considering POD, measurement error and POFC.

Objective 4: Develop a methodology to estimate the reliability and RUL of a pipeline when the pit density is low in some locations and it is high in other locations.

1.3 Assumptions

The assumptions that are involved in this research are as follows:

- ILI data (infrequent, discrete and low quality information) are available for the entire pipeline.
- Matched ILI data and mass ILI data are available for locations with low and high pit density respectively.
- An OLI (continuous, discrete, and high-quality information) sensor is installed to monitor a pit continuously.
- The ME, POD, and POFC are known for the ILI and OLI tools.
- The detected pits are stable pits, which means they passed the nucleation,

re-passivation and metastable phases and their growth are stabilized.

- Pits are not interacting each other.
- The detected pits are not mitigated by the maintenance activities.

1.4 Overview of the research

In this research different stochastic processes for modeling pitting corrosion are assessed and compiled and the most proper one is selected to take into account four types of uncertainty (measurement, local, temporal, and epistemic) and two characteristics (time and depth dependency of pit depth growing behavior) in pipeline pitting corrosion degradation modeling.

Two hybrid (POF and data-driven) degradation models and a hybrid (defect-based and population-based) reliability model are developed to estimate the degradation level and reliability of aged piggable oil and gas pipelines due to internal pitting corrosion. In those models, different sources of available information and data (i.e., POF knowledge, ILI and OLI data, operational parameters measurements) are fused together to reduce the uncertainty in the prediction of pitting corrosion degradation level. Table 1.1 shows the potential available information and data for piggable and non-piggable pipelines and their application in different available pitting corrosion degradation models in the literature and also in this dissertation.

The first model is a hybrid defect-based model that fuses the POF knowledge with the noisy ILI data of a numbers of individual pits and OLI of a single stable pit. This model is developed for the case when the density of the pits is low and

Oil and gas pipelines						
		Piggable			Non-piggable	
Available info./data	defect based	population based	this dis- sertation	defect- based	population- based	
POF knowledge	✓	✓	✓	-	✓	
Matched ILI	✓	-	✓	-	✓	
Mass ILI	-	✓	✓	-	-	
Oper. Param. Measurements	-	-	✓	-	✓	
Corrosion rate distribution	-	-	-	-	✓	

Table 1.1: Usage of potential information and data sources in the available pitting corrosion degradation model in the literature and this dissertation

their sequential ILI data can be matched properly. In addition, a change in operational conditions is considered in pipeline degradation modeling for the first time by developing a similarity-based RUL estimation model. This model is developed by using a hierarchical Bayesian model based on a non-homogeneous gamma process and augmented particle filtering method.

The second model is a hybrid population-based approach that fuse POF knowledge with the noisy mass ILI data of a population of pits. This model is developed for the case when the density of the pits is high and matching procedure is time consuming and prone to error. In this model the measurement error, probability of not detecting some of the existing pits, and POFC are taken into account.

Finally those two hybrid models are combined to develop a hybrid reliability model for a pipeline when in some locations the pit density is low and in some locations the pit density is high. Having a high confidence estimation of the reliability of a pipeline helps to decrease the frequency of unnecessary maintenance activities

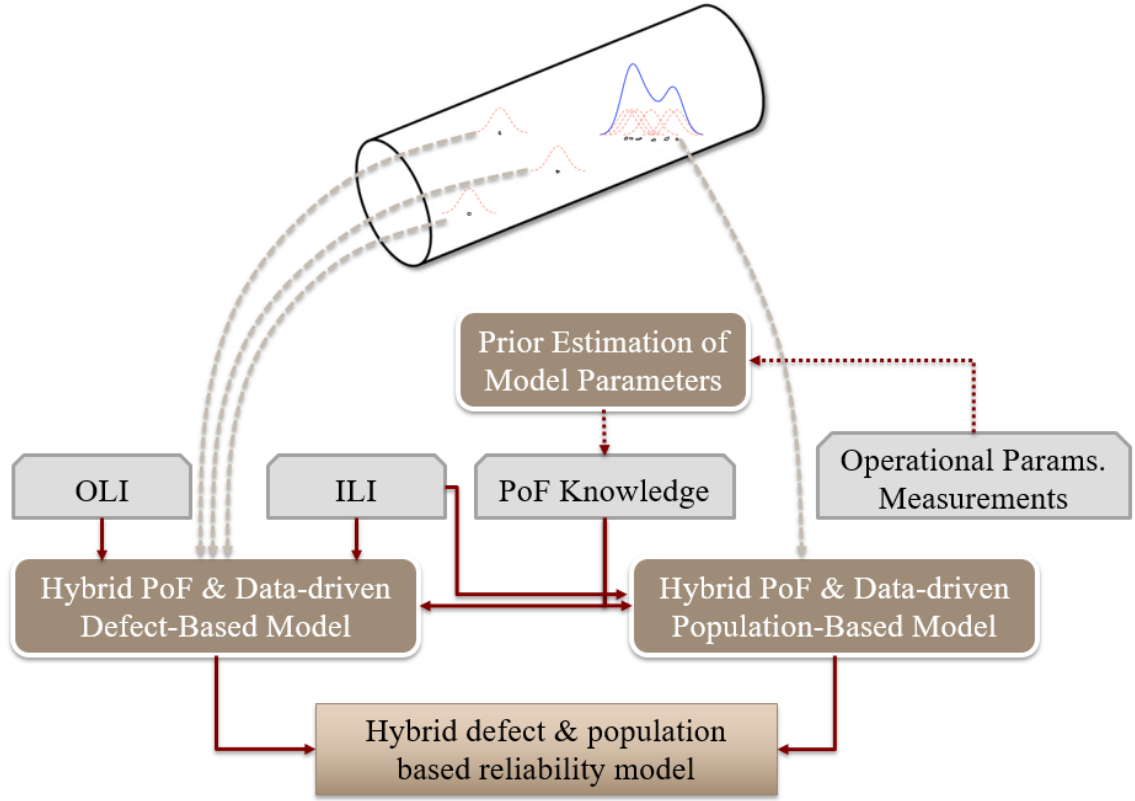


Figure 1.3: Summary of the proposed PHM degradation models for internal pitting corrosion of oil and gas pipelines

and unpredicted failures by making an optimal condition-based maintenance decision. Figure 1.3 shows the summary of the developed PHM degradation models for internal pitting corrosion of oil and gas pipelines.

1.5 Organization of this dissertation

This dissertation is organized as follows. Chapter 2 presents a literature review on PHM approaches, sensor data fusion, and similarity-based RUL estimation. Chapter 3 is a review paper which compiles and assesses different pitting corrosion rate models and modeling techniques applicable for oil and gas pipelines. Chapter 4 presents the development of a hybrid defect-based degradation model for a segment

of a pipeline when the pit density is low, considering change in operational conditions. Chapter 5 explains the development of a hybrid population-based degradation model for a segment of a pipeline when the pit density is high, considering POD, measurement error and POFC. Chapter 6 develops a methodology to estimate the reliability and RUL of a pipeline when the pit density is low in some locations and it is high in some other locations. The dissertation ends with conclusion, contributions, and suggested future work in Chapter 7.

Chapter 2: Literature review on PHM approaches, sensor data fusion, and similarity-based RUL estimation

This section is dedicated to the literature review on application of PHM approaches, sensor data fusion and similarity-based RUL estimation methods on pitting corrosion degradation modeling. In addition, a comprehensive literature review has been done on pitting corrosion modeling techniques that is presented in the next chapter.

2.1 Literature on PHM approaches

Generally, PHM approaches have two parts; prognostics, which is the process of predicting the reliability of the component/system, and health management, which is the process of monitoring the defects and determining a failure's impact on the performance of the system and mitigating the effects [5, 6]. In order to perform PHM, a comprehensive analysis needs to be done. The main steps of this analysis are shown in Figure 1.1. The first step is data acquisition which includes the process of data collection and storage from component/system under investigation. This data can be both sensor data and event data (e.g., failure, maintenance, and repair). The second step is data processing which includes data cleaning and data analy-

sis. Extracting useful features that indicate the failure progression of the system is performed in this step. The third step is to detect failures from collected and analyzed data. The fourth step is fault diagnostics which is the process of failure mode identification and degradation level assessment. The fifth step is prognostics which is the process of predicting the time to failure and RUL of the component/system. The sixth step is decision making step which includes selecting the proper maintenance action and finally the seventh step is developing a human-machine interface to visualize component health status [6].

PHM approaches can be categorized as physics-based (i.e., model-based), data-driven and hybrid approaches. In physics-based models, the degradation behavior of the component is described by mathematical models or equations derived from physical systems. Paris-Erdogan law [31] is a well-known physics-based model for fatigue crack growth. This mathematical model is combined with condition monitoring data to tune the model parameters, and then this model is used to estimate the RUL of the component. Physics-based models are more accurate in long-term RUL estimation. However, developing a physics-based model for complex systems with stochastic degradation behavior of components is challenging. Kalman filter and particle filters are two common Bayesian methods that are used widely to estimate the parameter of a physics-based model.

Data-driven prognostics approaches try to predict the RUL using the condition monitoring data. They can model the complex system, but the accuracy is highly dependent on the amount of the condition monitoring data. Gaussian Process Regression, Artificial Neural Networks, Fuzzy Logic, and Bayesian networks are some

examples of data-driven prognostics approaches. For example Zhang et al. [32] used long short-term memory recurrent neural network for RUL estimation of lithium-ion batteries.

The hybrid prognostics approaches try to combine the merits of different approaches while minimizing the limitations to better RUL estimation and health management [6]. Liao and Kottig [33] categorized hybrid approaches into five categories as follows. Experience-based model + data-driven based model; for example, Chinnam and Baruah [34] combined Artificial Neural Networks (ANN) and fuzzy logics to estimate RUL of a cutting tool. Experience-based model + physics-based model; for example, Swanson [35] combined Kalman filter and fuzzy logic to estimate crack growth in tension steels bands. Data-driven model + Data-driven model; for example Yan and Lee [36] used logistic regression and maximum likelihood estimation to estimate the tool wear condition in drilling operation. Data-driven model + physics-based model; for example, Rabiei et al. [37] used support vector regression and particle filtering to estimate RUL in a crack under fatigue load. And finally Experience-based + data-driven + physics-based models; for example, Gola and Nystad [38] proposed a hybrid approach to assess the health state of a choke valve under erosion by combining fluid dynamic model, ANN, and moving maxima filters.

2.2 Literature review on sensor data fusion

The integration of information from different sources is known as data fusion. Data fusion is a multidisciplinary area and many terminologies such as sensor

fusion, data fusion, information fusion, multi-sensor data fusion, and multi-sensor integration have been used in the literature interchangeably to address different techniques, technologies, systems, and applications that utilized data from multiple information sources [39]. Among different definitions for sensor data fusion exist in the literature, a well-known definition for sensor data fusion is provided in [40]: "data fusion techniques combine data from multiple sensors and related information from associated databases to achieve improved accuracy and more specific inferences than could be achieved by the use of a single sensor alone." Generally, performing sensor data fusion has several advantages such as improving detection confidence, reliability, and extending the temporal and spatial coverage of the sensors. It can also provide specific benefits in some application such as wireless sensor networks by decreasing energy consumption and increase the lifetime of the sensors by reducing the number of transmitted messages [41].

This section reviews the relevant literature related to sensor data fusion techniques and the focus is on those techniques that can be used for RUL estimation of the pipelines and subsequently optimal maintenance decision making.

2.2.1 Motivation for data fusion

Why data fusion is necessary for oil and gas integrity management? A brief answer to this question is to overcome the limitations of using a single sensor system. A single sensor system might suffer from the following problems [39]:

- Sensor Deprivation: the damage of a single sensor system leads to loss of

perception on the desired object.

- Limited Spatial coverage: Usually there is a limitation on the coverage area of a sensor. For example, a reading from a fixed ultrasonic measurement tool on a pipeline just provides an estimation of the depth of the pits near that tool.
- Limited temporal coverage: In some sensors or some applications there is a limitation on the measurement frequency. For instance, ILI of the pipelines is an expensive operation and usually carried out every 3-10 years.
- Imprecision: The precision of the measurement is limited to the precision of the employed single sensor. For example magnetic flux leakage or ultrasonic testing signals that commonly are used in ILI include both biased and scattering error [13]
- Uncertainty of detection or POD: which is the probability that a defect be detected by an inspection tool. In contrast to imprecision, uncertainty of detection depends on the observed object rather than the sensor. For instance, in case of pitting corrosion, the probability of detecting a large pit by using a sensor is higher than the probability of detecting a small pit with the same sensor.

2.2.2 Categorization of sensor data fusion techniques based on the data type

Various categorizations for sensor data fusion techniques exist in the literature. The common categories are relations between inputs [42], input/output types

and their nature [43], sensor data fusion level [44], and type of architecture [45]. Two of the most well-known categorizations are reviewed here. The following two paragraphs are adapted from [45].

Durrant-Whyte [42] categorized sensor data fusion techniques based on the relations between the data sources. According to this approach, when the information on the same target provided by two sensors with different fields of view, the sensor data fusion technique is considered as complementary fusion. When two or more sensors provide information about the same target and same fields of view, the sensor data fusion technique is considered redundant. When the provided information is combined into new information that is typically more complex than the original information (e.g., two sensor modalities), the sensor data fusion technique is considered as cooperative fusion.

Dasarathy [43] proposed one of the most well-known sensor data fusion categorization systems based on the types of input/output data. This categorization is composed of the following categories:

- Data in-data out: this category is the most elementary or lowest form of sensor data fusion techniques. Typically the results are more reliable and accurate in this level [45] since the level of detail in the information is highest at that level.
- Data in-feature out: at this level, the raw data from different sources (e.g., different sensors at the same time or different signals from a same sensor at different times) are combined to extract some form of a feature of the object in the environment. Table 2.1 shows some examples of features that can be

Domain	Type	Feature
Time	Signal characteristics	Absolute value, Range, Maximum, Minimum, Derivative, Integral, Root mean square error (RMSE), Jerk, Zero crossing
	Statistical characteristics	Mean, Median, Variance, Standard deviation, Skew, Kurtosis, Percentile, Cumulative histogram, Cross correlation, Entropy
Frequency		Fourier coefficients, Energy, Power, Wavelet features, Power spectral density

Table 2.1: Example features that can be extracted from sensor data [46]

extracted from sensor data.

- Feature in-feature out: at this level, both input and output of the fusion process are features. The derived features are combined either qualitatively or quantitatively.
- Feature in-decision out: In this level, the feature from different sensors are the inputs and a set of decisions are the outputs.
- Decision in-decision out: at this level input decisions are fused to obtain better or new decisions.

In practical situations, in order to achieve the optimal performance for a system, it is likely that sensor data fusion be incorporated in different levels. There is a persistent school of thought among researcher in sensor data fusion area that fusion at the data in-data out level is the best approach because at this level the detail in the information is the highest. However, it should be noted that at this level the level of the noise is also the highest. Therefore, there is a trade-off to be evaluated in choosing the optimal sensor data fusion level/s for a given application [43].

2.2.3 Sensor data fusion algorithms

Selecting a sensor data fusion algorithm depends on the target application. The common factors that influence selecting a proper sensor data fusion algorithm include the required output, required accuracy, available input data, computational complexity, and available processing power [46]. There is a wide range of sensor data fusion algorithms from low complexity sensor data fusion algorithms, such as weighted average, k-NN, and K-means, that are well suited for simple clustering applications, to high complexity algorithms such as support vector machine, ANN, and Bayesian networks. Different classification systems for sensor data fusion algorithms exist in the literature [40, 45, 47]. For instance, Klein [47] classified the sensor data fusion algorithms as Bayesian inference, Dempster-Shafer evidential theory, ANNs, Voting logic fusion, Fuzzy logic fusion, knowledge-based expert systems and pattern recognition. In this chapter, Bayesian inference and ANNs as the two more common algorithms in PHM analysis are discussed briefly and some of their applications in degradation modeling are reviewed.

2.2.4 Bayesian Inference for degradation level estimation

Bayesian inference is a probability-based reasoning method that is based on Bayes' theorem which enables fusion of pieces of data. In sensor data fusion context, Bayesian inference belongs to the class of sensor data fusion algorithms that calculate the conditional posterior probability of a hypothesis (e.g., being in a degraded state) being true, given supporting evidence and a prior knowledge about that hypothesis.

Bayes' theorem provides a method to compute the posterior probability distribution of being at state x_k at time k given the set of sensor measurements up to time k , $Z^k = z_1, \dots, z_k$, and the prior distribution, as following:

$$Pr(x_k|Z^k) = \frac{Pr(z_k|x_k)Pr(x_k|Z^{k-1})}{Pr(Z^k|Z^{k-1})} \quad (2.1)$$

Where $Pr(z_k|x_k)$ is the likelihood of observing z_k , if system is in state x_k , $Pr(x_k|Z^{k-1})$ is the prior distribution of being in state x_k given the sensor measurements up to time $k - 1$. This prior distribution can be obtained by using Equation 2.2, which incorporates the given state model (Equation 2.3) and measurement model of the system (Equation 2.4). The denominator is a normalization factor to ensure that the probability density function integrates to one, which is obtained by Equation 2.5.

$$Pr(x_k | Z^{k-1}) = \int Pr(x_k | x_{k-1})Pr(x_{k-1} | Z^{k-1})dx_{k-1} \quad (2.2)$$

$$x_k = f_k(x_k, \epsilon_k) \rightarrow Pr(x_k | x_{k-1}) \quad (2.3)$$

$$z_k = h_k(x_k, \omega_k) \rightarrow Pr(z_k | x_k) \quad (2.4)$$

$$Pr(Z^k | Z^{k-1}) = \int Pr(z_k | x_k)Pr(x_k | Z^{k-1})dx_k \quad (2.5)$$

where ϵ_k and ω_k are the state model noise and measurement model noise respectively.

In general, both the prior distribution and the normalizing factor, contain integrals that cannot be evaluated analytically. The numerical simulation-based techniques (e.g., MCMC, particle filtering) have been developed to find an approximation for the posterior distribution. In the following, some works that used Bayesian inference to fuse the inspection data to model degradation processes are reviewed.

Maes et al., [16] proposed a hierarchical Bayesian framework for corrosion defect growth. They fused m sets of ILI data of n pits to estimate the degradation level of each defect. Among different limitations that were mentioned in Section 2.2.1, this framework addresses the limitations that are related to frequency, uncertainty, and imprecision of using one sensor data. In [16] pitting corrosion process has been modeled by using a gamma process, and ILI data sets have been fused to estimate the parameters of that gamma process to be used for RUL estimation of the pipeline. Maes et al. [16] framework has been used by Zhang and Zhuo [13] to estimate the degradation level in a natural gas pipeline that is currently in service in Alberta, Canada. Zhang and Zhuo [13] proposed a methodology for reliability evaluation of onshore natural gas pipeline containing multiple active defects due to internal pressure. The difference between the growth model that proposed in [13] and the one that proposed by Maes et al. is that, it considers the corrosion initiation time in pitting corrosion modeling. In other words, Zhang and Zhuo assumed that initiation time of different pits are different.

Rabiei et al. [37] used augmented particle filtering to fuse two types of sensor

data (i.e., acoustic emission and modulus of elasticity) from a metallic alloy under fatigue to estimate the degradation level happening prior to crack initiation in that metal. Rabiei et al. [37] proposed a new damage prognostics framework based on the evolution of damage precursors representing the indirect damage indicators when measurement of conventional direct damage indicator such as crack size is difficult or impossible. They ([37]) focused on the time period before crack initiation in the component, for which the conventional crack growth damage models (e.g., Paris Law) are not applicable and cannot be applied to estimate damage level. Rabiei et al. [37] showed that their proposed methodology tracks the true damage evolution effectively based on the variation of modulus of elasticity along with captured AE signals from experiments they conducted.

2.2.5 Artificial Neural Networks (ANNs)

ANNs mimics the working process of the human brain using interconnections of a large number of units or nodes called artificial neurons. ANNs are popular because of their proven ability to find complex relationship between input and output variables that are most of the time not well understood. They are adaptive and because of their parallel information-processing structure, they are able to build functional relationships between data and provide a powerful toolbox for nonlinear, multidimensional interpolations [48]. Neural networks come in two classes: feedforward neural network and recurrent neural networks (RNN) [49]. In a feedforward network, the information flows only in the forward direction. In a graph repre-

sentation, the graph of a feedforward network is acyclic. It should be noted that feedforward networks are static. The most general neural network architecture is the recurrent neural network (RNN), whose connection graph exhibit cycles (i.e., at least one cycle). Since the output of a neuron cannot be a function of itself, it requires that time be explicitly taken into account. A special kind of RNN is Long Short-Term Memory (LSTM) method. LSTM is an RNN with a hidden layer, but each hidden node is replaced by a memory cell to store information. LSTM has achieved great success in machine translation and speech recognition. The main characteristic that makes LSTM so powerful, is the ability to of remember information for long periods of time. Due to the inherent sequential nature of sensor data, this method is suitable for RUL estimation using sensor data [50].

Generally, ANNs have a good performance in the RUL estimation of complex systems because they are capable of learning complex nonlinear relationship by training the multi-layer networks using data. On the other hand, they have some limitations. Besides their low transparency (i.e., they are black boxes and there is no meaningful insight into the nature of their prediction), they need a large number of high-quality training data, which are usually difficult to capture in industrial applications. Also, their structure and parameters need to be initialized manually and randomly (i.e., the number of hidden layers and neurons are selected manually and randomly) [51]. In the following, some works that used ANNs for degradation models updating and RUL estimation are reviewed.

Sinha and Pandey [52] proposed a fuzzy-ANN-based approach for reliability assessment of oil and gas pipelines. The input data for ANN include yield strength

of the pipe, PWT, pipe outer diameter, average crack depth, the standard deviation of crack depth, average crack length, the standard deviation of crack length, and operating pressure. The average and standard deviation of defect depth and length are estimated by using ILI data. The output of this ANN is the probability of failure, which is mapped into a set of fuzzy membership grades (i.e., very low, low, medium, high, and very high). The failure takes place when the failure pressure falls below the pipeline operating pressure. They sampled from the probability distribution of each input to create training and testing data for the ANN. Basically, the objective of that work was to see if simulation-based analysis could be replaced by a neural network to predict the probability of failure. However, to develop this model, simulated data have been used. This approach can be used in non-piggable pipelines to estimate the probability of failure where there are some online sensors. However, it is not suitable for RUL estimation because it does not consider defects' growing behavior.

Carvalho et al. [53] used ANN for pattern recognition of magnetic flux leakage (MFL) signals in weld joints of pipelines. They classified signal patterns with three types of defects in the weld joints: external corrosion (EC), internal corrosion (IC) and lack of weld penetration (LP). They used four specimens (Figure 2.1) with artificial defects inserted on them. The LP defect was introduced during the welding and the EC and IC defects were simulated with shallow grooves inserted manually by machining (Figure 2.2). They used MFL pig with 136 Hall sensors and a ring of coil type sensors to inspect those specimens. In this work, ANN is used for defect classification in weld bead in a reliable and fast way. They combined the signals of the three specimens in a single set of data and then randomly separated this set

into a training (70% of data) and test set (30% of data). The signals of the fourth specimen were used only for network validation. The results showed the constructed ANN is able to classify signals of defected and non-defected weld joints with 94.2% success rate, and for corrosion and LP signals with 92.5% success rate. Also, it is possible to classify the pattern signals of EC, IC, and LP with an average rate of success of 71.7%. Applying this approach on real ILI data is difficult because the actual depth of the pits are unknown and they cannot be used to train the ANN.

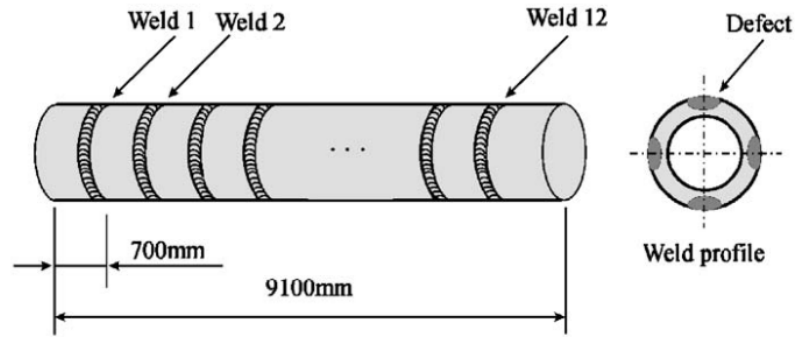


Figure 2.1: Specimens used to generate ground truth data [53]

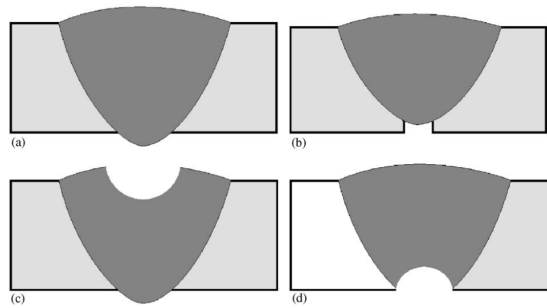


Figure 2.2: Sketch of the four studied conditions: a) non-defect; b) lack of penetration (LP); c) external corrosion (EC); d) internal corrosion(IN) [53]

Baraldi, Compare, Saucó, et al. [54] proposed an approach to extend particle filtering to the case in which an analytical measurement model is not available but a dataset containing pairs of state and the corresponding measurement is available.

They substituted the measurement model in PF with a bagged ensemble of ANNs. In the bagging method, several, classifiers (e.g., ANNs, SVR) are trained independently with different training set. The training sets are re-sampled and replaced from the original training dataset randomly. Then those classifiers are aggregated by a combination method such as the average of probabilities [55]. Baraldi et al. [54] applied this approach to a case study dealing with crack propagation in a component subject to fatigue load. In this case study, it is assumed that the state model is known. The measurement model is unknown and a dataset formed by N pairs of state and measurement is available. The verification of this approach shows that when the training set is sufficiently large, a good approximation of the measurement model may be obtained and its substitution in the PF does not significantly affect its performance. This approach is applicable for pitting corrosion in case of having raw inspection data and the actual depth of the pits to train the ANNs.

Yang et al. [36] proposed a method that fuses the particle filter and long short-term memory algorithms. Particle filter is used broadly in the literature for the purpose of prognostics by estimating the system state and identifying the model parameters. However, it does not have ideal performance due to the lack of measurement in the prediction phase. In this work, LSTM is used to forecast the measurements and the results are used as the future observations of PF. Then the predicted value by PF given back to the LSTM as a value for next prediction. This method is applied to the data of Proton Exchange Membrane Fuel Cell Stack from IEEE PHM 2014 data challenge. The results show that it can effectively integrate the advantages of PF and LSTM.

2.2.6 Literature review on similarity-based methods for RUL estimation

In this research a similarity-based RUL estimation model is developed. To do so, a literature review has been done on this topic as follows:

The basic idea in similarity-based models is to construct many off-line possible sub-models for degradation indicator and then choosing which sub-model is an appropriate one based on online monitoring information [56].

Wang et al. [57] proposed a similarity-based matching algorithm for RUL estimation. They assumed that a library of degradation patterns with complete run-to-failure historical data is available for multiple units of a system/component. Then, in order to predict the RUL of a test unit, instead of fitting a curve and extrapolating it, they matched the available data for the test unit with a certain life period of certain training units with the best matching score. They used Euclidian distance to find out the similarity between the test unit and training units. Finally, they estimated the RUL of the test unit by using real life data of matched training units (i.e., those with the highest similarities) minus the current life of the test unit. They used this approach on run-to-failure data of an unspecified engineering system to tackle the data challenge problem defined by the 2008 PHM data challenge competition.

Eker et al. [58] modified the previous approach by considering the most similar K percent of training samples rather than using the whole training set. They employed a genetic algorithm to find the best value for K by minimizing the RMSE

values out of RUL estimation.

Zio and Di Maio [59] proposed a similarity-based approach to predict the RUL of a system by defining a fuzzy-based algorithm. In this approach, a library of reference trajectory patterns to failure is created and a fuzzy-based similarity analysis is performed to predict the RUL of a newly developing failure trajectory (test trajectory). Based on this approach, the monitored signal for each system/component is divided into k segments. Then those segments of the reference trajectories that are most similar to the most recent segment of the test trajectory gain the higher weights in the extrapolation of the test trajectory to failure. In case of having two or more similar segments in a reference trajectory, the latest one is selected to have a more conservative estimation for RUL of the test trajectory. In all the above-mentioned approaches, the frequency of the observations for both the reference components and the test component is the same. In this dissertation, the author will propose a similarity-based approach for RUL estimation of a test component when the frequency of the observation is not equal for the test component (pit) and the reference components (pits).

Chapter 3: A Review of Data-Driven Oil and Gas Pipeline Pitting Corrosion Growth Models Applicable for Prognostic and Health Management

This chapter has been published in the International Journal of Prognostics and Health Management as Roohollah Heidary, Steven A. Gabriel, Mohammad Modarres, et al. "A Review of Data-Driven Oil and Gas Pipeline Pitting Corrosion Growth Models Applicable for Prognostic and Health Management". In: International Journal of Prognostics and Health Management 9.1 (2018).

3.1 Abstract

Pitting corrosion is a primary and most severe failure mechanism of oil and gas pipelines. To implement a PHM for oil and gas pipelines corroded by internal pitting, an appropriate degradation model is required. An appropriate and highly reliable pitting corrosion degradation assessment model should consider, in addition to epistemic uncertainty, the temporal aspects, the spatial heterogeneity, and inspection errors. It should also take into account the two well-known characteristics of pitting corrosion growing behavior: depth and time dependency of pit growth

rate. Analysis of these different levels of uncertainties in the amount of corrosion damage over time should be performed for continuous and failure-free operation of the pipelines. This paper reviews some of the leading probabilistic data-driven prediction models for PHM analysis for oil and gas pipelines corroded by internal pitting. These models categorized as random variable-based and stochastic process-based models are reviewed and the appropriateness of each category is discussed. Since stochastic process-based models are more versatile to predict the behavior of internal pitting corrosion in oil and gas pipelines, the capabilities of the two popular stochastic process-based models, Markov process-based and gamma process-based, are discussed in more detail.

3.2 Introduction

Corrosion is the main failure mechanism of oil and gas pipelines. Of all corrosion mechanisms, pitting corrosion is of most concern in pipelines because of the high rate at which pits can grow [2]. Failure data, provided in the literature, shows that 57.7% of oil and gas pipeline failures in Alberta, Canada between 1980 and 2005 [4] and 15% of all transmission pipeline incidents between 1994 and 2004 in the US were due to internal corrosion [60]. Moreover, 90% of corrosion failures of transmission pipeline sector in the US, between 1970 and 1984 were due to localized pitting corrosion [4]. Therefore, this review paper primarily discusses pitting corrosion growth prediction models applicable for PHM of oil and gas pipelines.

Despite significant research efforts in forecasting pitting corrosion, there are

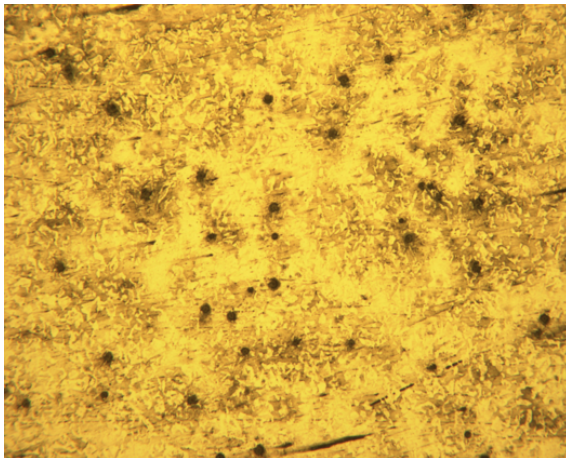


Figure 3.1: An example of pitting corrosion on X70 carbon steel surface in a corrosive environment (magnification scale: 200X) [63]

still many unanswered questions due to the highly stochastic nature of the pitting corrosion mechanism and a large number of dependent and independent influential parameters [61, 62]. For example, parameters that may influence internal pitting corrosion are the pH value in the water phase, the water chemistry, the protective scale, the CO_2 partial pressure, the amount of H_2S , the effect of oil wetting, the metal alloy composition, the temperature, the multi-phase flow, and the flow rate. Due to the large variations in these parameters, inter-dependencies between them, and also non-monotonic effects of some of them, there is a multitude of degradation paths for every single pit. In addition to this variation in degradation paths for each pit, there is usually more than one pit in a segment of a pipeline and each pit must be analyzed individually (by considering dependencies and correlations between pits) because the failure at each pit is equal to the failure of the whole pipeline. Figure 3.1 depicts an example of pitting corrosion on X70 carbon steel surface in a corrosive environment.

In comparison with conventional reliability analysis that mostly gives a population-

based assessment, PHM approaches can handle corrosion complexity more efficiently, especially by utilizing fast developing information and inspection technologies that make it possible to have real-time data management and processing for each individual pipeline and also individual pit [5]. Pipeline PHM approaches predict the RUL of a pipeline based on imprecise past and current degradation data gathered through some monitoring regime; this imprecision is due to uncertain inspection date. This estimation of RUL is vital in condition-based maintenance by avoiding unnecessary maintenance and unpredicted failures [7, 37].

Most PHM methods rely on POF-based or data-driven based models [7]. POF-based models have advantages in long-term damage behavior prediction, but since they are based on some approximations and simplifying assumptions when the degradation process is complex (e.g., pitting corrosion), it is difficult to estimate the model parameters and validate the results [8]. However, studying POF-based models is important to identify the root causes of pitting corrosion that can provide useful information for prognostic purposes. Because of the complexity and inherent randomness of pitting corrosion over time, probabilistic data-driven models are more suitable to describe pitting corrosion behavior especially when the results of modeling are used to perform reliability analysis [30, 64, 65].

In probabilistic data-driven models, the knowledge about dependencies between pit depth and independent covariates, and also the uncertainties about the degrading process, are encapsulated in the inspection data. The extrapolated RUL prediction is valid and applicable as long as the resulting model from these inspection data is used for predicting RUL in pipelines with a similar operational condition.

Among different probabilistic data-driven PHM approaches [5, 8], this paper discusses regression-based, gamma process-based, and Markov process-based models that are usually used to represent pitting corrosion process in oil and gas pipelines.

To emphasize the contribution of this review paper, the readers should make note of some other review papers [4, 9, 60, 61] that categorize different corrosion rate models and modeling approaches. Key conclusions of these review papers will follow.

Nyborg [12] compared the performance of fourteen uniform CO_2 ¹ corrosion rate models for oil and gas production systems by applying these models to some reliable data from some operating companies. Some of these models are empirical and were obtained by using empirical regression analysis. On the other hand, some of them are mechanistic that take the chemical, electro-chemical or transport processes into account and some of them are a combination of these two approaches and are semi-empirical. Among all these models, just four of them have considered the localized corrosion (e.g., pitting corrosion, crevice corrosion). Nyborg [12] concluded that none of these fourteen models significantly performed better than the others for all cases and none of these models can claim better than $\pm 50\%$ accuracy for a wide range of conditions. Two main factors that cause this variability are corrosion films and oil wetting effects modeling approaches. As it has been shown in [12],

¹It worth noting that internal corrosion of oil and gas pipelines made from carbon steel is often referred to as "sweet CO_2 corrosion". However other corrosive species such as hydrogen sulfide, H_2S (sour corrosion), organic acid, etc., might be involved in this corrosion process as well [9]. Among these corrosion species, presence of H_2S , changes corrosion mechanism tremendously because of production of iron sulfide instead of iron carbonate. Therefore, using sweet corrosion model, even by adding sulfide correction factor, will not give reliable results [12]. Based on field corrosion data, H_2S is related to the occurrence of localized corrosion, however, the mechanism and location of happening are not well understood [9].

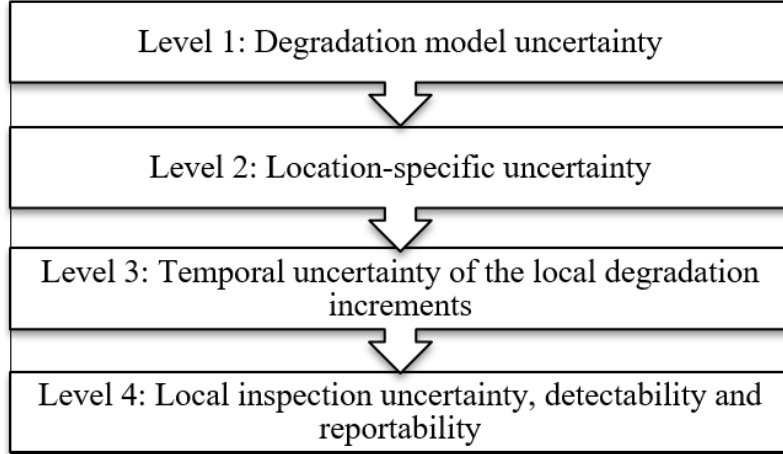


Figure 3.2: Hierarchical levels of uncertainty in degrading systems (modified) [16]

those models that are mostly based on regression analysis and POF analysis, cannot depict the inherent uncertainties in the corrosion process even for uniform corrosion. One reason for this inaccuracy is that these models mostly have considered level 1 uncertainty in Figure 3.2, which is related to lack of knowledge about the corrosion process (epistemic uncertainty), and they do not take into account the other three levels of uncertainty that are discussed later.

Nesic [9] categorized available CO_2 corrosion rate models for uniform internal corrosion of oil and gas pipelines into mechanistic models, empirical models and semi-empirical models and discussed advantages and disadvantages of each category. Mechanistic models have a strong theoretical background and give accurate and physically realistic interpolation and extrapolation prediction when they are calibrated with a reliable experimental database. However, the main disadvantage of mechanistic models is that the prediction results might be unrealistic if many simplifying assumptions are used. Re-calibrating mechanistic models by adding correction factors (to expand the range of application) leads to semi-empirical mod-

els. However, using semi-empirical models for extrapolation can result in having unreliable or unrealistic results. The third category is the empirical models (e.g., regression-based models, neural network-based models) that have very little or no theoretical background. These models perform very well within their calibration range but have to be used cautiously outside this range. Localized CO_2 corrosion is considered briefly in [9] as a process that is still not well understood and some recent works that have been done in this area are addressed

Papavinasam[60], has reviewed different models that predict internal pitting corrosion of oil and gas pipelines. However, most of the models that are discussed in that review are addressing uniform CO_2 corrosion rate.

In a nutshell, the above-mentioned models, including the probabilistic ones mostly correspond to level 1 in Figure 3.2 and they do not consider the other three levels of uncertainty.

Figure 3.2 shows the four hierarchical levels of uncertainty in degrading structures. Level 1, captures all model uncertainties (epistemic uncertainties) that are applicable to all points within a pipeline segment. The other three levels, apply to each local point in that segment; Level 2 indicates location-specific uncertainties that are related to uncertainties in known covariates (e.g., temperature, pressure, material properties) or aleatory effects due to unknown or omitted covariates (e.g., top of line corrosion that sometimes happens due to water condensation in natural gas pipelines); Level 3 reflects the temporal uncertainty that models the difference between two defects, which even have the same load conditions and also in a similar location but can grow differently; and level 4 represents three kinds of inspection

uncertainties (measurement error, POD and reportability error) that need to be taken into account. Measurement error is a function of in-line inspection (ILI) device and measurement conditions, POD is a function of the actual defect size, and reportability is a function of the lower detection threshold of the ILI device [16].

This paper defines an appropriate pitting corrosion degradation model for PHM analysis of oil and gas pipelines as a model that considers all of these four levels of uncertainty. In addition to the above-mentioned criteria, pitting corrosion rate has some characteristics all of which should be satisfied by an appropriate pitting corrosion degradation model. First, the pitting corrosion growth rate is depth-dependent (characteristic I; the corrosion rate of a deeper pit is greater than the corrosion rate of a shallower one) and second, the pitting corrosion rate is time-dependent (i.e., for a single pit the corrosion rate decreases over time [9, 66] and this declining behavior follows a power law model with a less than one positive exponent (characteristic II) [2, 17, 63].

To the best of the authors' knowledge, there is no comprehensive review paper on pitting corrosion growth models applicable for PHM of oil and gas pipeline. This paper reviewed the commonly used pitting corrosion growth models; we focused on most highly cited and also more recently developed models. We then evaluated the published models by checking if they can model the above-mentioned characteristics and different uncertainty levels.

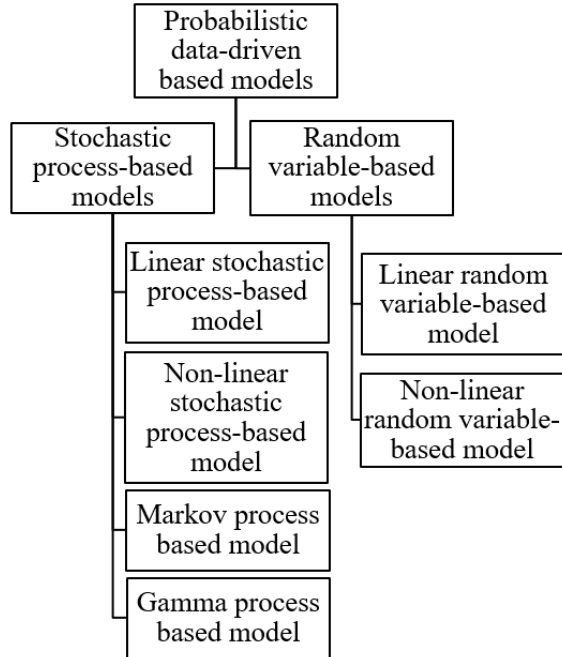


Figure 3.3: Breakdown of probabilistic data-driven based models for internal localized corrosion in pipelines

3.3 Probabilistic data driven models

Probabilistic data-driven based models can be classified into random-variable based and stochastic-process based models. The main difference between these two categories is that the latter one deals with the temporal variability of the degradation process, which leads to more realistic prediction [13], while the former one does not consider the third level of uncertainty in Figure 3.2.

Figure 3.3 shows this classification and also the corresponding sub-classes for each class. These models are the most commonly used probabilistic data-driven ones that have been used in the literature to model pitting corrosion growth in the oil and gas pipelines. These models are explained in more detail in the following sections.

3.3.1 Random-variable based corrosion growth models

The random variable-based corrosion growth models are the most common ones in the literature for reliability analysis of corroding pipelines [13]. These models consider corrosion uncertainty in terms of time-independent random variables. Linear and nonlinear random variable-based growth models are discussed below.

3.3.1.1 Linear random variable corrosion growth model

By having inspection data for at least two time instances, the growth rate for each pit depth can be estimated by the linear Equation 3.1 and the probability distribution function of corrosion rate for a population of defects can be extracted accordingly.

$$v_d = (D(t_2) - D(t_1))/(t_2 - t_1) \quad (3.1)$$

where v_d is the random variable that indicates the growth rate of a specific pit (d), $D(t_2)$ is the maximum depth of that pit (d) at time t_2 and $D(t_1)$ is the maximum depth of that pit (d) at time t_1 . The randomness of the corrosion rate is due to the large variation in the depth of the pits caused by variations of the metal properties and the environmental conditions.

Linear random variable models are used commonly because they are simple and can be adjusted to limited corrosion data easily (i.e., only two sets of data, however, these models can be applied to one set of data as well, by assuming that

stable pits start to grow from the beginning of corrosion process) [30]. However, extrapolating this model over time overestimates the corrosion degradation and may give a conservative estimation of the reliability of the pipeline, because as mentioned before, the behavior of pitting corrosion growth follows a nonlinear power function with a positive exponent of less than one [17, 30, 63]. Another drawback of the linear models is that if they are projected backward, the pitting initiation time t_0 is often found to be negative which is physically meaningless [30]. This model considers level 1 in Figure 3.2 nor the above-mentioned characteristics I and II. Temporal variability can be added to this model by using a Poisson square wave process that is explained in Section 3.3.2.

3.3.1.2 Non-Linear random variable corrosion growth model

As mentioned above, it is widely accepted that the pitting corrosion growth can be described by a power function with positive exponents of less than one [17, 30, 63]. Equation 3.2 shows this model that is proposed in [67].

$$D_{max}(t) = kt^\alpha \quad (3.2)$$

Considering the corrosion initiation time, a more accurate version of this model as shown in Equation 3.3 is used by some other researchers [2, 17].

$$D_{max}(t) = k(t - t_0)^\alpha \quad (3.3)$$

where $D_{max}(t)$ is the maximum defect depth at time t , t_0 is the corrosion

initiation time, k is a proportionality factor and α is an exponent factor. Note that in external corrosion, t_0 represents the time that is required for coating damage plus the time period of effectiveness of cathodic protection, and in internal corrosion, t_0 represents the initiation time of stable pit growth [66]. In an extension to the model in Equation 3.3, Velazquez et al. [2] performed a multivariate regression analysis to correlate the dependent variable (D_{max}) and independent variables (e.g., exposure time, soil and pipeline properties) for external pitting corrosion. They expressed k and α as linear combinations of the soil and pipe variables as shown in Equation 3.4.

$$D_{max} = k(t - t_0)^\alpha = [k_0 + \sum_{i=1}^n k_i x_i](t - t_0)^{n_0 + \sum_{j=1}^m n_j x_j} \quad (3.4)$$

where x_i is the i_{th} random predictor variable (e.g., pH) and k_i and n_j are regression coefficients for this predictor.

Based on [2], the proportionality coefficient k is mostly correlated to pH, resistivity, dissolved ion concentrations, and redox potential. On the other hand, the exponent coefficient α is a function of water content, bulk density, coating type, and the pipe-to-soil potential.

In order to validate this model, Velazquez et al. [2] plotted actual depth vs. predicted depth for 123 pits collected from another pipeline. Based on the visual examination of the plot, they concluded that the scatter of the predicted depth around the perfect correlation line was acceptable.

Ossai et al. [17] used Equation 3.5 to model internal pitting corrosion of

sixty non-piggable oil and gas pipelines based on ten years of corrosion data. They assumed that the pitting initiation time is zero. The regression model that they used is shown in Equation 3.5.

$$D_{max} = k(t - 0)^\alpha = (e^{\gamma_0 + \sum_{j=1}^k \gamma_j y_j}) t^\alpha \quad (3.5)$$

Here γ_0 is the intercept, γ_j is regression coefficient and y_j is j_{th} predictor variable (i.e., operational parameters) that affects internal pitting corrosion. That study [17] shows that CO_2 partial pressure, flow rate, and chloride ion concentration are moderately correlated with maximum pit depth. In contrary, water cut, pH and sulfate ion concentration are weakly correlated with maximum pit depth.

Ossai et al. [17] validated this model by calculating the root mean square percentage error (RMSPE) for the prediction data from three different pipelines with pits divided into four different pitting rate categories (low, moderate, high and severe). They calculated RMSPE for each combination with results ranging from $0.52 \sim 3.54$, $0.59 \sim 7.26$, $0.51 \sim 1.03$ and $0.6 \sim 1.20$ for low, moderate, high, and severe pitting corrosion rate category respectively. These ranges show the level of prediction accuracy of this model for each category. This model considers level 1 in Figure 3.2 (epistemic uncertainty) and also characteristics II (having power law behavior) but it neither addresses the other levels in Figure 3.2 nor the characteristics I (dependency of the corrosion rate on the depth of the pit). Temporal variability can be added to this model by using a Poisson square wave process that is explained in Section 3.2.2.

3.3.2 Stochastic-process based corrosion growth models

The most commonly used stochastic processes that have been used to characterize the growth of corrosion defects are Markov process and gamma process [13]. Two other stochastic processes, inverse Gaussian process [68] and Bayesian dynamic linear model [69], also have been used for this modeling purpose and are discussed briefly at the end of the gamma process section. Before describing these processes, two other regression-based stochastic process-based models are presented.

3.3.2.1 Linear stochastic process corrosion growth model

As it was discussed in Section 3.3.1, random variable models do not consider the variability of corrosion growth over time (level 3 in Figure 3.2). To consider this temporal variability, Bazan and Beck [30] modeled the defect growth rate as a Poisson square wave process (PSWP). Figure 4 shows a realization of a PSWP that represents the stochastic behavior of the defect growth rate (blue line). Moreover, this figure portrays a realization of the resulting stochastic defect size (red line), which is the accumulation of corrosion degradation at each random time interval. In this process, both pulse height (Y_i) and pulse duration ($t_{i+1} - t_i$) are expressed as random variables. Pulse durations are characterized as independent and identically distributed (i.i.d) random variables that are exponentially distributed (Poisson process) and pulse heights (i.e., maximum pit depth growth rate) are characterized as i.i.d random variables that can be modeled by any strictly positive random variable distribution (e.g., the gamma distribution [30]). In this model, the maximum pit

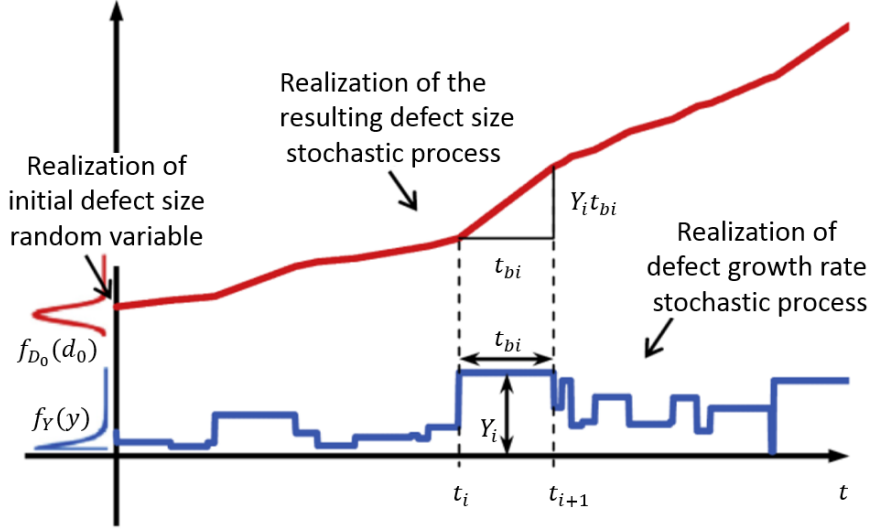


Figure 3.4: Linear stochastic process model [30]

depth at each time instance can be estimated by using Equation 3.6.

$$D_{max}(t_{i+1}) = D_{max}(t_i) + Y_i(t_{i+1} - t_i); i = 0, 1, \dots, n \quad (3.6)$$

where n is the number of pulses, $D_{max}(t)$ is maximum pit depth at time t , and Y_i is the pulse height. Bazan and Beck [30] used a data-fitting optimization algorithm to find out the parameters of this model (exponential distribution parameter for pulse durations, scale and shape parameter of gamma distribution for pulse heights) based on two sets of available inspection data. This model also (similar to the linear random variable model) has the limitation that backward extrapolation may lead to negative corrosion initiation time that is meaningless and violates the physics of the corrosion process.

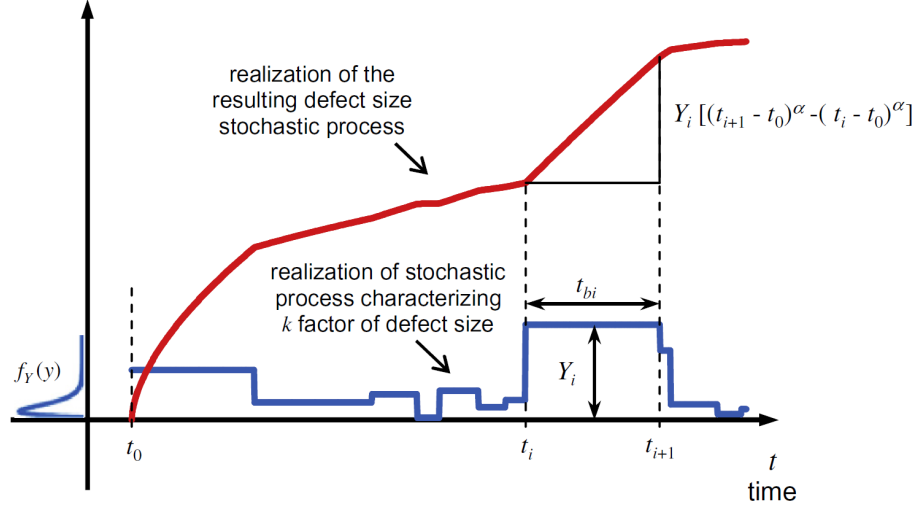


Figure 3.5: Non-Linear stochastic process model [30]

3.3.2.2 Non-Linear stochastic process corrosion growth model

To add temporal variability to the model in Section 3.1, Bazan and Beck [30] used PSWP with pulse heights (Y_i) and durations ($t_{i+1} - t_i$) according to Equation 3.7 that shows the increment in defect size in each interval. Figure 3.5 shows a realization of this stochastic process.

$$D_{max}(t_{i+1}) = D_{max}(t_i) + Y_i[(t_{i+1} - t_0)^\alpha - (t_i - t_0)^\alpha]; i = 0, 1, \dots, n \quad (3.7)$$

In Equation 3.7, Y_i is the proportionality coefficient of maximum pit depth and operation parameters, α is the exponent coefficient, n is the number of the pulses, and t_0 is the corrosion initiation time.

Having distributions of maximum pit depths at two time instances, parameters of this model were estimated by applying a data-fitting optimization algorithm

[30]. These parameters include the exponential distribution parameter (for pulse duration), scale and shape parameters of the gamma distribution (for pulse height), and scale and location parameters for lognormal distribution (for exponent factor). In contrast to linear models (Equation 3.6), the non-Linear stochastic process corrosion rate model (Equation 3.7) does not estimate the corrosion initiation time as a negative value.

Bazan and Beck [30] calibrated these four models (linear random, non-linear random, linear stochastic and non-linear stochastic models) to the same set of corrosion data to explore the difference between them. They used actual corrosion data in a pipeline collected for only two inspections. Therefore, without data on the third set of inspections, they could not evaluate the prediction capabilities of these four models. However, they showed that non-linear stochastic process model represents problem physics much better and it matches the available corrosion data reasonably well.

3.3.3 Markov process based corrosion growth models

Markov processes have been used by many researchers to model corrosion process. The stochastic process $D(t), t \geq 0$ is a continuous-time Markov chain (Markov process), if for all $s, t \geq 0, d(u), 0 \leq u \leq s$, and non-negative integers i and j :

$$P[D(t+s) = j | D(s) = i, D(u) = d(u), 0 \leq u < s] = P[D(t+s) = j | D(s) = i] \quad (3.8)$$

where $D(s)$, represents the condition (state) of the system at time s .

In other words, given that the system is in state i at time s ($D(s) = i$), the future states ($D(t + s)$) do not depend on the previous states ($D(u) = d(u), 0 \leq u < s$). This is the so-called Markovian property and a continuous-time stochastic process is a Markov process if it satisfies the Markovian property. In addition, if $P[D(t + s) = j | D(s) = i]$ is independent of s , the Markov process is said to have homogeneous or stationary transition probability [70]. In a Markov process, transition rate, λ_i , between states i and j , are defined in such a way that the probability of transition between states i and j in the infinitesimal time interval δt , is $\lambda_i \delta t$ and the probability of more than one transition in this time interval is negligible. The Kolmogorov differential equation that represents this process is given in Equation 3.9 [70, 71]

$$\begin{aligned} \frac{dP_1(t)}{dt} &= -\lambda_1 P_1(t) \\ \frac{dP_i(t)}{dt} &= -\lambda_{i-1} P_{i-1}(t) - \lambda_i P_i(t), \\ & i = 2, \dots, N \end{aligned} \tag{3.9}$$

Here $P_i(t)$ represents probability of being in state i at time t .

In Markov process-based corrosion rate models, the thickness of the pipeline is divided into N finite states and presence of the maximum pit depth in each state at any point in time can be represented by a discrete random variable $D(t)$. The ultimate goal of the analysis is to predict probability of being in each state at each point in time ($P[D(t) = i] = P_i(t), i = 1, 2, \dots, N$). The important issue in these

models is how to find the transition rate between states and how to correlate these transition rates to corrosion rates. In other words, these models try to find a valid set of transition rates between states by using available corrosion data for a specific pipeline to predict both the corrosion growth behavior of current pits and also new pits in the same or comparable pipelines. See [70, 71] for more details on Markov processes. In the following subsections, some main works that have been done in this area are presented.

Non-homogeneous Markov process corrosion growth model Provan and Rodriguez [72] proposed a non-homogeneous (transition rates are time-dependent) Markov process model to describe the growth of the maximum pit depth over time for a specific system for the first time. The gist of this model is the proposed non-homogeneous transition rate relationship shown in Equation 3.10.

$$\lambda_j(t) = \frac{\lambda_j(1 + \lambda t)}{1 + \lambda t^k}; j = 1, 2, \dots, N \quad (3.10)$$

where λ_j is the transition rate from state j to state $j + 1$, t is exposure time, and positive values λ and k are the parameters of the pitting corrosion system. As mentioned before, the thickness of the pipeline is divided into a discretized space of states and being in each state indicates that the maximum depth of the pit is in that state. This model satisfies characteristic I and II that were mentioned previously. In other words, for greater j (i.e., pit depth is in the deeper state) λ_j is greater. Also for a constant j , transition rate (which is proportional to corrosion rate [65]) decreases over time (as long as k is greater than 1, which is the case of

two examples that have been used in Provan and Rodriguez [72]. To determine the parameters of the pitting corrosion system (λ and k), Provan and Rodriguez used an iteration procedure to find the proper values of λ and k (which depend on the selected number of the states) that give the closest fit to their own experimental corrosion data for stainless steel [72] and also corrosion data for aluminum given in [73]. To validate their model, Provan and Rodriguez visually compared the actual and predicted probability histograms of maximum pit depth at different points in time and concluded that their results give ample confidence in their proposed approach. The main drawback of this model (Equation 3.10) is that there is no physical meaning behind it and also there is no explanation about how to use this model for more than one pit [65]. Also, this model does not address level 2, 3 and 4 uncertainties in Figure 3.2.

Non-homogeneous Poisson process for pit initiation and non-homogeneous Markov processes for pit growth Hong [74] proposed a model in which pit initiation was modeled by a non-homogeneous Poisson process (which is a valid assumption because most of the pits are generating at the beginning of the corrosion process [73], therefore pit initiation times are not homogeneously distributed). Also, pit growth process was modeled by a non-homogeneous Markov process. To find a closed-form solution for the Kolmogorov differential equation (Equation 3.9), first, the author has assumed homogeneity for both pits initiation times (homogeneous Poisson process) and pits growth process (homogeneous Markov process) and then the time dependency that causes non-homogeneity was modeled by using the so-called time-condensation method [75]. To do this transformation, the variable t

(that represents time) in the homogeneous equations is replaced by t^β , in which β is a constant of the pitting corrosion that can be obtained by minimizing the errors of observed and predicted mean values of the maximum pit depths. This model (Equation 3.11) gives the probability ($\theta_i(t)$) that maximum pit depth be in a state less than or equal to state i at time t by considering all pits that have been generated in time interval $[0, t]$.

$$\theta_i(t) = \exp(-\nu t^\beta (1 - \frac{1}{\lambda t^\beta} \sum_{j=1}^i \frac{\gamma(j, \lambda t^\beta)}{(j-1)!})), \quad (3.11)$$

$$i = 1, \dots, N - 1$$

where ν is pit generation rate, β is the model parameter, λ is the growth rate, n is the number of discretized states, and $\gamma(j, \lambda t^\beta)$ is an incomplete gamma function.

To validate this model, Hong [74] compared the mean of actual and predicted values of maximum pit depth visually. But Hong did not discuss any validation against additional data.

One drawback of Hong's model is that the proposed probability distribution of maximum pit depth is not a Gumbel distribution as it would be expected according to the published results in the literature [65]; because it is well-known that extreme-value analysis using the Gumbel distribution is the most successful application in statistical analysis to predict the maximum pit depth in a large area by using a small number of samples within a small area [64]. Another drawback is that the results of the model depend on the number of states [65]. In addition, it does not

consider level 2, 3 and 4 uncertainties in Figure 3.2.

Non-homogeneous Linear Pure Birth Markov Process This model [65, 76] proposes, for the first time, a methodology to link pit initiation and pit growth stages for multiple pits. For pit initiation, the Weibull distribution is used by interpreting the initiation time of each pit as the time to the first failure of a part of a system [77]. A continuous-time, non-homogeneous linear pure birth Markov process was used to model temporal non-homogeneity of pit evolution. In this process, transition rates from one state to another satisfy the forward Kolmogorov Equation [70, 71]) with the following equation.

$$\lambda_j(t) = j\lambda(t) \quad (3.12)$$

where $\lambda_j(t)$ represents the transition rate between the j_{th} to the $(j+1)_{th}$ state during the time interval $[t + \delta t]$. δt is an arbitrarily small unit of time that the probability of more than one transition is negligible. Since $\lambda_i(t) > \lambda_j(t)$ for $i > j$, characteristic I is already satisfied.

An advantage of using linear pure birth Markov process is that it has a closed-form solution for the transition probability from the m_{th} state to the n_{th} state in the interval (t_0, t) . This closed-form solution for this process that represents the negative binomial distribution is shown in Equation 3.13 [76].

$$P_{m,n}(t_0, t) = \frac{(n-1)!}{(n-m)!(m+1)!} e^{-(\rho(t)-\rho(t_0))m} (1 - e^{-(\rho(t)-\rho(t_0))})^{n-m} \quad (3.13)$$

where $\rho(t) = \int_0^t \lambda(\tau) d\tau$.

According to this equation by having $\lambda(t)$, $\rho(t)$ can be estimated and subsequently $P_{m,n}(t_0, t)$ can be calculated by Equation 3.13 and by having the initial pit depth distribution ($p_m(t_0)$), the probability of being in each state at each point in time ($p_n(t)$) can be estimated according to Equation 3.14.

$$p_n(t) = \sum_{m=1}^n p_m(t_0) p_{m,n}(t_0, t) \quad (3.14)$$

The gist of this model is the proposed approach to find the transition rate $\lambda(t)$ based on the estimated corrosion growth model. This model is based on this assumption that the mean of the stochastic process (linear pure birth Markov process (Equation 3.16) can be assumed to be equal to the mean of the deterministic damage process (Equation 3.3. This assumption is valid for some processes under specific assumptions that are given in [78]. By equating these two means, $\lambda(t)$ can be obtained from Equation 3.15.

$$\lambda(t) = \frac{\alpha}{t - t_0} \quad (3.15)$$

where α and t_0 are the exponent coefficient and corrosion initiation time in the power law model (Equation 3.3.

The mean of the linear growth Markov process can be estimated by Eq. (16).

$$M(t) = \sum_{m=1}^n m p_m(t) \quad (3.16)$$

Where n is the number of the states and $p_m(t)$ is the probability of being in state m at time t . In this approach, there is no limitation on the number of discretized states because there is a closed-form solution for this model. However, there are two important unanswered questions about this model that have been mentioned by the authors of this paper themselves. First, the validity of the assumption of equating stochastic and deterministic means for the case of pitting corrosion and second, the applicability of this model for different kind of pit populations.

An important question that has been answered by this model in [65] is that how to use Equation 3.13 for multiple pits with different pit initiation times. By assuming that m pits initiate and grow independently and also assuming that all of them are in state 1 at initiation time, the probability that the deepest pit is in a state less than or equal to state i at time t can be estimated by Equation 3.17.

$$\theta(i, t) = \prod_{k=1}^m [1 - (1 - e^{-\rho(t-t_k)})]^i \quad (3.17)$$

Where pit initiation process is considered by parameters t_k and pit growth process is considered by $\rho(t)$.

Valor et al. [65] showed that for large m , this cumulative distribution function (Equation 3.17 follows a Gumbel distribution and for a special case (assuming pit initiation times are equal for all pits) they found a lower bound for m as an important parameter when pit initiation and growth are combined in their proposed model.

The parameters of the proposed model ($t_k, \rho(t)$ and m) can be obtained by

minimizing a total error function E_T given in Equation 3.18.

$$E_T = \sum_{i=1}^N \sqrt{(\mu_e^i - \mu_p^i)^2} + \sqrt{(\sigma_e^i - \sigma_p^i)^2} \quad (3.18)$$

Where (μ_p^i, σ_p^i) and (μ_e^i, σ_e^i) are the mean value and variance of the i_{th} predicted and experimental extreme value distribution; respectively.

Valor et al. [65]) validated this model by calculating the mean MRSE. They used experimental data published by Aziz [73], Provan and Rodriguez [72], Melchers [79], Strutt, Nicholls, Barbier [80], and showed that the results of their proposed model using those experimental data are better (lower MRSE) than reported results in those works. This model had the most extensive validation in comparison with the other works that are reviewed in the current paper.

This model considered characteristic I and II. Also, this model considers pit initiation process, pit growth process, and multiple independent pits growth. However, it does not consider level 2, 3 and 4 uncertainties in Figure 3.2.

Another drawback of Markov process-based models is that it is not straightforward to update these models by Bayesian inference in case of new imperfect ILLI data [69].

3.3.4 Gamma process based corrosion growth models

The gamma process is a stochastic process with independent, non-negative, gamma distributed increments. Mathematically speaking, a gamma process with shape function $\alpha(t)$ and scale parameter β is a stochastic process $[D(t), t \leq 0]$ with

the following properties:

- $\alpha(t) > 0$ is a non-decreasing, right-continuous, real-valued function for $t \leq 0$ and $\alpha(0) = 0$
- $\beta > 0$
- $D(0) = 0$ with probability 1
- $D(\tau) - D(t) \sim Ga(\alpha(\tau) - \alpha(t), \beta)$ for all $\tau > t \leq 0$;
- $D(t)$ has independent increment

Where Ga indicates gamma distribution with following probability density function.

$$Ga(d | \alpha, \beta) = \frac{\beta^\alpha}{\Gamma(\alpha)} d^{\alpha-1} \exp(-\beta d) \times I_{(0, \infty)}(d) \quad (3.19)$$

where $I_{(0, \text{inf})}(d) = 1$ for $d > 0$ and zero otherwise and $\Gamma(\alpha) = \int_{t=0}^{\infty} t^{\alpha-1} e^{-t} dt$ is the gamma function [3].

Due to the monotonic increasing nature of the gamma process, it is an appropriate process for degradation mechanisms such as wear, fatigue, corrosion, creep, etc. Also, mathematical tractability is another advantage of this process. Using this process implies that the defect size is always increasing when there is no maintenance [81, 82].

Van Noortwijk [3] published a comprehensive survey of the application of the gamma process in maintenance. The following briefly explains two examples of those works that have used the gamma process to model the pipeline corrosion defect growth.

Maes et al. [16] proposed a hierarchical Bayes framework (Figure 3.6) to model

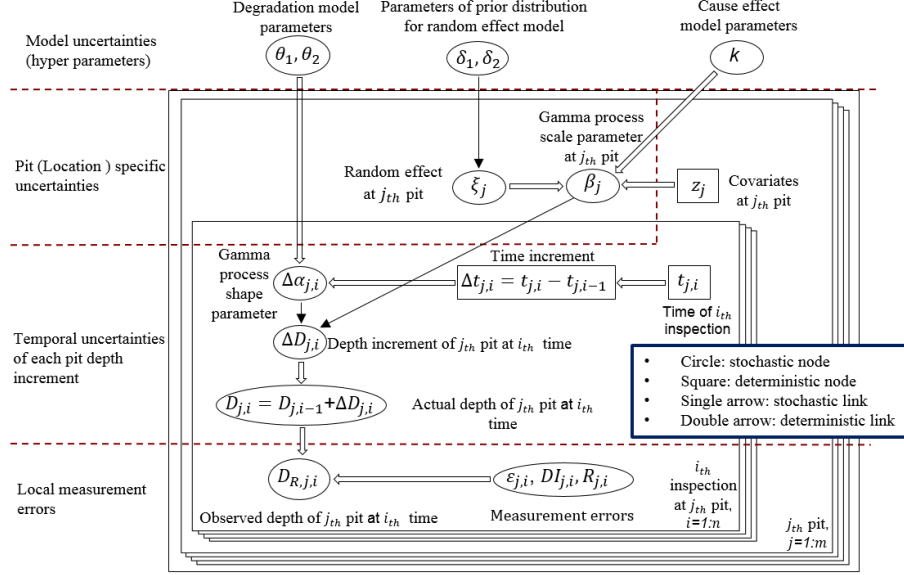


Figure 3.6: Hierarchical Bayes framework for heterogeneous degradation, modified from [83]

pipeline defect growth subject to ILI uncertainty. This framework can incorporate new inspection data and update the corrosion growth model accordingly.

Different levels of uncertainty are considered in this work as follows. Level 4 in Figure 3.2 is related to inspection uncertainties. These uncertainties can be categorized to measurement error, detectability, and reportability error. In [16] measurement errors are assumed to be normally distributed with means equal to zero and known location dependent variances (that might be correlated to the other locations (level 2 and 4 in Figure 3.2)). Equation 3.20 shows the relationship between measured size, $D_{M,j,i}$, and actual true degradation, $D_{j,i}$, for the j_{th} defect at i_{th} inspection time.

$$D_{M,j,i} = D_{j,i} + \epsilon_{j,i} \quad (3.20)$$

Where $\epsilon_{j,i}$ is the measurement error for a specific inspection device and measurement conditions at a given location that is usually correlated to inspection device bias and interpretation algorithm. To model POD that depends on the size of the defect, a detection indicator variable, $(DI_{j,i})$, that follows Bernoulli distribution is defined according to Equation 3.21. Then the observable degradation, $(D_{O,j,i})$, would be the product of this detection indicator ($DI_{j,i}$; with $DI_{j,i} = 1$ corresponding to successful detection) and the uncertain measurement due to sizing error, $(DX_{M,j,i})$ (Equation 3.22).

$$DI_{j,i} \mid PD(D_{j,i}) \sim \text{Bernoulli}(PD(D_{j,i})) \quad (3.21)$$

Where PD indicates POD.

$$D_{O,j,i} = DI_{j,i} \cdot D_{M,j,i} \quad (3.22)$$

The reportability factor (that represents lower detection threshold of the ILI device) is defined as a binary indicator random variable, $(R_{j,i})$ (Equation 3.23). Production of this factor to the observed degradation measurement, $(D_{O,j,i})$, gives the degradation value reported by the inspection device (Equation 3.24).

$$R_{j,i}(D_{O,j,i}) = \begin{cases} 0 & \text{if } D_{O,j,i} < \text{ILI device threshold} \\ 1 & \text{if } D_{O,j,i} \geq \text{ILI device threshold} \end{cases} \quad (3.23)$$

$$D_{R,j,i} = R_{j,i} D_{O,j,i} \quad (3.24)$$

Temporal uncertainties (level 3 in Figure 3.2) are modeled by considering the actual degradation at each inspection time as the summation of actual degradation at the previous inspection time and degradation increment between these two inspections. Because of two reasons, gamma process is an appropriate process to model the degradation increment behavior (Equation 3.25); independent degradation increments assumption [3] and restriction that such increments must be positive.

$$\Delta D_{j,i} \mid \Delta \alpha_{j,i}, \beta_j \sim \text{gamma}(\Delta \alpha_{j,i}, \beta_j) \quad (3.25)$$

Where $\Delta \alpha_{j,i}$ is the shape parameter and β_j is the scale parameter of the gamma distribution given in Equation 3.19.

The shape parameter reflects the time dependency of the physics of the degradation process (level three of the uncertainty in Figure 3.2). By selecting a proper functional form for the shape parameter, different degradation processes can be modeled. Power law function (Equation 3.19) is a versatile function that can represent constant, increasing or decreasing degradation rate based on the exponent of the model.

$$\Delta \alpha_{j,i} = \theta_1 [(t_{j,i-1} + \Delta t_{j,i-1})^{\theta_2} - t_{j,i-1}^{\theta_2}] \quad (3.26)$$

Where θ_1 and θ_2 are degradation model's parameters that are related to epistemic uncertainty. $\theta_2 > 1$ stands for an increasing degradation process, $\theta_2 < 1$ expresses a decreasing degradation process, and $\theta_2 = 1$ represents a constant degradation process.

The scale parameter of the gamma process is a positive location specific parameter that reflects the heterogeneity of the defects between the locations (level 2 of uncertainty in Figure 3.2). The location heterogeneity is represented by z_j , k and ζ_j . z_j are local covariates (e.g., pressure, temperature, pH), k is a vector of cause and effect regression coefficients associated with z_j and ζ_j are local aleatory effects that cannot be explained by defined covariates (e.g., top of line corrosion).

$$\beta_j = \exp[z_j^T k + \zeta_j] \quad (3.27)$$

Figure 3.6 summarizes this hierarchical Bayesian framework. In this figure, δ_1 and δ_2 are prior distribution Parameters for local aleatory effect model. According to this framework, by assuming prior probability density functions for system-wide parameters $(\theta_1, \theta_2, \delta_1, \delta_2, k)$, the actual true degradation, $D_{j,i}$, for j th defect at i th inspection time can be predicted. Then, as soon as inspection data $(D_{R,j,i})$ become available (by knowing measurement error for each location and inspection time), the model's parameters can be updated by using a Bayesian updating simulation techniques such as Markov chain Monte Carlo (MCMC).

As it was explained briefly, this hierarchical framework can model different level of uncertainties in the degradation systems and also characteristic II of pitting corrosion can be modeled by selecting proper values for θ_1 and θ_2 . However, characteristic I is not addressed in this model directly.

Zhang and Zhou [13] modified the above framework by considering corrosion initiation time in their model and used homogeneous gamma process ($\theta_2 = 1$) to

characterize the growth of the depth of corrosion defects. Zhang and Zhou [13] used ILI data obtained in 2000, 2004 and 2007 for 62 defects to estimate their model parameters and they validated their model by comparing the defects' actual depths (obtained after excavation and field measurement) in 2010 with the corresponding depth predicted by their proposed growth model. This validation shows that 90% of the predicted depths fall within the region bounded by the two lines representing actual depth $\pm 10\%$ PWT.

Finally, two other works that used the similar Bayesian framework are discussed briefly. Zhang et al. [68] used this framework by considering inverse Gaussian process (IGP) instead of homogeneous gamma process (HGP) to characterize the growth of the depth of corrosion defects. By applying this model to the same set of ILI corrosion data, they concluded that the predictions of the IGP-based model are negligibly different from those of the HGP-based model, but significantly better than random variable-based models. In another work, Zhang and Zhou [69] applied a similar Bayesian framework by using a Bayesian dynamic linear model (BDLM) and compared the results with their previous results based on HGP and IGP. They showed that the absolute difference between predicted depths and corresponding field-measured depth is less than or equal to 10% PWT for about 92% of the defects for BDLM, while this value for IGP and HGP is about 90% of the defects. This model is validated against a small number of corrosion data and it needs to be validated with larger data set to be able to be used it in practical application [69].

Model	Lev.1	Lev.2	Lev.3	Lev.4	Char.I	Char.II	Practicality
Lin. Random variable	✓						PI 1
Non-Lin. Random variable	✓					✓	PI 1
Lin. Stochastic Process	✓		✓			✓	PI 2
Non-Lin. Stochastic Process-based	✓		✓			✓	PI 2
Markov process-based	✓		✓		✓	✓	PI 3
Gamma process-based	✓	✓	✓	✓		✓	PI 3

Table 3.1: Evaluation of different commonly used probabilistic data-driven pitting corrosion growth models in oil and gas pipelines

3.4 Discussions

Now we address the question of "when should each model be used?" To answer this question, two criteria are defined: appropriateness and practicality. As it is explained in Section 1, an appropriate pitting corrosion growth model should consider four levels of uncertainty and also two well-known characteristics of pitting corrosion growing behavior: depth and time dependency of pit growth rate. The practicality criterion, indicates the level of knowledge that is required to perform each model. Table 3.1 summarizes this evaluation for those models that are discussed in this paper.

The first category in this table corresponds to linear random variable-based model which is the simplest probabilistic approach and also is the most commonly used approach in the industry that usually overestimates the pit growth rate.

The second category corresponds to non-linear random variable-based model which is the one that considers the well-known non-linear behavior (power law function with a less than one positive exponent) of pitting corrosion process. None of these random variable-based models consider spatial heterogeneity, temporal vari-

ation, and measurement errors. They also do not take into account the depth dependency of the pitting corrosion rate.

The third and fourth categories correspond to linear and non-linear stochastic process-based models that consider the temporal variability of pitting corrosion process. As it was discussed in Section 3.2, these models are combinations of PSWP and linear and non-linear random variable-based models. The two stochastic process-based models also do not consider spatial heterogeneity and measurement errors. They also do not take into account the depth dependency of the pitting corrosion rate.

The fifth category corresponds to Markov process-based models. In these models, the main issue involves extracting proper transition rates between states. Markov process based-models consider epistemic uncertainty, temporal variability, non-linearity and also depth dependency of the pitting corrosion rates. However, the spatial heterogeneity and measurement uncertainties are not addressed properly in Markov process-based models and it is not straightforward to update these models by Bayesian inference in case of new imperfect ILI data.

The last category of this table corresponds to the gamma process-based models which are the most versatile models that can address different levels of uncertainties. Besides, they can model the non-linearity in the pitting corrosion growth process. These models can also be updated properly by Bayesian inference in case of new imperfect ILI data. However, depth-dependency has not been considered directly in these models. In the first six columns of Table 1 appropriateness of the above-mentioned categories are evaluated.

The last column of Table 1 is allocated to practicality criterion. In this column, PI stands for Practicality Index. PI 1 is assigned to the first two categories and it means that these models can be developed by the common field engineers that are familiar with regression analysis using common application tools like Excel. PI 2 is assigned to the next two categories and it means that these models need more advanced knowledge of statistics such as PSWP. PI 3 is assigned to the last two categories and it needs a deep understanding of Markov process and gamma process.

3.5 Conclusion

This paper reviews various pitting corrosion degradation models for PHM analysis. Degradation model is a key element of the PHM approach to predict the RUL of a degrading system. Despite a large number of studies that have tried to find a comprehensive pitting corrosion growth model (degradation model), there is no universally accepted model that is able to predict the pitting corrosion growth properly for all occasions. Among available POF and data-driven based pitting corrosion growth models, this review paper focused on the latter as they are more suitable to describe pitting corrosion behavior because of the complexity and inherent randomness of pitting corrosion over time. The reason is that pitting corrosion process is a stochastic process that depends on a large number of dependent and independent factors (epistemic uncertainties); moreover, this process has temporal and spatial heterogeneity; also, inspection uncertainties (measurement errors, POD and reportability errors) add another level of uncertainty to the pitting corrosion

growth estimation.

In addition to these different levels of uncertainties, an appropriate pitting corrosion growth model must be able to take into account the two other well-known characteristics of pitting corrosion; the corrosion rate of a deeper pit is greater than the corrosion rate of a shallower one, and for a single pit, the corrosion rate declines over time following a power-law function with a less than one positive exponent. This paper discussed the appropriateness of some probabilistic data-driven based models that are commonly used to predict pitting corrosion growth. In addition to the appropriateness, the practicality of these models is also discussed in this paper.

Chapter 4: Development of a hybrid defect-based degradation model for a pipeline segment with low pit density

This chapter has been published in the Structural Health Monitoring journal as Roohollah Heidary and Katrina M. Groth. “A hybrid model of internal pitting corrosion degradation under changing operational conditions for pipeline integrity management”. In: Structural Health Monitoring (2019). DOI: 10.1177/1475921719877656

4.1 Abstract

This paper proposes a new framework to estimate the degradation level in oil and gas pipelines corroded by internal pitting when operational conditions change over time. Despite the fact that the operational conditions of a pipeline change at various times, this change has not been addressed in the current available pipeline corrosion degradation models. In this framework, a hierarchical Bayesian method and augmented particle filtering are used for data fusion to address this issue. This framework is applied on a case study and the results are compared with the estimations of a state of the art pitting corrosion degradation model.

Symbol	Description	Symbol	Description	Unit
SI	Similarity Index	k	Coefficient of power law model	mm
ILI	In-line inspection	t	Time	year
OLI	Online inspection	τ	Time	year
PF	Particle filtering	t_0	Pit initiation time	year
APF	Augmented particle filtering	T	Time at which operational conditions change	year
HB-NHGP	Hierarchical Bayesian based on a non-homogeneous gamma process	d	Maximum pit depth	mm
PWT	Pipe wall thickness	θ	Vector of model parameters	
EMPD	Estimated maximum pit depth	ν	Exponent of power law model	
RUL	Remaining useful life	V_q	q_{th} operational parameter	
PHM	Prognostics and health management	γ_q	Regression coefficient for the q_{th} operational parameter	
PM-SD	Process model standard deviation in APF	γ_0	The intercept of the regression model	
POF	Physics of Failure	Q	No. of operational parameters	
Metric R	RMSE between actual and predicted maximum depth of all pits	y	Measured maximum pit depth	mm
Metric N	The percentage of all pits that their predicted depths fall within the $\pm 10\%$ of their actual maximum depth	ϵ	Random scattering error	mm
a	Constant biased error	m	No. of in-line inspected pits	
b	Proportional biased error	n	No. of ILI operations	
i	Pit index	$Pit M$	The online inspected pit	
j	Time index	h	Kernel smoothing factor	
p	Particle index	Actual depth	Synthetic actual depth of a pit without measurement error	
P	Number of particles	Measured depth	Synthetic measured depth of a pit	
		Estimated depth	An estimation of the synthetic actual depth of a pit	

4.2 Introduction

Although pipelines are the most reliable and economical mode of transportation of oil and gas in large quantities [1], their failures and maintenance activities can impose a high cost to industry. In order to avoid unpredicted failures and also unnecessary maintenance activities, having a high confidence estimation of pipeline degradation due to different potential failure mechanisms is critical in pipeline integrity management.

Among different failure mechanisms, corrosion is especially significant for oil and gas pipelines, and pitting corrosion is of the most concerning because of the high pits growth rate [2]. According to the available literature, 15% of all transmission pipeline incidents between 1994 and 2004 in the US [60] and 58% of oil and gas pipeline failure in Alberta, Canada, were due to internal corrosion [4]. Furthermore, 90% of corrosion failures of transmission pipelines in the US between 1970 and 1984 were due to localized corrosion [4]. Therefore, investigation of internal localized corrosion is an essential task in pipeline integrity management.

While there has been significant progress in understanding uniform corrosion, localized corrosion is still not well understood [9]. Internal pitting corrosion, as a localized corrosion mechanism, is a highly stochastic process which is affected by a large number of dependent and independent parameters [61, 62]. Some of these parameters are pH value in the water phase, the water chemistry, the protective scale, the CO₂ partial pressure, the amount of H₂S, the effect of oil wetting, the metal alloy composition, the temperature, the multi-phase flow, and the flow rate. In addition,

there is temporal and local heterogeneity in some of these parameters, and interdependence between them [15]. There has been some progress on development of different pitting corrosion degradation models in the literature. We reviewed some of the leading probabilistic prediction models for oil and gas pipelines corroded by pitting corrosion and ranked them based on their comprehensiveness, the required data and the level of knowledge that are required to develop each of those models [15]. To the best of authors' knowledge, the available degradation models for internal pitting corrosion of oil and gas pipelines have been developed based on the assumption that all pits are under the same operational conditions for the operating life of the pipelines [13, 16, 17]. However, operational conditions of a pipeline can change due to changing nature of the field, flow reversal, product change, or conversion to service [85]. For example a pipeline that was constructed in 1953 to deliver crude oil, was converted to natural gas service in 2002 in Austin Texas, U.S. [19]. Another example for conversion to service is the use of the current natural gas pipelines to deliver hydrogen across U.S., which is in the feasibility study phase [86, 87]. This option is under investigation in U.K. as well [21]. An example for change in the product is the continuous change in the product properties within an uncertain range in the natural gas pipelines [88]. According to PHMSA (Pipeline and Hazardous Materials Safety Administration) changes in operational conditions may impact various aspects of a pipelines operation, maintenance, monitoring, integrity management, material compatibility, and corrosion susceptibility [89]. Therefore, the focus of this paper is on developing a hybrid PHM degradation model for internal pitting corrosion in pipelines when operational conditions change over time.

This model provides the main input (i.e., estimated degradation level) for condition based maintenance optimization of the pipeline.

The rest of this paper is organized as following. In the next section, related works, approach, and contributions are discussed. Two Bayesian inference methods that are used in this framework are explained afterwards. Then, the problem is defined and the proposed framework is explained by applying that on a case study. The Results section is dedicated to discuss the results and conclusion is the last section of this paper.

4.3 Related work, approach, and contributions

The integrity management of piggable pipelines is commonly performed by using in-line inspection data that are obtained by utilizing a non-destructive tool (e.g., magnetic flux leakage (MFL) or ultrasonic test (UT)) [24]. Maes et al. proposed a hierarchical Bayesian (HB) model based on a gamma process to project pit growth in piggable pipelines [16]. They considered four types of uncertainty in modeling: epistemic uncertainty, spatial heterogeneity, temporal variation, and measurement errors [16]. Zhang and Zhou [13] used Maes model to estimate maximum pit depth ¹ for a gas pipeline in Alberta, Canada. They showed that for 90% of the 62 pits, the absolute difference between the predicted depths and the field measured depths are less than or equal to 10% of the PWT. Zhang et al. [68] extended Maes model by assuming pits' depth growth follow an inverse Gaussian process instead of a gamma

¹Estimation of maximum (vs. mean, etc.) pit depth is the main concern in pitting corrosion literature because the deepest pits are the first that cause leaks [90].

process. By applying this new approach, on the same ILI data-set in [13], they showed that the new results are essentially equivalent to those based on a gamma process. In another work, Zhang et al. [69] again extended the Maes model by using a Bayesian dynamic linear model instead of a gamma process. In this case, they showed that the absolute difference between predicted depth and the corresponding field measurement is less than or equal to 10% of the PWT for about 92% of the pits. To the best knowledge of the authors, the family of hierarchical Bayesian models are the state of the art degradation models for piggable pipelines.

In contrast to the above-mentioned family of models, there is another approach that is applicable for non-piggable pipelines. In this family of models, a generic degradation model is developed for all pits by correlating the maximum pit depth with the operational parameters. One of the most comprehensive internal pitting corrosion degradation model that has been developed based on this approach, is proposed by Ossai et al.[14]. This model correlated eleven operational parameters with the maximum pit depth, by performing a non-linear regression analysis. Ossai model was developed by using ten years recorded pit depth data from UT, and operating parameters data that were obtained via routine quality control procedures. The Ossai model is explained in more details in Synthetic data generation procedure.

These two families of models are hybrid PHM models that combine inspection and measurement data with POF of the pitting corrosion process, by relying on this well-accepted assumption that maximum depth of a pit follows a power function with a positive exponent less than one [2, 63]. The hierarchical Bayesian models rely more heavily on the inspection data, because in these approaches specific inspection data

were available for each individual pit. In contrast, in the generic models, the POF aspect is emphasized by taking into account the different covariates in degradation modeling. However, the data are not pit-specific in this family of models. One contribution of this paper is to propose a hybrid framework that has the advantages of both approaches described above, by considering both specific ILI data of each pit and also the effect of operational parameters on POF in degradation modeling.

Another contribution of this work, as mentioned above, is to consider changes in operational conditions in pitting corrosion degradation modeling. Considering change in degradation rate in condition-based maintenance optimization is addressed in [91] by using online inspection data for one component/item. However, in the case of long pipelines, it is not feasible to install online sensors on all pits to detect change in their degradation rates in order to consider that in maintenance optimization. This paper proposes a novel framework to monitor change in degradation rate (due to change in operational conditions) in the reference pit, and then make a logical and reliable inference about the change in the degradation rate and degradation level of other active pits along the pipeline.

4.4 Bayesian inference methods

The proposed framework is founded on two Bayesian inference techniques: augmented particle filtering and hierarchical Bayesian methods. APF is used to fuse OLI data and estimate the degradation level of the reference pit. A hierarchical Bayesian method is used to fuse ILI data and estimate degradation level of ILI pits

at ILI times. These two methods are discussed in the following sections.

4.4.1 Augmented particle filtering (APF)

Particle filtering (PF) or sequential Monte Carlo method is a technique that uses recursive Bayesian approaches to estimate the state of a dynamic system that changes over time using a sequence of noisy measurements made on the system [92]. Because of its flexible and powerful diagnostic and prognostic features for nonlinear and non-Gaussian systems, application of PF in reliability engineering has increased rapidly in the recent years [37]. PF is able to process data online as it arrives, which is crucial both from the point of view of storage costs and also for rapid adaptation to changing data characteristics [92]. This makes it a proper choice for modeling degradation processes with change in degradation rate.

In order to make inference about a dynamic system using particle filtering, at least two models are required; the process model (Equation 4.1) that describes the evolution of the state with time, and the measurement model (Equation 4.2) that relates the noisy measurements to the state of the system [92].

$$d_j = f_j(d_{j-1}, V_{j-1}) \rightarrow Pr(d_j|d_{j-1}) \quad (4.1)$$

Where d represents the state of the system (in this paper maximum pit depth), f represents a possibly nonlinear process function, j represents the time index, and

V is an i.i.d process noise.

$$y_j = g_j(d_j, \omega_j) \rightarrow Pr(y_j|d_j) \quad (4.2)$$

where y represents the noisy measurement of the state of the system (in this paper measured maximum pit depth), g is a possible nonlinear measurement function, and ω is an i.i.d measurement noise sequence.

In order to infer the posterior density function (pdf) of the state of the system given previous noisy measurements, Bayes' rule can be used according to Equation 4.3.

$$\begin{aligned} Pr(d_j|y_{1:j}) &= \frac{Pr(y_j|d_j)Pr(d_j|y_{1:j-1})}{Pr(y_j|y_{1:j-1})} \\ &\propto Pr(y_j|d_j)Pr(d_j|y_{1:j-1}) \end{aligned} \quad (4.3)$$

In this equation $Pr(y_j|d_j)$ can be calculated by using Equation 4.2 and the prior pdf of the state of the system, $Pr(d_j|y_{1:j-1})$, can be calculated by using Chapman-Kolmogorov Equation:

$$\begin{aligned} Pr(d_j|y_{1:j-1}) &= \int Pr(d_j|d_{j-1}, y_{1:j-1}) \\ &\quad Pr(d_{j-1}|y_{1:j-1})dx_{j-1} \end{aligned} \quad (4.4)$$

Assuming that the measurements are conditionally independent and also assuming first order Markovian property, Equation 4.4 can be simplified as Equation

4.5.

$$Pr(d_j|y_{1:j-1}) = \int Pr(d_j|d_{j-1})Pr(d_{j-1}|y_{1:j-1})dx_{j-1} \quad (4.5)$$

In this integral, the first term can be calculated by using Equation 4.1 and the second term can be calculated recursively forward in time by assuming that the pdf of the initial condition of the state of the system, $Pr(d_0)$, is known. The denominator in Equation 4.3 is a normalizing factor which is independent of the state of the system and usually does not have an analytical closed form solution, and numerical solution is usually computationally expensive. In PF, there is no need to calculate the denominator.

Except for special cases (i.e., linear Gaussian state space models), it is not possible to evaluate the posterior distribution in Equation 4.3 analytically. The key idea in PF is to approximate the posterior density function of the state of the system with a discrete weighted distribution of some random samples (i.e., particles) (Equation 4.6).

$$Pr(d_j|y_{1:j}) \simeq \sum_{p=1}^P w_j^p \delta(d_j - d_j^p) \quad (4.6)$$

In this equation, δ represents the Dirac's delta function, w_j^p represents the normalized weight of the p_{th} particle at the j_{th} time step, and P is the number of particles. In order to perform PF, P number of samples or particles are generated from initial pdf of the state of the system and then at each time step, those particles are evolved by using the process model (prediction step). Subsequently, the measurements corresponding to that time step will be used to update the assigned

weight to each particle (updating step) [92]. Those weights are chosen using the principle of importance sampling [93, 94]. The concept of importance sampling is as following. Suppose $e(d) \propto r(d)$ is a probability density function that is difficult to draw samples from (e.g., posterior distribution of nonlinear non-Gaussian systems in Bayes' rule in Equation 4.3). But we can easily sample from another pdf, $s(d)$, (e.g., a normal distribution). In this case a weighted approximation of $e(d)$ can be obtained by using Equation 4.7

$$e(d) \approx \sum_{p=1}^P w^p \delta(d - d^p) \quad (4.7)$$

Where $w^p \propto \frac{r(d^p)}{s(d^p)}$ is the normalized weight of the p th sample (i.e., particle).

By using this concept, it can simply be proven [92] that the sequence of the assigned weight of particles at each time can be obtained by Equation 4.8.

$$w_j^p \propto w_{j-1}^p \frac{Pr(y_j | d_j^p) Pr(d_j^p | d_{j-1}^p)}{G(d_j^p | d_{j-1}^p, y_j)} \quad (4.8)$$

By using this equation in Equation 4.6, the posterior distribution of the state of the system can be approximated.

In the standard PF, it is assumed that the parameters of the process model are known. However, for most of the practical cases, those parameters are unknown, but the form of the process model is known based on the physics of the process. In that case, augmented particle filtering (APF) can be used to estimate the state of the system and the process model parameters simultaneously. The process model

in APF is shown in Equation 4.9.

$$d_k = f_k(d_{k-1}, \theta_k, V_{k-1}) \rightarrow Pr(d_k | d_{k-1}, \theta_k) \quad (4.9)$$

Where θ represents the vector of the state model parameters.

Kitagawa [95] and Liu and West [96] used a Gaussian random walk to define the evolution model for degradation model parameters to enable their adaptation to new data. It has been identified in [96, 97] that using random walk results in posteriors more diffused than the actual one. To solve this issue, Liu and West [96] proposed a kernel smoothing approach to reduce the variability in the posterior distributions. Following that approach, the posterior distribution of the model parameters can be approximated by Equation 4.10 [96].

$$Pr(\theta_j | y_{1:j}) \simeq \sum_{p=1}^P w_j^p N(\theta_j | \mu_j^p, h^2 \zeta_j) \quad (4.10)$$

Where $N(\cdot | \mu, S)$ is a multivariate normal density with mean μ (Equation 4.11) and variance S . In this equation h is the kernel smoothing parameter, and ζ is Monte Carlo posterior variance.

$$\mu_j^p = h\theta_j^p + (1 - h)\bar{\theta}_j \quad (4.11)$$

Selection of kernel smoothing factor is also a challenge in using APF. Based on the prior knowledge, if the parameters are slowly varying or if they are fixed, the smoothing factor should be set to a small positive value (e.g., $0 < h < 0.2$) to reflect

the steady property of the parameters. On the other hand, when the parameters are expected to change significantly over time, the h value should take a value close to one (e.g., $0.8 < h < 1$) to incorporate the dynamic behavior of the process [98]. The kernel smoothing factor can also be tuned on a validation data-set and then be applied to the future data [98].

In this work, the latter approach is followed. We considered 70% of the OLI data, up to time T , as the validation data-set and we find the optimum h value that gives the minimum RMSE between the online measurements and the predictions of APF.

For the case of pitting corrosion, it is well accepted that maximum depth of a pit follows a power function with a positive exponent less than one (Equation 4.12) [2, 63].

$$d_j = k(t_j - t_0)^\nu \quad (4.12)$$

Where k and ν represent the parameters of pitting corrosion degradation model and t_0 represents the pit initiation time. The recursive format of this model to be used in APF analysis is shown in Equation 4.13. In this equation a white Gaussian noise with mean zero and standard deviation $PM-SD$ is assumed as the state model noise.

$$d_j = d_{j-1} + k\nu(t_j - t_0)^{\nu-1}\Delta t + N(0, PM - SD) \quad (4.13)$$

By considering a general form of the measurement model for an inspection tool,

which includes both the biased and random scattering errors, the actual and measured maximum depth of a pit are related according to Equation 4.14

$$y_{ij} = a_j + b_j d_{ij} + N(0, \epsilon_{ij}) \quad (4.14)$$

Where y_{ij} represents the measured maximum depth of i_{th} pit at the j_{th} inspection ($j = 1, 2, \dots, n$), a_j and b_j are the constant and the proportional biases of the inspection tool employed in the j_{th} inspection, and ϵ_{ij} denotes the standard deviation of normally distributed random scattering error associated with the measured depth of i_{th} pit at the j_{th} inspection. By using Equation 4.14 the measurement model in APF can be derived according to Equation 4.15.

$$Pr(y_{ij}|d_{ij}) = \frac{1}{2\pi\epsilon_{ij}^2} \exp\left(-\frac{(y_{ij} - (a_j + b_j d_{i,j}))^2}{2\epsilon_{ij}^2}\right) \quad (4.15)$$

Using Equation 4.13 and 4.14, the pseudo code in Table 4.1 has been used in this study for APF analysis.

4.4.2 Hierarchical Bayesian method

Another method that is used in this framework is a hierarchical Bayesian method based on a non-homogeneous gamma process [16]. Hierarchical Bayesian modeling is an appropriate method to make scientific inference about a population, based on many individuals, and it is called "hierarchical" because it uses hierarchical or multistage prior distributions [99]. This method is used in this framework to fuse ILLI data of various pits along the pipeline.

```

For  $p = 1:P$ 
  Sample  $d_0^p$  from maximum pit depth prior distribution.
  Sample  $\theta_0^p$  from model parameters prior distributions:
  Normal (prior value, 0.1*prior value).
  Calculate  $\bar{\theta}_0, \text{var}(\theta_0)$ .
  Assign particles' weight:  $w_0^p = 1$ .
End
For  $j = 1$ : Number of OLI data
   $k_j = (1 - h^2)^{0.5}k_{j-1} + (1 - (1 - h^2)^{0.5})\bar{k}_{j-1}$ 
   $\nu_j = (1 - h^2)^{0.5}\nu_{j-1} + (1 - (1 - h^2)^{0.5})\bar{\nu}_{j-1}$ 
  Prediction step
   $d_j^p = d_{j-1}^p + k\nu(t_j - t_0)^{\nu-1} + \text{rand}.N(0, PM - SD)$ 
   $k_j = k_{j-1} + \text{rand}.N(0, h^2\text{var}(k_{j-1}))$ 
   $\nu_j = \nu_{j-1} + \text{rand}.N(0, h^2\text{var}(\nu_{j-1}))$ 
  Updating step
   $w_j^i = w_{j-1}^i \Pr(y_j | d_j, k_j, \nu_j)$ 
  Normalize the weights
  Resample  $d_j, k_j, \nu_j$ 
End

```

Table 4.1: Pseudo code for APF

Since 1975 when the gamma process was introduced in the area of reliability engineering [100], it has been used widely to model degradation processes such as corrosion, wear, and fatigue, which involve monotonically accumulating damage over time in a sequence of tiny increments [3, 82].

A gamma process is a continuous-time stochastic process $\{X(t), t > 0\}$ with the following properties.

- $X(0) = 0$ with the probability 1.
- $\Delta X = X(\tau) - X(t) \sim Ga(\Delta\alpha = (\alpha(\tau) - \alpha(t)), \beta)$ for all $0 \leq t < \tau$
- $X(t)$ has independent increment

Where Ga represents pdf of gamma distribution. A random quantity (in this

study maximum pit depth) has a gamma distribution with shape parameter $\alpha > 0$ and a rate parameter (inverse of scale parameter) $\beta > 0$ if its pdf is given by:

$$f_{X(t)}(x) = Ga(x; \alpha, \beta) = \frac{\beta^{\alpha(t)}}{\Gamma(\alpha(t))} x^{\alpha(t)-1} \exp(-\beta x) \quad (4.16)$$

Where $\Gamma(\cdot)$ denotes the gamma function. The expectation and variance of the gamma process are given in Equations 4.17 and 4.18 respectively.

$$E(X(t)) = \frac{\alpha(t)}{\beta} \quad (4.17)$$

$$Var(X(t)) = \frac{\alpha(t)}{\beta^2} \quad (4.18)$$

According to Equation 4.17 the shape parameter of a gamma process reflects the average trend of the random quantity as a function of time. Therefore, by selecting an appropriate form for the shape parameter of a gamma process, it can model degradation processes with increasing, decreasing, or constant degradation rates. For pitting corrosion process, as it was mentioned previously, a well-accepted format of its degradation model is shown in Equation 4.12. Therefore, in that case, the shape parameter of a gamma process is correlated with the degradation model parameters according to Equation 4.19.

$$\alpha_j = k'(t_j - t_0)^{\nu'} \quad (4.19)$$

Based on this assumption, the increments in degradation level follow a gamma

distribution given in Equation 4.20.

$$\begin{aligned} \Delta d_{ij} = d_{ij} - d_{ij-1} \sim Ga(\Delta\alpha_{ij} = \\ (k'((t_j - t_0)^{\nu'} - (t_{j-1} - t_0)^{\nu'}), \beta_i) \end{aligned} \quad (4.20)$$

When new measurements are available at each inspection time, the posterior distribution of the depth increment of each pit will be updated by using Equation 4.21.

$$Pr(\Delta d_{ij}|Y_i) \propto Pr(Y_i|\Delta d_{ij})Ga(\Delta d_{ij}|\Delta\alpha_{ij}, \beta_i) \quad (4.21)$$

In this equation, the likelihood of the inspection data Y_i given the increments can be written as shown in Equation 4.22 by considering the measurement model that is given in Equation 4.14.

$$\begin{aligned} Pr(Y_i|\Delta D_i) = (2\pi)^{-n/2} \exp(-1/2(Y_i - (A + BS_{\Delta D_i}))' \times \\ \sum_{\epsilon}^{-1} \times (Y_i - (A + BS_{\Delta D_i}))) \end{aligned} \quad (4.22)$$

Where $Y_i = (y_{i1}, y_{i2}, \dots, y_{in})'$, $A = (a_1, a_2, \dots, a_n)'$, B is an n -by- n diagonal matrix with diagonal elements equal to b_j , \sum_{ϵ}^{-1} is the n -by- n diagonal covariance matrix with diagonal elements equal to the variance of the random scattering errors associated with the tool used in inspection time j , and $S_{\Delta D_i}$ is an $n \times 1$ vector with the j th element equal to $\sum_{k=1}^j \Delta d_{ik}$.

The hierarchical Bayesian model that is used to estimate these hyper-parameters $(t_0, p_1, q_1, p_2, q_2, p_3, q_3)$ is shown in Figure 4.1.

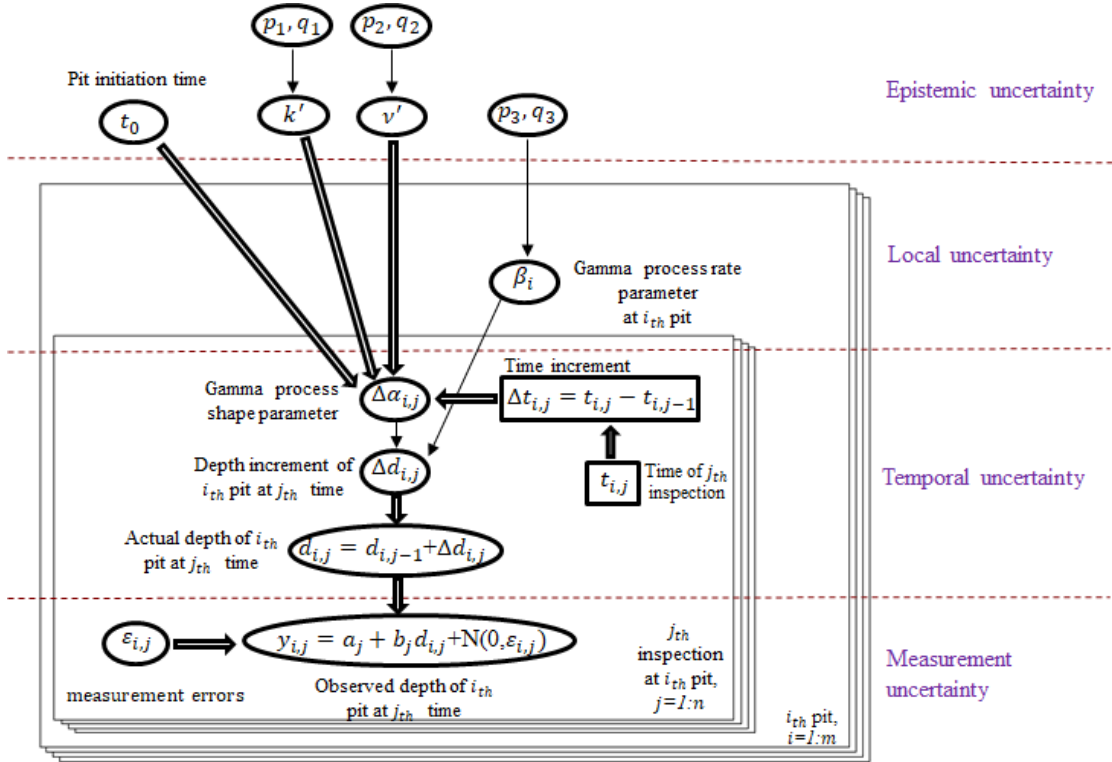


Figure 4.1: Hierarchical Bayesian model based on a non-homogeneous gamma process modified from the approach that is proposed in [16]

4.5 Proposed framework

Consider a long piggable oil or gas pipeline, for which n ILI data sets are available for m number of active pits at times t_1, t_2, \dots, t_n . In addition, an active pit (the reference pit, pit M) is monitored continuously by using an online inspection tool. This pipeline is in operation since time t_0 , which is assumed to be the initiation time for all pits. The operational conditions are monitored and measured as part of the routine operating condition monitoring procedure of the pipelines. The question,

which is addressed in this paper, is how to estimate the maximum depth of the existing pits at time t_{n+1} when the operational conditions change at time T , $t_n < T < t_{n+1}$ and there is no new ILI data for those pits.

In order to answer the above-mentioned question, we propose a data fusion framework that has three phases that are shown in Figure 4.2. The required input data for this framework are shown in the left side of this figure. In phase I, prior values for the degradation model parameters and the standard deviation of the state model noise in APF are estimated for use in phase II and III. In phase II, a similarity index (SI) between pit i ($i = 1, 2, \dots, m$) (an ILI-pit) and pit M (the reference pit) is defined. Finally in phase III by using that SI, some dummy observations are generated and used to estimate the maximum depth of each ILI pit at time t_{n+1} . These phases are explained in more details in the next paragraphs by referring to the steps in Figure 4.2.

4.5.1 Phase I: estimating the standard deviation of the white noise of APF process model (PM-SD) and the prior values for degradation model parameters

In phase I the standard deviation of the process model white noise in APF analysis and also the prior values for degradation model parameters are estimated by using the historical data of operational parameters and corrosion rate of the considered pipeline or pipelines under similar operational condition. Practically, operational parameters are measured by routine monitoring of the pipeline at a

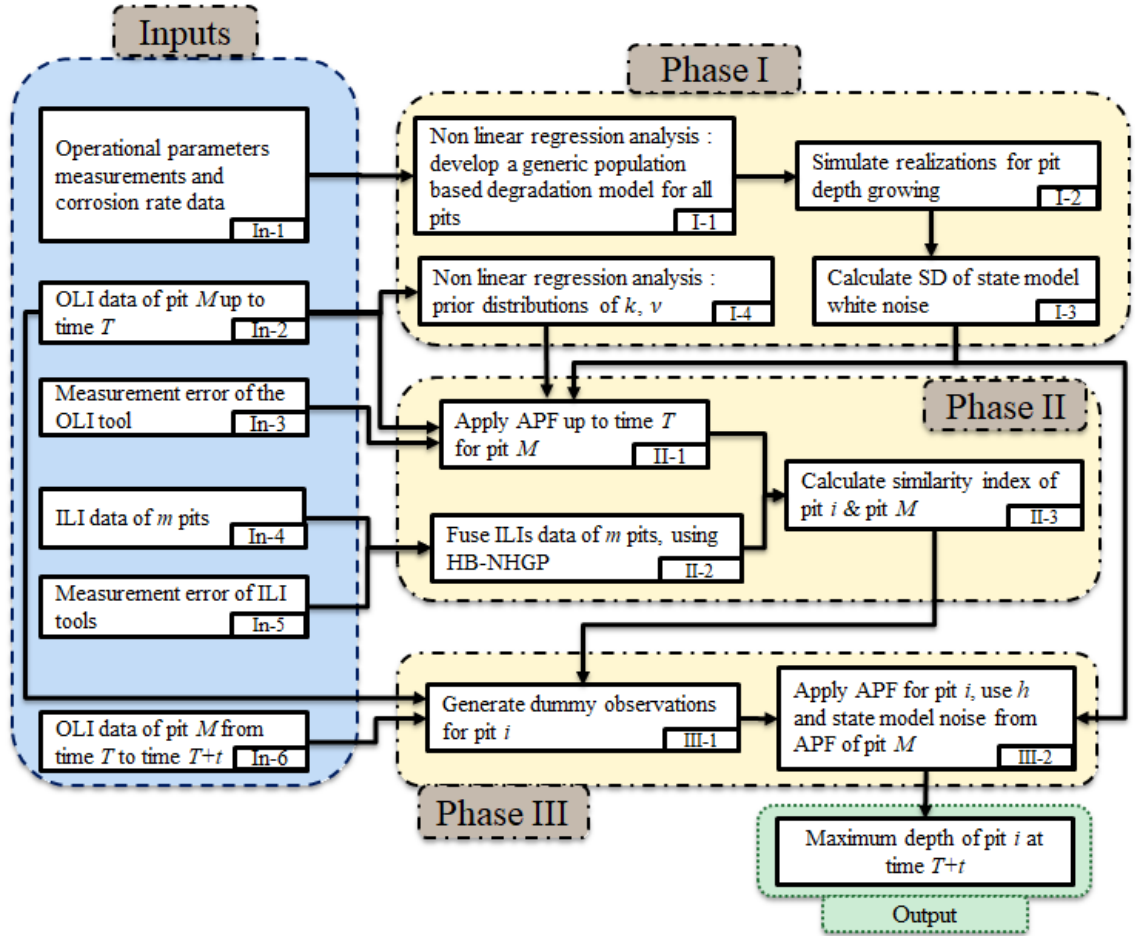


Figure 4.2: Flowchart of the proposed framework

limited number of locations, and it is not feasible to measure them in all locations. However, valuable information about the physics of the corrosion failure mechanism are embedded in those limited data. In this phase, we propose an approach to use those data to estimate the noise of process model in PF. In this way, a generic degradation model (Equation 4.23) is developed for all pits by using a multivariate nonlinear regression analysis (Step I-1), to correlate the average of the maximum pits depth (\bar{d}) with the operational parameters (e.g., pressure, temperature, pH,

etc.) and time.

$$\bar{d}(t) = f(P, T, pH, \dots, t) \quad (4.23)$$

This model is then used to simulate realizations of actual (vs. measured) maximum depth growing behavior for a number of pits (Step I-2). Figure 4.3 shows an example of these realizations. In order to simulate those realizations, at each time interval (Δt), new samples should be extracted from the pdf of each operational parameter (from Step In-1) to be inserted in the developed generic model (Equation 4.23) to obtain the corresponding pit depth increment Δd . This depth increment will be used recursively to simulate those realizations (Equation 4.24).

$$\bar{d}(t) = \bar{d}(t - 1) + \Delta \bar{d} = \bar{d}(t - 1) + \frac{\partial f}{\partial t}(P, T, pH, \dots, t) \Delta t \quad (4.24)$$

In Step I-3, the standard deviation of depth increments is calculated for each pit and then the PM-SD is estimated as the average of those standard deviations of all pits (Equation 4.25).

$$PM - SD = \frac{1}{m} \sum_{i=1}^m STD \text{ of } \Delta \bar{d}_{i,j} \quad (4.25)$$

Where j is the time step index and i is the pit index.

In addition, by using regression analysis on the OLI data up to time T (Step In-2), and fitting a power law function, prior values for the degradation model parameters (k, ν) are obtained in Step I-4.

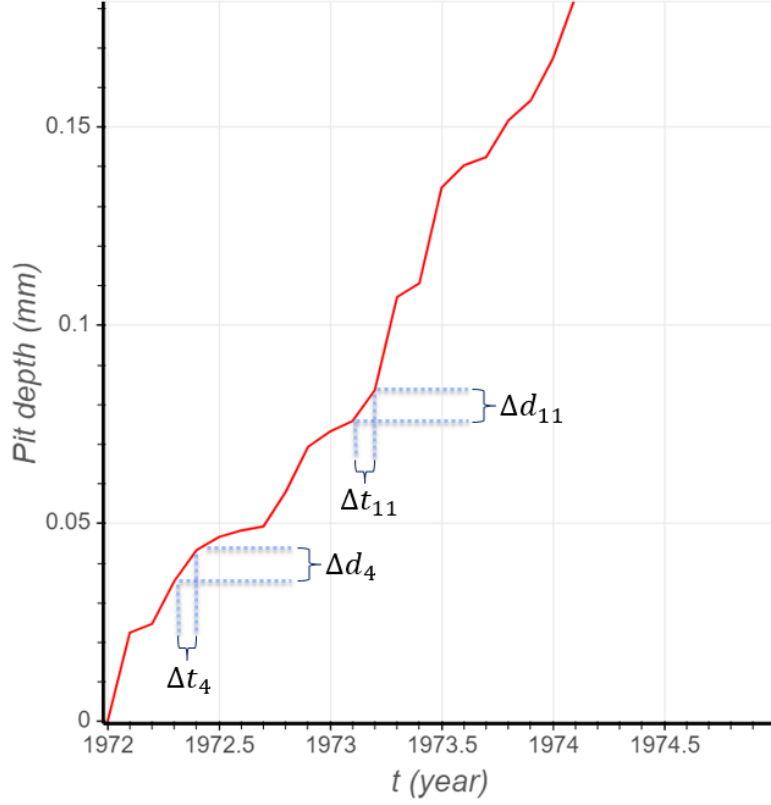


Figure 4.3: A realization of simulated actual maximum pit depth

4.5.2 Phase II: Defining a similarity index between pit i and pit M

In phase II a similarity index (SI) is defined (Step II-3) between each ILI (pit i) and pit M . This SI is defined as a ratio of the estimated maximum pit depth (EMPD) of pit i over EMPD of pit M at ILI times (Equation 4.26).

$$SI(i) = \frac{1}{nP} \sum_{j=1}^n \sum_{p=1}^P \frac{d_{jp} \text{ of pit } i \text{ by HB-NHGP}}{d_{jp} \text{ of pit } M \text{ by APF}} \quad (4.26)$$

Where n is the number of ILI operations and P is the number of particles and p is the particle index.

The denominator is an estimation of the maximum pit depth of the reference

pit M and it is obtained by using APF to fuse the OLI data (Step In-3) of this pit up to time T . In the denominator, d_{jp} is the state of particle p at the j th ILI. The other inputs for APF analysis of pit M are the preliminary estimation of k and ν (Step I-4) and the estimated PM-SD (Step I-3) and the characteristics of the OLI tool (Step In-3).

The numerator of this ratio is estimated by fusing ILI data of all pits, by using the hierarchical Bayesian model based on a non-homogeneous gamma process (HB-NHGP) that is explained in the Hierarchical Bayesian method section (Step II-2). Inputs of this step are ILI data of all pits (Step In-4), and the characteristics of ILI tools (Step In-5), including biased and scattering errors of those tools (a , b and ϵ in Equation 4.14). The output of Step II-2 is an estimate of mean and standard deviation of the posterior distribution of EMPD of each ILI pit. We used Monte Carlo simulation to extract random samples from that posterior distribution to have an estimation corresponding to each particle (d_{jp} in the numerator).

4.5.3 Phase III: Inferring the degradation level of pit i

Finally in phase III, APF is used to estimate maximum depth of pit i at time t_{n+1} (Step III-2) by fusing the generated dummy observations for that pit. Those dummy observations are generated by multiplying the real OLI data of pit M by the corresponding SI of pit i (Step III-1). In this phase, h and PM-SD that were estimated for the OLI pit previously, are used for ILI pits as well, because these two parameters show the stochasticity of a stochastic process at each time and OLI and

ILI pits are exposing to the same corrosion environment at each time.

4.6 Demonstration of the proposed framework

In this section, the proposed framework is demonstrated in a case study. Consider a long oil or gas pipeline (e.g., 50 miles length) in operation since 1972. This pipeline is inspected by ILI, ultrasonic test, in years 2000, 2005, 2010, and 2015. A number of active pits are detected and monitored at those times. After the first ILI, an OLI sensor is installed to monitor the degradation behavior of an active pit (the reference pit) continuously. The operational conditions change causing change from moderate to severe corrosion condition in 2015. The goal is to estimate the maximum depth of ILI pits in 2020 when there is no new ILI data available, by inferring from OLI data of the reference pit.

4.6.1 Performing phase I of the proposed framework

In practice input data given in Steps In-2, In-4, and In-6 from Figure 4.2 should be gathered from ILI and OLI of the pipeline. These input data can hardly be found altogether in the existing literature for a pipeline. Therefore, we used the model that was developed in [14] as the starting point (output of Step I-1) to generate synthetic actual (vs.measured) depths in Step I-2. We added random measurement noise to those synthetic actual depths to generate synthetic ILI and OLI data for this case study. The characteristics of the inspection tools that are given in [13] are used in Steps In-3 and In-5. This synthetic data generation procedure is explained

Param.	Units	Description	Best fit dist.	Original dist. parameters	Modified dist. parameters
				Scale, Shape	Scale, Shape
T	C	Temperature	Lognormal	3.72, 0.4052	3.35, 0.12
Pc	MPa	CO ₂ partial pressure	Weibull	0.1598, 1.2797	0.065, 1.25
pH	-	pH	Extreme value	7.9418, 0.4747	8.2, 16.5
S	MgL ⁻¹	Sulphate ion	Weibull	38.9576, 0.4052	40.5, 1.5
C	MgL ⁻¹	Chloride ion	Weibull	3613.8, 1.3	1413.8, 1.5
W	-	Water cut	Lognormal	-1.7178, 1.4696	3.15, 0.8
r	Pa	Wall shear stress	Lognormal	3.447, 0.9151	3.447, 0.9151
Gs	m ³ day ⁻¹	Gas production rate	Extreme value	335310, 120120	335310, 120120
OL	m ³ day ⁻¹	Oil production rate	Weibull	136.33, 2.1145	136.33, 2.1145
Wt	m ³ day ⁻¹	Water production rate	Weibull	94.9241, 0.4847	94.9241, 0.4847
Pt	MPa	Operating pressure	Extreme value	8.1274, 3.2704	8.1274, 3.2704

Table 4.2: Best fit distribution of the operational parameters [14] and modified values for moderate corrosion rate category

in more details as following.

4.6.1.1 Synthetic data generation procedure

We reviewed different pitting corrosion degradation models [15] and among them we used a model that was developed by Ossai, Boswell, and Davies [14], as the output of Step I-1. This model is chosen because it has been developed based on the field data (rather than experimental data) and to the best of our knowledge, that model is the most comprehensive available generic internal pitting corrosion degradation model in the literature, that correlates eleven covariates (Table 4.2) with the average maximum pit depth over time. This model has been developed by using ten years of measurement data from sixty X52 pipelines that were used for oil and gas pipelines in Nigeria. Ossai et al. carried out multivariate regression

Estimate	Coefficients (γ_q)	Standard error	t Stat	P-value
Log(T)	0.037	0.083	0.4465	0.6616
Log(Pc)	-0.014	0.0373	-0.3745	0.7133
Log(pH)	-0.8446	0.7418	-1.1386	0.2727
Log(S)	-0.0033	0.0835	-0.0392	0.9692
Log(C)	0.0613	0.0494	1.2388	0.2345
Log(W)	0.042	0.0337	1.2463	0.2318
Log(r)	0.0037	0.0433	0.0857	0.9329
Log(Gs)	-0.0467	0.0554	-0.8441	0.4119
Log(OL)	-0.0002	0.0657	-0.0037	0.9971
Log(Wt)	-0.0076	0.021	-0.3621	0.7223
Log(Pt)	-0.0142	0.0488	-0.2915	0.7746
Intercept γ_0	0.44	0.7572	0.5811	0.5698
Log(t)	0.8032	0.0458	17.5346	0

Table 4.3: Parametric estimate for power model development [14]

modeling to develop this model which is shown in Equation 4.27.

$$\bar{d}(t) = k(t - t_0)^\nu = \exp(\gamma_0 + \sum_{q=1}^Q \gamma_q V_q)(t - t_0)^\nu \quad (4.27)$$

Where \bar{d} represents the average maximum pit depth, t represents time of evaluation, k and ν are the power law model parameters, t_0 is the pit initiation time (Ossai et al. assumed that pit initiation time is equal to the operation initiation time for all pits), γ_0 represents the intercept, γ_q represents the mean value of the regression coefficient (Table 4.3) of the q_{th} operational parameter, V_q represents q_{th} operational parameter (Table 4.2), and Q represents the number of operational parameters.

Considering natural log of the mean value of the operational parameters and the mean value of the estimated regression coefficients in Equation 4.27, the average

maximum pit depth is determined by using Equation 4.28 [14].

$$\bar{d}(t) = 0.732 t^{0.803} \quad (4.28)$$

We used this model as the degradation model for time $t > T$, ($T = 2015$ in this case study). For time $t < T$ (from 1972 to 2015) we used the model that has been developed for moderate corrosion rate category in [17] (Equation 4.29).

$$\bar{d}(t) = 0.269 t^{0.741} \quad (4.29)$$

Since the best fit probability distribution of the operational parameters for the moderate corrosion rate category are not given in [17], we modified the scale and the shape parameters of the distributions that are given in Table 4.2, to have approximately the same mean and standard deviation that are given for moderate corrosion rate category in Table 1 of [17] (Both [14] and [17] are based on the same data set). These modified values are given in the last column of Table 4.2. We used Monte Carlo simulation to sample from the distributions of the operational parameters that are given in Table 4.2.

In addition, the variation in the estimated coefficients of the degradation model is also taken into account in the synthetic data generation by considering the given standard errors. The details are given in the following pseudo code.

In this pseudo code (Table 4.4), `std.N.rand` is a positive random number generated from the standard normal distribution. `DOF` is the degree of freedom of the student's t-distribution which is equal to the number of samples minus one, minus

<p>For $i = 1: m$ (m, number of pits = 100 in this study) $d_{i,0} = 0$ For $j = 1$: No. of time steps Generate $V_{q,i,j}$ by Monte Carlo simulation (using the distribution parameters in Table 4.2). Generate $\gamma_{q,i,j} = \gamma_q$ (given in Table 4.3) + $t.\text{inv}(\text{std.N.rand}(i,j), \text{DOF}) \times$ corresponding standard error given in Table 4.3. $\bar{d}_{i,j} = \nu \times \exp(\gamma_0 + \sum_{q=1}^Q \gamma_{q,i,j} V_q) \times t^{\nu-1}$. $\Delta \bar{d}_{i,j} = \bar{d}_{i,j} - \bar{d}_{i,j-1}$. End End</p>

Table 4.4: Pseudo code for synthetic data generation

number of parameters (in this case eleven). According to [17], number of samples is more than 70 and 300 for moderate and severe corrosion rate categories respectively. Therefore DOF is more than 30, for both cases. Which means student's t-distribution can be approximated by a standard normal distribution [101] and DOF does not play an important role in sampling process.

Additionally, in order to take into account the temporal variation of corrosion process, we sampled from the parameters and the coefficients distribution every 0.1 year (Δt in Figure 4.3). We assumed that there are 100 pits on this pipeline. This pit density is selected based on examples in the literature (e.g., 62 pits in 80 km [13], 554 pits in 129 km [102], 1 pit per km [29]). These examples show that the pit density is a small number and we can reasonably assume that the pits are not interacting each other. However, in case of interaction between pits, the common practical and conservative approach can be used which is to coalesce the adjacent pits by following available codes (e.g., DNV RP-F101 [103]) and considering the

	First ILI	Second ILI	Third ILI	Fourth ILI	OLI
<i>a</i>	2.04% PWT	2.04% PWT	-15.28% PWT	-10.38% PWT	0
<i>b</i>	0.97	0.97	1.4	1.13	1
ϵ	5.97%PWT	5.97%PWT	9.05%PWT	7.62%PWT	2.0%PWT

Table 4.5: Constant (a) and proportional (b) biased error and scattering error of inspection tools [13]

composite pit in this framework.

Having this synthetic data, an estimation for the standard deviation of the white noise of the state model in APF is calculated by using Equation 4.25.

In order to generate ILI data (Step In-4 in Figure (4.2)), the measurement error of ILI tools are added to the synthetic data according to Equation 4.14. We used the same equation to consider measurement error in generating OLI data for the reference pit (Steps In-2 and In-6) by using characteristics of the OLI tool. This information for each ILI tool and also the OLI tool is given in Table 4.5. We assumed that the scattering error is independent and identically distributed for each pit at each time and it follows a white noise with mean value equal to zero and standard deviations ($\epsilon_{i,j}$) that are given in Table 4.5 for ILI and OLI tools.

Figure 4.4 shows an example of synthetic actual and measured maximum pit depth for the OLI and an ILI pit. This figure shows that the frequency of the OLI data is higher than the frequency of ILI data. In addition, the measurement error of OLI tool is smaller than the measurement error of ILI tool.

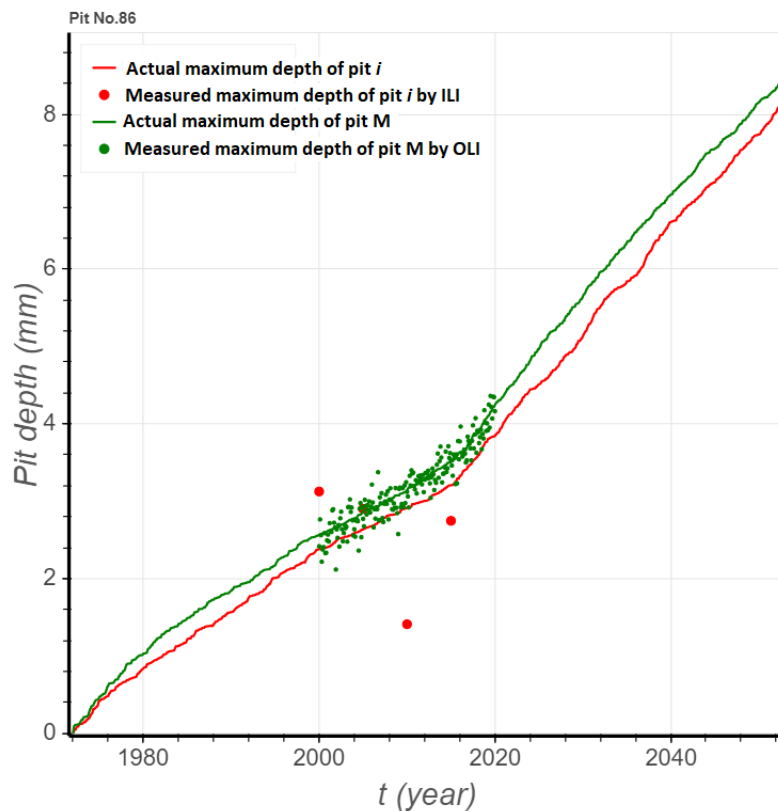


Figure 4.4: Generated synthetic data for an OLI and an ILI pit

4.6.2 Performing phase II of the proposed framework

The assumptions on phase II for this case study are as following. In Step II-1, 10,000 particles are randomly selected to approximate the posterior distributions of the maximum depth and the degradation model parameters by APF. In order to select a proper value for h (kernel smoothing factor), we used 70% of OLI data up to time T (i.e., 2015 in this case) as the training data set for APF, and then we found the optimal value of h which gives the minimum RMSE between the predicted value by APF and the measured maximum pit depth by online inspection for the test data set (e.g., remaining 30% of the OLI data). Based on this approach the selected h value for this case study is 0.01. We also assumed that degradation model

parameters follow normal distributions with mean values that obtained in Step I-4 (e.g., we used 0.23 and 0.73 for a seed number) and standard deviation equal to 0.1 of the corresponding mean value. In addition, the PM-SD of process model noise is obtained in Step I-3 (e.g., we used 0.008 for a seed number).

In Step II-2 the posterior probability distribution of maximum depth of ILI pits at ILI times are obtained. In this step, a gamma distribution with shape and scale parameters equal to ten and one, is selected as the prior distribution for k . The same assumption has been made for ν and β_i with the shape and scale parameters both equal to one [13]. The generated synthetic ILI data of 100 pits are used as the evidence in the hierarchical Bayesian analysis to update the posterior distributions of the maximum pit depth (d). We employed the Markov chain Monte Carlo simulation technique by using the software OpenBUGS for this analysis. Since this model is a multi-parameter model, we run two chains, starting at two different points to decide when convergence to the posterior distribution has occurred [99]. For each chain 100,000 simulation sequences were generated and 10,000 sequences were discarded as the burn in period. A thinning interval of 10 was selected to reduce the auto-correlation between the samples.

In Step II-3, by having estimations of maximum depth of ILI and OLI pits from Steps II-1 and II-2, a similarity index between each ILI and the reference pit is defined by using Equation 4.26.

4.6.3 Performing phase III of the proposed framework

Finally in Step III-2, the posterior distribution of maximum depth for each ILI pit at 2020 is estimated by following the given APF pseudo code in Table 4.1 and using dummy observations of each in-line inspected pit. Those dummy observations were generated in Step III-1 following the procedure that is explained in Phase III. The results of this case study are discussed in the next section.

4.7 Results

In this section, the results of APF analysis in estimation of maximum depth for the OLI-pit is discussed first. Then, the performance of this framework is validated by comparing its results with the results of Maes model, assuming there is no change in operational conditions. Finally, assuming the operational conditions change at time T (i.e., 2015 in this case), from moderate to severe corrosion rate category, we illustrate the effects of considering this change (and using this framework) on pipeline degradation level estimation.

Figure 4.5 shows the estimation of the model parameters for the reference pit by using APF, when the operational conditions are the same during pipeline life-cycle. This figure depicts that approximately seven years after the first inspection, when there is enough data to update the posterior distribution of the model parameters, the variation of the model parameters reduces and they converge to constant values that can be used for prognostic purposes.

Figure 4.6 shows the estimated maximum depth of pit M by using APF. Ac-

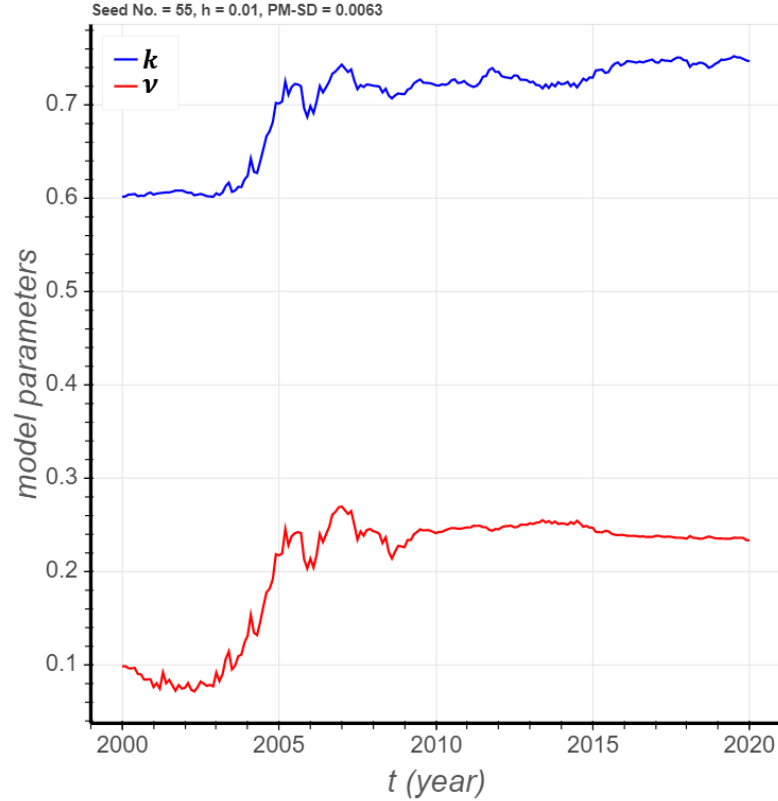


Figure 4.5: Estimated model parameters for the reference pit by using APF for a random seed number

According to this figure, between years 2000 to 2020, that OLI data are available, there is no significant error in maximum pit depth estimation. After 2020, as it was expected for particle filtering method, the estimation error increases over time because of lack of new inspection data. However, even after 2020, the actual maximum pit depth is within the lower and upper bounds of this estimation. Figures 4 and 5 indicate that APF is an appropriate method to estimate maximum pit depth, when online inspection data are available.

In order to validate the performance of this framework we defined two metrics. The first validation metric (Metric R) is the RMSE of maximum pit depth prediction at 2020 (Equation 4.30). This RMSE should be less than or almost equal to the

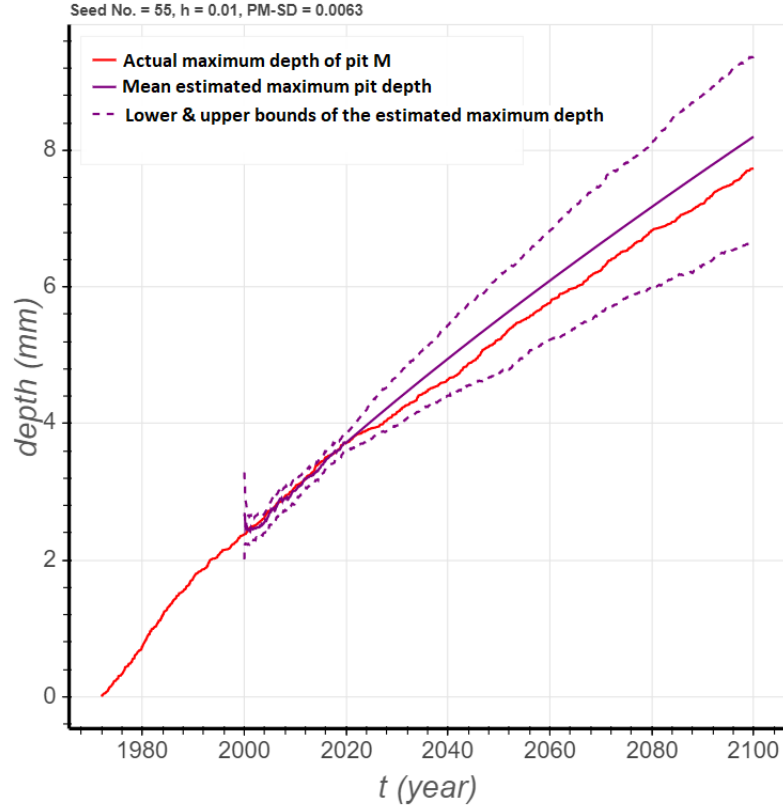


Figure 4.6: Estimated maximum depth of the reference pit by APF

RMSE of Maes model. The second validation metric (Metric N) is the percentage of all pits that their predicted depths fall within the $\pm 10\%$ of their actual maximum depth. The $\pm 10\%$ PWT is commonly used in the pipeline industry as a confidence interval for the accuracy of the inspection tools [13] and we modified that in this work as a metric for accuracy of the prediction. This metric should be greater than or equal to the one for Maes model. The second metric is defined because a pipeline is a series system and failure at each location (i.e., pit) is equal to the failure of the whole pipeline [104, 105]. Therefore having smaller RMSE, does not necessarily mean that the proposed framework has a better performance. It might be the case that the estimation errors of a few pits are so small that it causes decrement in the

Seed No.	Metric R(mm), Maes	Metric R(mm), Framework	Ratio	Metric N(%), Maes	Metric N(%), Framework
1653	0.324	0.308	0.951	72	75
251	0.331	0.308	0.930	69	77
2652	0.337	0.293	0.870	61	73
5412875	0.352	0.352	1.000	68	67
93	0.291	0.365	1.259	78	69
...
3987	0.288	0.288	0.997	79	78
Average	0.316	0.318	1.010	74	75

Table 4.6: Comparing the results in case of no change in operational conditions

RMSE, but for the majority of the pits, the estimation error have increased. Hence, both of these metrics should be satisfied to conclude that the performance of the proposed framework is at least as good as the performance of Maes model when the operational conditions do not change.

$$RMSE = \left(\sum_{i=1}^m \frac{(d_i - y_i)^2}{m} \right)^{0.5} \quad (4.30)$$

Figure 4.7 and 4.8 depict two examples of the estimated maximum depth at 2020 for two ILI pits by using this framework and Maes model. The SI are 0.98 and 1.17 for pit No.29 and pit No.53 respectively. According to Figure 4.7, for pit No.29 the estimation error of this framework is less than the estimation error of Maes model and according to Figure 4.8, for pit No.53 it is vice versa. In order to quantify the estimation error for all pits to compare the performance of Maes model and this framework, the RMSE for both models is calculated. The results for some random seed numbers are given in Table 4.6. As shown in the table, the

ratio of the RMSE of this framework over the RMSE of Maes model is around one for all seed numbers (30 seed numbers) and the average of that ratio for all seed numbers is 1.010. With respect to Metric N, on average for 73.6% and 74.9% of pits, for Maes model and this framework respectively, the predicted depth is within the $\pm 10\%$ of the actual maximum pit depth. These metrics indicate that when there is no change in operational conditions, the performance of this framework is similar to the performance of Maes model as a validated state of the art pitting corrosion degradation model for piggable pipelines.

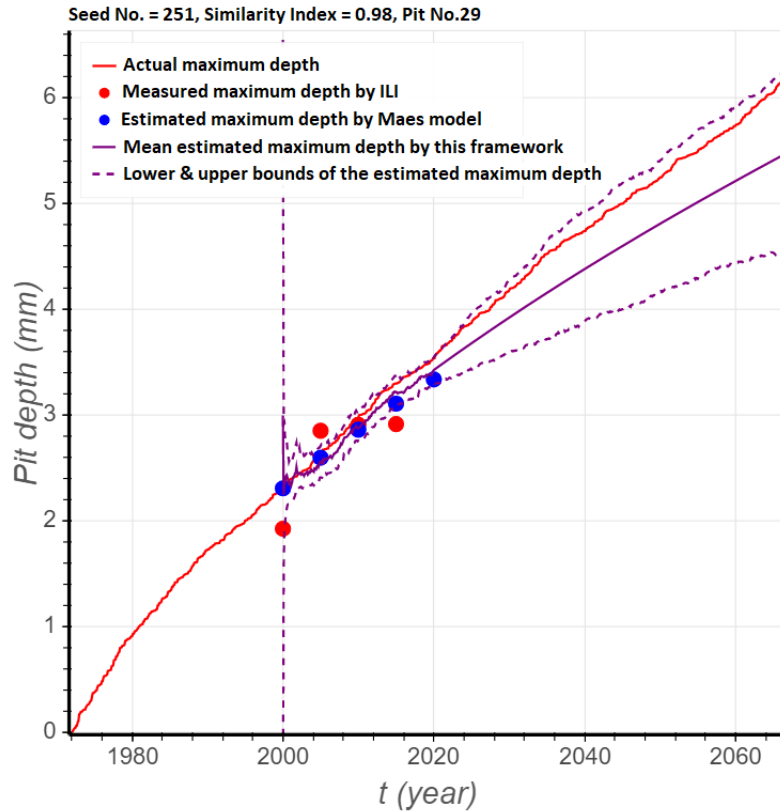


Figure 4.7: Estimated maximum depth of pit No.29 by this framework and Maes model, without change in operational conditions

Relying on the validation results, we used this framework to estimate maximum pit depth at year 2020 when operational conditions change at 2015. Figure

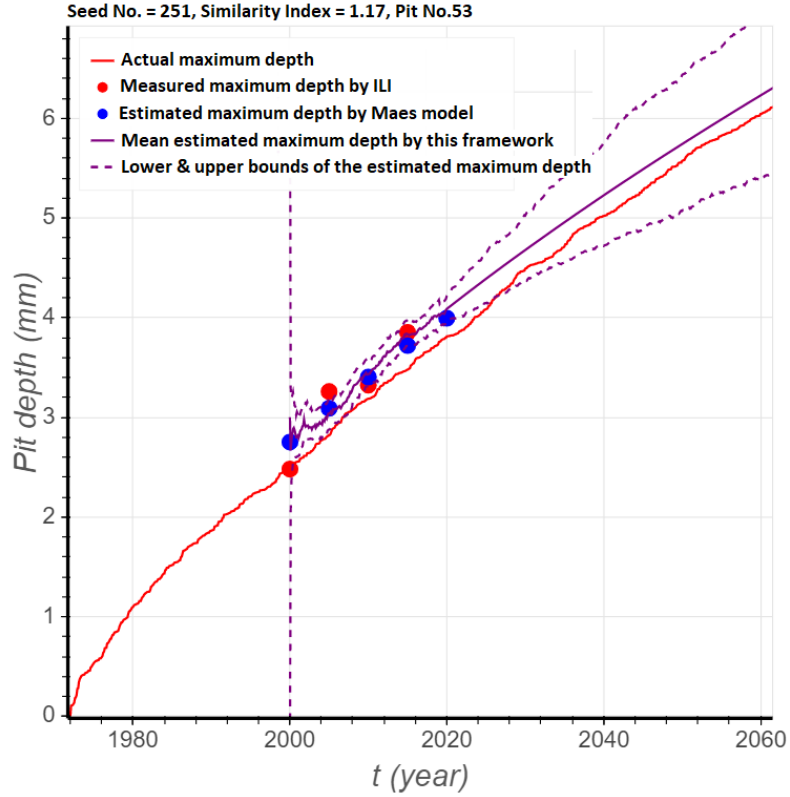


Figure 4.8: Estimated maximum depth of pit No.53 by this framework and Maes model, without change in operational conditions

Seed No.	Metric R(mm), Maes	Metric R(mm), Framework	Ratio	Metric N(%), Maes	Metric N(%), Framework
1653	0.631	0.344	0.545	31	73
251	0.596	0.407	0.683	40	67
2652	0.599	0.328	0.549	29	73
5412875	0.543	0.391	0.718	44	69
93	0.612	0.367	0.601	27	77
...
3987	0.519	0.322	0.621	42	75
Average	0.556	0.334	0.634	39	75

Table 4.7: Comparing the results in case of considering change in operational conditions

4.9 and 4.10 are two examples of the maximum pit depth estimation for pit No.50 and pit No.31 respectively. Pit No.50 is an example that shows when operational

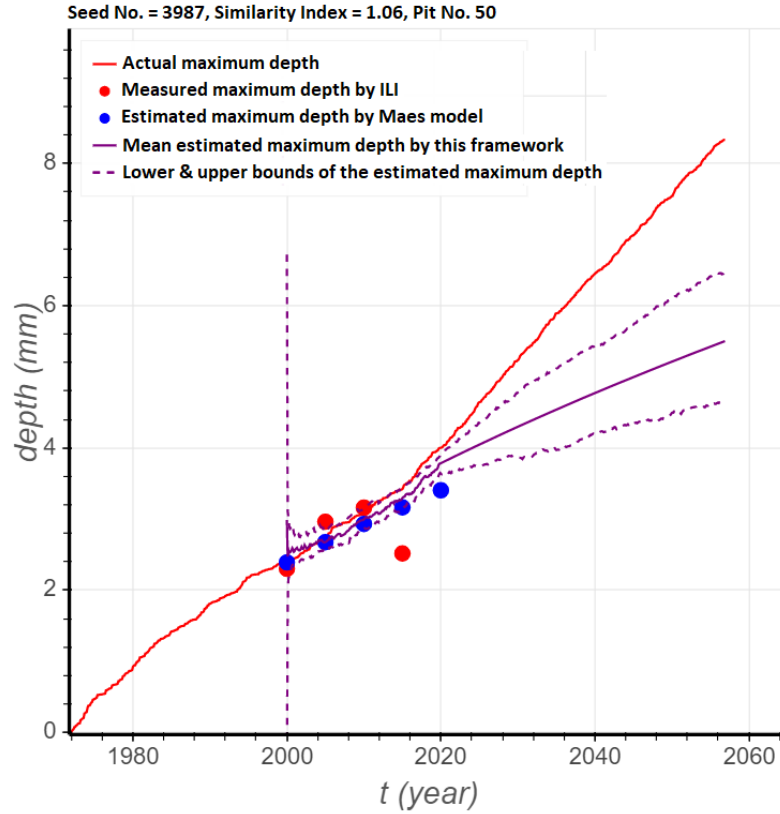


Figure 4.9: Estimated maximum depth of pit No.50 by this framework and Maes model with change in operational conditions

conditions change, using this framework decreases the estimation error, however, the opposite is true for Pit No.31. In order to compare the estimation error for all pits, Metrics R and N are given in Table 4.7, for both methods and for some example seed numbers. For example for seed number 3987, the RMSE of Maes model is 0.519 and for this framework it is 0.322. Which means the RMSE of this framework is 62% of the RMSE of Maes model, that is a significant improvement in accuracy of maximum pit depth prediction. As it was mentioned before, this metric is necessary but not sufficient to conclude that there is an improvement in degradation level estimation for the whole pipeline. Metric N must also be considered. As it is shown in Table 4.7, for seed number 3987, Metric N is 42 for Maes model and it is 75 for

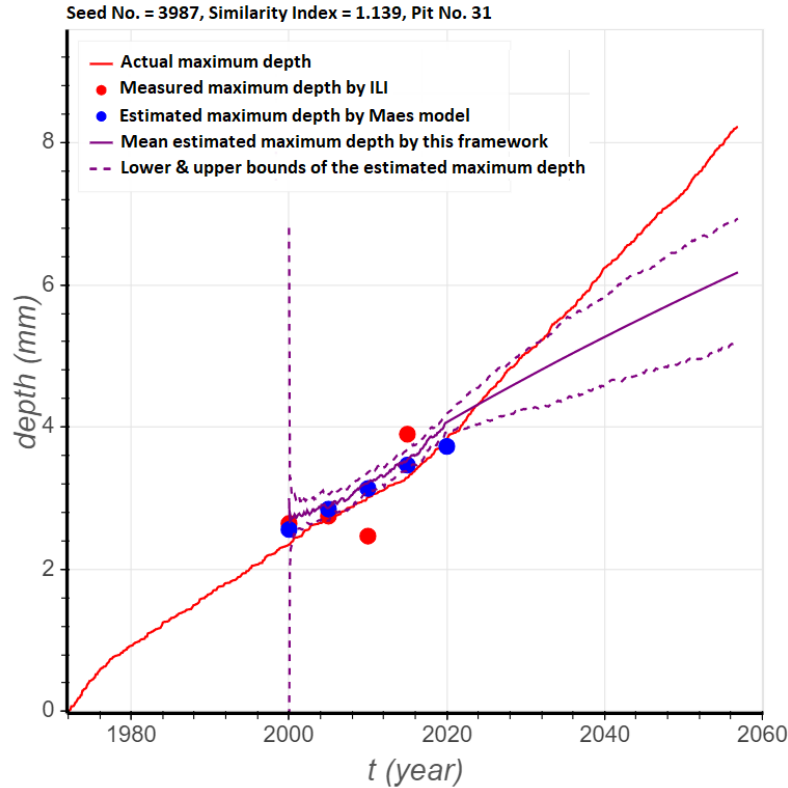


Figure 4.10: Estimated maximum depth of pit No. 31 by this framework and Maes model with change in operational conditions

this framework. This means that for seed 3987, out of 100 pits, the Maes model prediction for 42 of them is within $\pm 10\%$ of their actual maximum depth, whereas our framework is accurate for 75. The average of these two metrics for all seed numbers are also given in Table 4.7. According to this table, on average, by using this framework the RMSE is 40% lower than the RMSE of using Maes model when there is change in operational conditions. In addition, for 75.5% of the pits, the predicted maximum depth is within $\pm 10\%$ of their actual maximum depth for this framework in comparison to 39.4% of the pits for Maes model. These results show a significant improvement in maximum pit depth prediction that leads to avoiding either unnecessary maintenance or unpredicted failures.

It is worth noting that when there is a change in operational conditions, going forward in time, even for the proposed framework, prediction error increases significantly because there is not enough observations to update and learn the model parameters properly. However, this error will be reduced by implementing future OLI and ILI inspections.

4.8 Conclusion

In this work, a novel data fusion framework is proposed to develop an internal pitting corrosion degradation model for oil and gas pipelines when operational conditions change over time. The change in operational conditions is taken into account by monitoring the change in degradation level of an active pit (the reference pit) and accordingly inferring about the change in degradation level of other active pits. This framework consists of three phases. In phase I, historical data of the considered pipeline or pipelines with similar operational conditions, are used to develop a generic degradation model for all pits. This model is used to generate synthetic actual maximum pit depth realizations for a number of pits. The standard deviation of the white noise that is used in process model in APF is extracted from these synthetic data. In addition, at this phase, prior values for degradation model parameters are obtained by performing a nonlinear regression analysis on the OLI data of the reference pit. In phase II, a similarity index between each ILI pit and the reference pit is calculated as a ratio of the estimated maximum depth of the ILI pit (by using a hierarchical Bayesian method based on a non-homogeneous gamma

process) and the estimated maximum depth of the reference pit (by using APF) at ILI times. In Phase III, dummy online observations are generated for each ILI pit by multiplying its similarity index with the OLI data of the reference pit. Then those dummy observations are used in APF to estimate the maximum depth of ILI pits when there is no new ILI data.

The application of this framework is discussed by using this framework on a number of pits and the results are compared with the results of a state of the art degradation model (Maes model), that has been validated by real field data and is available in the literature. Two metrics are used to compare the results of this framework with the results of the Maes model. The first metric is Metric R which is the average of RMSE between actual and predicted maximum pit depth for all seed numbers. This metric is necessary but not sufficient to compare the performances of this framework and the Maes model. The reason is that, it is possible that the estimation errors of a few pits are so small that it causes decrement in the RMSE, but for the majority of the pits, the estimation error have increased. We defined the second metric, Metric N, as the percentage of all pits that the corresponding predictions are within $\pm 10\%$ bounds of their actual maximum depth.

When there is no change in operational conditions, in terms of Metric R, the results are approximately the same for the new framework and the Maes model (i.e., on average of approximately 0.31). In addition, on average for 73% of all pits, for both this framework and Maes model, the predicted depth is within the $\pm 10\%$ bounds of their actual maximum pit depth (Metric N).

We also conduct this validation on case study with a change in operational

conditions. Based on the presented results, by considering change in operational conditions and using this framework, Metric R, the RMSE, would be approximately 60% of the RMSE of the Maes model which is a significant improvement in maximum pit depth prediction. In addition, in the case of change in operational conditions, the predicted depth of 75.5% of pits are within the $\pm 10\%$ of their actual maximum pit depth by using this framework. This number is 39.45% for Maes model. In the other words, this framework provides 91% improvement with respect to the number of pits with a high confidence level estimation. These results show that when there is a change in operational conditions, using the proposed framework resulted in decrease in the prediction error for the majority of the pits. These improvements enable avoiding either unnecessary maintenance or unpredicted failures.

In the next step of this research, we will use the results of this paper to estimate the probability of occurrence of different failure modes (i.e., small leak, large leak and rupture) in a pipeline segment and then define an optimal maintenance policy which takes into account the cost of each failure mode and also the cost of different maintenance actions (i.e., do nothing, sleeving, and replacement). That optimal policy will include the optimal maintenance action and time for each segment and also the optimal next ILI time for the whole pipeline.

Lack of the real field corrosion inspection data is a big challenge in PHM of the oil and gas pipelines. Hence, it is highly recommended that oil and gas pipelines' owners and pipeline operating companies collect the operational conditions and inspection data and make them available in the public domain to make it possible for the researchers to validate their new corrosion degradation models that finally leads

to the decrease in the number of unexpected failures and unnecessary maintenance.

Chapter 5: Development of a hybrid population-based degradation model for a pipeline segment with high pit density

5.1 abstract

This paper presents a novel algorithm to develop a population-based pitting corrosion degradation model for pigged oil and gas pipelines. The algorithm is developed to estimate and predict the distribution of actual depth of the existing pits on a pipeline segment, given two or more sets of ILI data that have uncertainty in size and number of the detected pits. This algorithm eliminates the need for a defect-matching procedure that is required in developing defect-based pitting corrosion degradation models. A hierarchical Bayesian model based on a non-homogeneous gamma process is developed in this paper to fuse the uncertain ILI data and POF knowledge of pitting corrosion process. Measurement error, POD and POFC are addressed in the developed algorithm. The application of the developed algorithm is demonstrated by implementing it on a case study and the results are compared with the simulated data from a generic degradation model that is available in the literature.

Symbol	Description	Unit
a	Constant biased error	
b	Proportional biased error	
c	Pit initiation time index, 1 for those pits that are initiated before ILL_1 , 2 for those that are initiated between ILL_1 and ILL_2 , ...	
d	Maximum pit depth	mm
d_{ijc}	Actual depth of a truly detected pit i at t_j with the pit initiation time's index c	mm
d_d	Minimum detection threshold depth of the inspection tool	mm
h	Bin index	
H	Number of bins of a histogram	
i	Pit index	
j	ILI time index	
k	Parameter of the power law model	mm
m_j	Number of detected pits at ILL_j at t_j	
m_{jc}	Number of detected pits at ILL_j that have been initiated at time t_{c-1}	
m'_{jc}	Expected number of detected pits at ILL_j that have been generated at time t_{c-1}	
M_j	Actual number of existing pits at t_{c-1} , $M_0 = 0$	
M_{jc}	Actual number of existing pits at ILL_j that have been initiated at time t_{c-1}	
n_h	Number of pits in bin h	
t_0	Pit initiation time	year
t	Time	year
t_j	Time of ILL_j	
t_{c-1}	Pit initiation time	
x_{ijc}	Actual depth of an existing pit i at t_j with the pit initiation time's index c	mm
y	Measured maximum pit depth	mm
y_{ijc}	Measured depth of a truly detected pit i at t_j with the pit initiation time's index c	mm
y_c	Mean credible measured depth of the inspection tool	mm
y'	Predicted value for the measured depth of a pit	mm
n_h	Number of pits in bin h	
ν	Exponent of the power law model	
θ	Vector of degradation model's hyper-parameters k, ν, β	
α'_{jc}	Shape parameter of the gamma process at time t_j for those pits that have been initiated at time t_{c-1} by using k, ν that have been estimated based on the inspection data at $ILL_1, ILL_2, \dots, ILL_{j-1}$	
α_{jc}	Shape parameter of the gamma process at time t_j for those pits that have been initiated at time t_{c-1} by using k, ν that have been estimated based on the inspection data at $ILL_1, ILL_2, \dots, ILL_j$	

Table 5.1: Nomenclature

Symbol	Description	Unit
ϵ	Random scattering error	mm
β	Scale parameter of the gamma process	
Actual depth	Synthetic actual depth of a pit without measurement error	mm
Estimated depth	An estimation of the synthetic actual depth of a pit	mm
Measured depth	Synthetic measured depth of a pit with measurement error	mm

Table 5.2: Nomenclature (Cont.)

5.2 Introduction

Having a high confidence estimation of pipelines' degradation level plays an important role in pipeline integrity management. Estimated degradation level is the main input for time to failure or remaining useful life estimation and subsequently condition-based maintenance optimization of the pipelines. In this way, taking into account all potential failure mechanisms is necessary. Among different potential failure mechanism of pipelines, pitting corrosion is one of the main concerns because of the high rate at which pits can grow [2] and cause unpredicted failures, that may impose a huge cost to the industry and environment, or unnecessary maintenance. Hence, in terms of the failure mechanism, the scope of this paper is on pitting corrosion process.

In terms of the investigated system, the scope of this paper is on piggable pipelines which approximately includes fifty percent of the pipelines under operation all over the world [1]. The so-called piggable pipelines are those that their diameter, geometry, operating condition, product, etc., do not limit the use of available commercial smart pigs (in-line inspection (ILI)) for their inspection. The ILIs of pipelines are commonly based on a MFL or UT techniques [85] and those re-

ports contain the measured maximum depth of the detected pits after processing the raw collected data (i.e., MFL or UT signals) which have uncertainty in the pit depth measurement (i.e., ME) and number of pits (i.e., POD and POFC) [106]. Despite significant advancement in the smart pigs technologies and the continuous improvement in their accuracy, their measurements still include of different types of uncertainty including measurement error in sizing, probability of not detecting some of the existing defects, and false call (false positive) for some defects that do not exist [107]. In order to address those types of uncertainty in pitting corrosion degradation modeling, two categories of algorithms are developed in the literature: defect-based and population-based.

The defect-based algorithms, in which the results of sequential ILI of each individual pits are used to evaluate the growing pattern of that pit, are more common in literature. In those algorithms, it is essential to match the results of sequential ILIs based on the location of the pits. Assuming that matched ILI data sets are available, Maes and Dann [16] proposed a defect-based hierarchical Bayesian (HB) model to estimate the degradation level of oil and gas pipelines due to localized corrosion. To address the temporal stochasticity of the pitting corrosion process they used a gamma process as the underlying stochastic process of their model. Zhang and Zue [13] validated Maes model by applying that model on four real pitting corrosion data sets of sixty two pits on an 80 km natural gas pipeline in Alberta, Canada. They also extended Maes model by assuming inverse-Gaussian [68] and Bayesian dynamic linear model [69] as the underlying stochastic process. In all those models, the underlying assumption about the operational conditions is that

the operational conditions of the pipelines remains the same for the operating life of the pipelines. Heidary and Groth [84] developed a defect-based pitting corrosion degradation model to cover the case when the operational conditions of a pipeline change over time.

Despite the fact that defect-based algorithms are more common in the oil and gas industry, they are less suitable when the pit density is high, because the matching procedure is time consuming and prone to error [18, 24]. A population-based algorithm can be applied as soon as new ILI data become available without further matching procedure and the results of this algorithm can be used to evaluate the criticality of the pipeline segment to decide about necessity of extra effort of a local corrosion growth analysis using matched features [18]. To eliminate the matching procedure step in the case of having high density pits (e.g., as experienced in upstream and subsea pipelines [18]), a few population-based methodologies have been proposed in the literature. The most recent one was proposed by Dann and Maes [18]. They used KL divergence method to estimate the hyper-parameters of the degradation model and used a homogeneous gamma process as the underlying stochastic process. They applied their model in a case study with two sets of ILI data and did not consider the initiation of new defects after the most recent inspection. Lu [108] Developed a population based pitting corrosion model, for nuclear power plants, based on gamma process based on a “repair-on-detection” strategy, which at least for pipelines is not applicable.

In this paper, we propose a novel population-based algorithm to estimate the degradation level of piggable pipelines due to pitting corrosion process. In this algo-

rithm we use non-homogeneous gamma process (NHGP) as the underlying stochastic process to take into account the temporal uncertainty in pitting corrosion process. Another reason for using non-homogeneous (vs. homogeneous) gamma process is that it makes it possible to consider POF knowledge about pitting corrosion process that is embedded in this well-accepted assumption that growing behavior of maximum depth of pits follows a power function with a positive power less than one [63, 109]. Moreover, this algorithm is not limited to two sets of ILI data and it can be used for two or more ILI data sets, which is the common practice in the industry. We also address the initiation of new pits between the last inspection and the prediction time. We utilize HB modeling to fuse the available two or more unmatched ILI data sets and the POF knowledge about pitting corrosion process. In this way, we propose a novel algorithm to cluster the ILI data at each inspection time based on the initiation time of the different pits. Those clustered data are used in their corresponding Bayesian model to estimate and update the hyper-parameters of the pitting corrosion degradation model and the actual depth of the existing pits at inspection times and also at each point in time in the future. In order to validate our algorithm, we simulate the actual maximum depth for a number of pits as the existing pits based on a non-homogeneous gamma process and. We removed some of them based on their probability of detecting to consider uncertainty in pit detection. We add measurement error and probability of false call to the simulated data and use them as the input data of our algorithm. we also assume that the number of initiated pits at each interval follows a homogeneous Poisson process. Finally, we compare the assumed and the estimated distributions of the actual maximum pit,

the number of the existing pits, and the pit generation rate of the homogeneous Poisson process.

More details about this algorithm, the case study, and the results are presented in this paper as follows. Section 5.3 is dedicated to the requirements and assumptions. In this section theoretical background about gamma process and HB model and the reasons that they are suitable for this degradation modeling are explained. In addition the assumptions behind this algorithm are articulated. In Section 5.4 the developed algorithm is presented in detail and in Section 5.5 it is demonstrated by a case study. The conclusion is presented in Section 5.6.

5.3 Assumptions and methods

In this section the assumptions that the algorithm is founded on and the methods that have been used in the algorithm are explained.

5.3.1 Assumptions

This algorithm is developed based on the following assumptions:

- Operational conditions (i.e., probability density function of temperature, pressure, flow rate, etc.) of the pipeline do not change over time and all pits are under the same operational conditions at each time [13, 14, 16].
- Pits are not interacting each other[18].
- The number of new initiated pits between each two ILI follows a homogeneous Poisson process (HPP) [64, 110]. Which means pits' initiation times follow the

corresponding uniform distribution and time between pits' initiation follow the corresponding exponential distribution.

- The detected pits are not mitigated by the maintenance activities.
- n ($n \geq 2$) sets of population-based ILI data sets are available. These data sets are reported by the ILI service companies that had performed the n ILI operations at t_1, t_2, \dots, t_n . And those reported ILI datasets include both true calls and false calls of the uncertain measurement (y_i) of the maximum depth of each pit of the population.
- The measurement model of the inspection tools is available and follows Equation 5.1[111].

$$y_i = a + b * d_i + N(0, \epsilon) \quad (5.1)$$

where a and b are biased error and ϵ is the random scattering error of the inspection tool which are assumed to be given by the ILI service companies. y_i is the measured depth of pit i and N stands for a normal distribution. This equation is used to estimate the actual depth of a pit given its measured depth.

- The detection threshold and the credible pit depth of the inspection tools are given by the ILI service companies. Which are used to calculate the POD (Equation 5.2) of each pit given its actual depth and the probability of false call (Equation 5.3) corresponding to each measured depth.

$$POD(Pit_i | d_i, d_d) = 1 - exp(-d_i/d_d) \quad (5.2)$$

where d_i represents the actual depth of Pit_i and d_d represents the minimum detection depth threshold of the inspection tool [13, 24].

$$POFC(Measurement_i | y_i, y_c) = exp(-y_i/y_c) \quad (5.3)$$

where y_i represents the i_{th} measured depth and y_c represents the mean credible measured depth of the inspection tool [24].

5.3.2 Homogeneous Poisson Process (HPP)

It is well accepted that pitting corrosion comprises two main processes: pit initiation and stable pit growth. The pit initiation process can be a consequence of the breakdown of the passive layer caused by random fluctuations in local conditions which takes some time, usually called induction (nucleation or initiation) period [66]. The pit initiation time varies depending on the corrosive environment and the material properties. In some experimental works, it has been confirmed that the distribution of the pit initiation time follows an exponential distribution, and therefore pit initiation can be modeled by using the homogeneous Poisson process (HPP) [64, 110]. In some other experiments, it has been observed that the pit initiation time is not distributed uniformly and pit generation rate is a decreasing function of time for long duration corrosion test [73, 112]. To model this behavior non-homogeneous Poisson process (NHPP) has been used to model the stochasticity in pit initiation time [65]. Zhang and Zhou [113] used NHPP by assuming that pit generation rate is an increasing function of time. Ossai et al. [114] assumed that all

pits initiated at the starting time of the pipeline operation.

In this paper, we assumed that pit initiation time follows an exponential distribution and the number of initiated pits at each time interval follows the corresponding HPP. A counting process is a HPP with parameter $\lambda(> 0)$ if [70]:

- $N(0) = 0$.
- The process has independent increments
- The number of events (i.e., pits) in any interval of length Δt is distributed according to a Poisson distribution with parameter $\lambda\Delta t$:

$$Pr[n \text{ pits in any interval of length } \Delta t] = \frac{[\lambda(\Delta t)]^n}{n!} \cdot e^{-\lambda\Delta t}$$

5.3.3 Non-homogeneous gamma process

The probabilistic pitting corrosion models can be categorized as random-variable based and stochastic-process based models [15]. The main difference between these categories is that the latter one deals with the temporal variability of the pitting corrosion process, while the former one does not capture it [13]. Among different stochastic-process based models, gamma process is more appropriate to model pitting corrosion process [15]. Gamma process has been used widely to model degradation processes such as wear, fatigue, and corrosion, which involve monotonically accumulating damage over time in a sequence of tiny increments [3, 100].

A gamma process is a continuous-time stochastic process $\{X(t), t > 0\}$ with the following properties.

- $X(0) = 0$ with the probability 1.
- $\Delta X = X(\tau) - X(t) \sim Ga(\Delta\alpha = \alpha(\tau) - \alpha(t), \beta)$ for all $0 \leq t < \tau$
- $X(t)$ has independent increment.

Where Ga represents probability density function (PDF) of a gamma distribution. A random quantity (x) (in this study maximum pit depth) has a gamma distribution with shape parameter $\alpha > 0$ and a rate parameter $\beta > 0$ if its PDF is given by:

$$f_{X(t)}(x) = Ga(x; \alpha, \beta) = \frac{\beta^{\alpha(t)}}{\Gamma(\alpha(t))} x^{\alpha(t)-1} \exp(-\beta x) \quad (5.4)$$

Where $\Gamma(\cdot)$ denotes the gamma function. Equations 5.5 and 5.6 shows the expectation and variance of the gamma process respectively.

$$E(X(t)) = \frac{\alpha(t)}{\beta} \quad (5.5)$$

$$Var(X(t)) = \frac{\alpha(t)}{\beta^2} \quad (5.6)$$

Since the rate parameter of a gamma process is constant and time independent, according to Equation 4.17, the shape parameter of a gamma process can address the temporal trend of the average a random variable that follows a gamma process. Hence, different degradation rate (i.e., increasing, decreasing, or constant) can be modeled by selecting an appropriate form for the shape parameter of the gamma process [16].

In the case of pitting corrosion, it is well-accepted that the mean value of the maximum depth of an active pit follows a power law function with a positive exponent less than one [2, 63, 109]. It has been found that pitting corrosion growth in stainless, mild steels and aluminum alloys follows this form of function [115, 116]. Therefore, in the case of pitting corrosion in carbon steel pipelines, the shape parameter of the underlying gamma process follows a power function according to Equation 5.7 and the corresponding gamma process is a non-homogeneous (non-stationary) gamma process, i.e., $\nu \neq 1$ [3].

$$\alpha(t) = k(t - t_0)^\nu \quad (5.7)$$

where k and ν represent the parameters of the pitting corrosion degradation model and t_0 represents the pit initiation time. Accordingly, the distribution of the actual depth of a pit population at time t follows a gamma distribution given in Equation 5.8.

$$f_{X(t)}(x) = Ga(\alpha = (k(t - t_0)^\nu), \beta) \quad (5.8)$$

5.3.4 Hierarchical Bayesian

In this study, we use a HB model to estimate the hyper-parameters (k , ν , β) of the pitting corrosion degradation model, and also the actual depth of the existing pits, given uncertain measurement data and pitting corrosion PoF knowledge. HB modeling is an appropriate method to make scientific inference about hyper-parameters of the distribution of an unknown of a population, based on ob-

servations of many individuals. It is called "hierarchical" because it uses hierarchical or multistage prior distributions [99]. This method has been used in the literature to develop a defect-based algorithm to model different types of uncertainty (temporal, spacial, epistemic [117], measurement) related to corrosion growth in the pipelines [13, 16, 68].

The general population-based HB model that is developed in this study is depicted in Figure 5.1. In this figure, the temporal plate indicates the time of the ILI_j . Based on the assumption that operational conditions do not change over time and all pits are under the same operational condition at each time, a same gamma process is used for all pits for the entire life of the pipeline. Therefore, the hyper-parameters (k, ν, β) of that gamma process are outside of the temporal plate. However, the shape parameter of the gamma process, α , is time dependent (because of the change in t_j and t_{c-1} in Equation 5.7). Therefore, α_{jc} is inside of the temporal plate and it varies at each inspection time for each category of pits based on their initiation time. Despite the assumption of HPP for pits' initiation time, with respect to degradation level estimation we made this conservative assumption that for those pits that have been initiated before the first ILI, the initiation time is $t_{c-1} = t_0 = 0$ and for those that have been initiated between each two ILIs, the initiation time of all of them is exactly after the most recent ILI. Hence, after each ILI, it is necessary to figure out which detected pits are new and which pits have been initiated previously that may or may not be detected in the previous ILIs. This clustering step will be discussed in more details in Section 5.4.3.

In Figure 5.1, x_{ijc} indicates the actual depth of an existing pit i at t_j with the

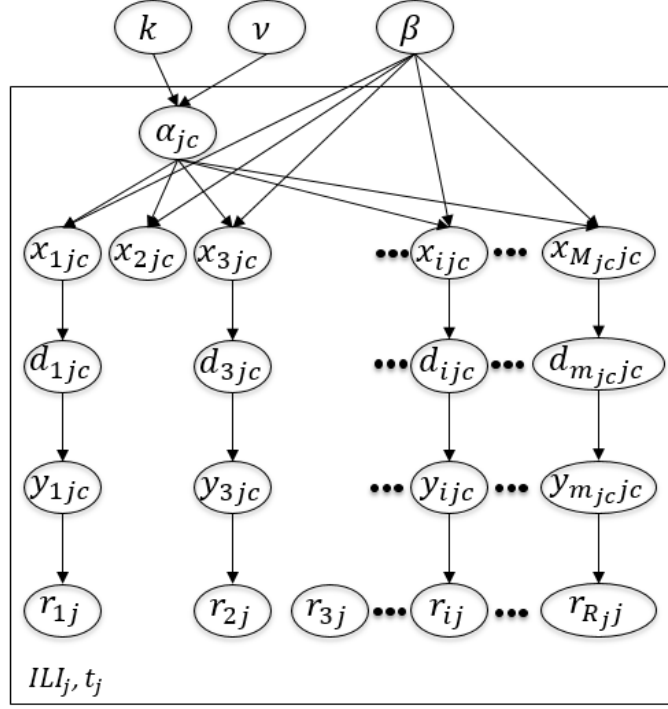


Figure 5.1: General HB model for each category of pits at each ILI time based on their initiation time

initiation time index c , d_{ijc} indicates the actual depth of a detected pit i at t_j with the pit initiation time index c , y_{ijc} indicates the measured depth of a detected pit i at t_j with the initiation time index c , and r_{ij} indicates the measured depth of a reported pit i at t_j . In addition, R_j indicates the number of reported pits at ILI_j including both false and true calls, m_{jc} indicates the number of pits that have been initiated at time t_{c-1} and are detected truly (i.e., true calls) at ILI_j , M_{jc} indicates the number of existing pits at ILI_j that have been initiated at time t_{c-1} . As it is shown in this figure, some existed pit (e.g., x_{2jc}) might be missed to be detected by the ILI tool at time t_j . In addition, some reported pits might be a false call (e.g., r_{3j}).

Since at each ILI there are some false call detection and also some existing

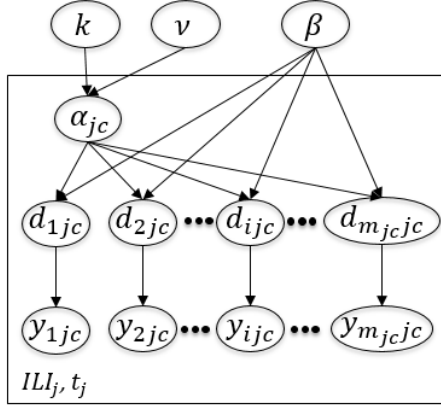


Figure 5.2: Modified general HB model for each category of pits at each ILI time based on their initiation time

pits that are not detected, the original HB model is modified to the one that is shown in Figure 5.2. The process of filtering true called pits from the reported pits is explained in Section 5.4.

This HB model is used to estimate the hyper-parameters and actual depth of the detected pits by using the Bayes rule according to Equation 5.9.

$$\begin{aligned}
 Pr(d_{ijc}, k, \nu, \beta | y_{ijc}) &= Pr(d_{ijc}, \theta | y_{ijc}) \\
 &\propto Pr(y_{ijc} | \theta, d_{ijc}) \times Pr(\theta, d_{ijc})
 \end{aligned}
 \tag{5.9}$$

5.4 Developed algorithm

In this section, firstly, the general structure of the algorithm, which comprises three phases, is illustrated and then each phase is articulated step by step.

5.4.1 General structure of the developed algorithm

Figure 5.3 depicts the general structure of the algorithm which includes three phases. According to this figure, in phase I, the first ILI dataset is used to estimate the hyper-parameters of the degradation model, the number of existing pits at time t_1 and the PMF of the actual depth of those pits at that time. In phase II, the other ILI data sets are used to update the hyper-parameters, and to estimate the number of existing pits and the PMF of their actual depth at time t_2, \dots, t_n . The main difference between phase I and phase II is in a clustering step. Since it is assumed that all existing pits at time t_1 , has been initiated at $t = 0$, hence all of them follow a same degradation model. However, at other inspections times and also in prediction time, there are clusters of pits with different initiation times. Therefore, we developed a clustering algorithm to categorise the detected pits at each inspection time based on their initiation times to be used on their corresponding Bayesian models. In phase III the rate parameter of the assumed HPP and the number of pits that are expected to be initiated between the time of the last ILI and the prediction time are estimated. Finally, the PMF of the actual depth of the existing pits at time t_{n+1} is estimated. The details of these three phases are given in the following subsections.

5.4.2 Phase I: Using the first ILI dataset

In phase I the first set of reported ILI data is used to find the first estimation of hyper-parameters (k, ν, β) of the NHGP representing the maximum pit depth

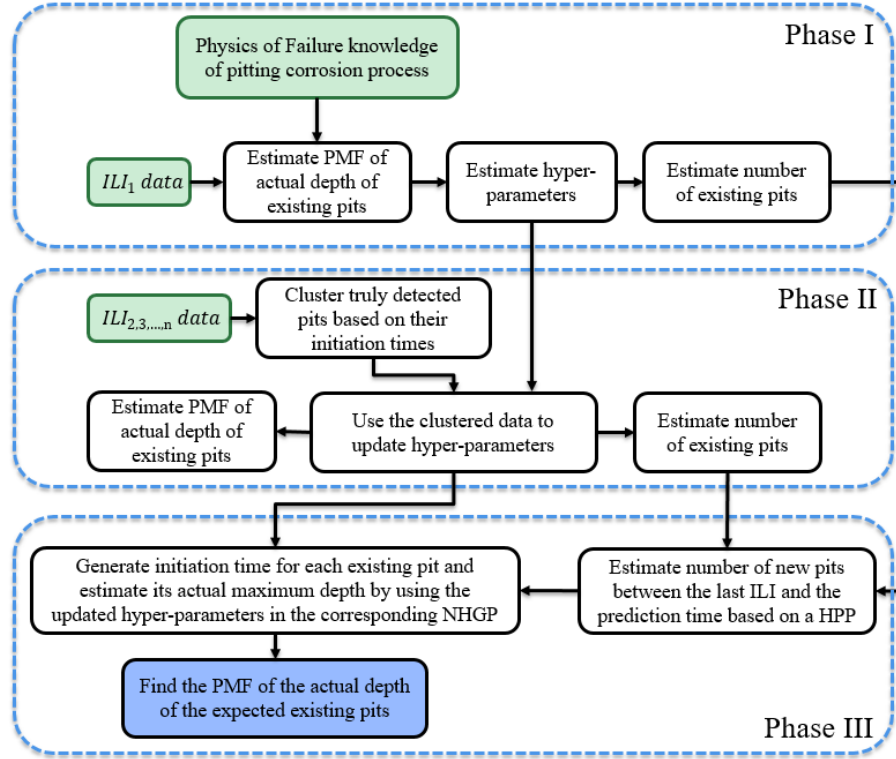


Figure 5.3: General structure of the developed algorithm

growing behavior, the number of the existing pits, and the probability mass function (PMF) of their actual depth at time t_1 , by performing the following steps:

- Step I-1: Filter the truly detected pits from the reported pits:

For each reported measured depth, generate a random uniform number between zero and one. If the probability of false call of that measured pit depth (use Equation 5.3) is higher than that random number, remove that measurement from the dataset and if not keep it.

- Step I-2: Estimate the hyper-parameters and the actual depth of the detected pits:

Use the measured depth of the m_{11} truly detected pits at ILI_1 and the prior values $(p_{1,2,3}, q_{1,2,3})$ in the corresponding HB (Figure 5.4) to obtain the first

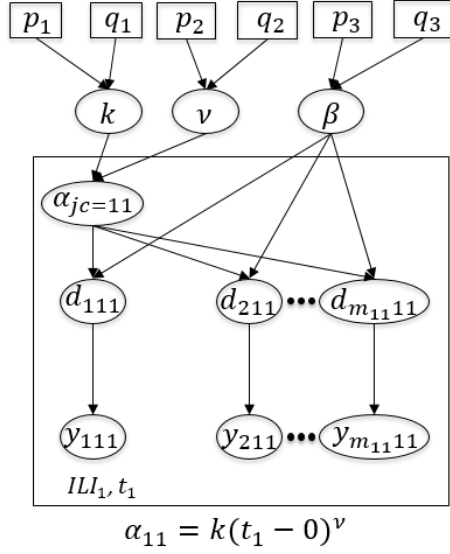


Figure 5.4: Modified HB model for ILL_1

estimate of the hyper-parameters and the actual depth of the truly detected pits at t_1 by using the Bayes rule (Equation 5.9). Non informative prior distributions (i.e., uniform distributions) can be selected for prior distributions of the hyper-parameters in this Bayesian model (Figure 5.4). In other words $p_{1,2,3} > 0$ are the lower bounds of the prior uniform distributions and $q_{1,2,3} > 0$ are the upper bounds. The only prior information is that the upper bound of ν (q_1) is equal to one based on PoF knowledge of internal pitting corrosion process.

- Step I-3: Estimate the number of existing pits at t_1 (M_1) given the number of truly detected pits (m_{11}):

Discretize the PMF of d_{i11} to H number of bins and estimate the number of

existing pits at each bin by using Equation 5.10 [29, 106].

$$n_h(PMF(X_1)) = n_h(PMF(D_1))/POD_h \quad (5.10)$$

$$h = 1, 2, \dots, H$$

where n_h is the number of pits in bin h and POD_h is the corresponding POD which can be calculated by using the mean value of bin h in Equation 5.2 [add ref]. The total number of existing pits at time t_1 can be estimated by summing the frequency of all bins of the PMF of x_{i11} by using Equation 5.11.

$$M_1 = \sum_{h=1}^H n_h(PMF(x_{i11})) \quad (5.11)$$

- Step I-4: Estimate the PMF of the actual depth of the existing pits:

For those bins that the frequency in PMF of x_{i11} is higher than the frequency of PMF of d_{i11} , generate $n_h(PMF(x_{i11})) - n_h(PMF(d_{i11}))$ number of random uniform values between the start and end depth of that bin.

The output of this phase are an for the hyper-parameters (k, ν, β) , the number of the existing pits, and the probability mass function (PMF) of their actual depth at time t_1 .

5.4.3 Phase II: Incorporating additional data sets

In phase II, the additional ILI data sets are incorporated to update the degradation model's hyper-parameters, and to estimate the number and the actual depth of the existing pits at $t_j, j = 2, \dots, n$. As mentioned previously, in this phase, a

clustering step is required to categorise detected pits based on their initiation times.

Phase is explained in detail for ILL_2 as following and the same approach is applicable for the next ILLs.

- Step II-1: Filter the truly detected pits from the reported pits at ILL_2 :

For each reported measured depth, generate a random uniform number between zero and one. If the probability of false call of that measurement (use Equation 5.3) is higher than that random number, remove that measurement from the dataset and if not keep it.

- Step II-2: Estimate the number of pits of each cluster that are expected to have been detected at t_2 :

The general idea of the clustering algorithm is to estimate how many of those pits that have been initiated before ILL_1 (M_1) are expected to have been detected at ILL_2 (m'_{21}). Then subtract that number from the number of truly detected pits at ILL_2 (m_2) to find the expected number of those pits that have been initiated between ILL_1 and ILL_2 and are expected to have been detected at ILL_2 . The general idea of the this step is shown in Figure 5.5. According to this figure, at each inspection time, there are a number of truly detected and undetected pits. The goal is to estimate how many of those pits that were initiated before ILL_1 (M_1), are expected to have been detected at ILL_2 (m'_{21}), given the first estimation of the hyper-parameters that are obtained in Phase I, and the number of truly detected pits at t_2 (m_2).

Since in a gamma process the rate parameter is time independent, the estimated rate parameter at time t_1 , can be used in time t_2 . However, for the

shape parameter, which is time dependent, the estimated k and ν , in phase I, in conjunction with t_2 are used in Equation 5.7 to find $\alpha'_{21} = k(t_2 - 0)^\nu$. By using those rate and shape parameters, the expected PDF of the actual maximum pit depth of the pit population can be estimated by using Equation 5.8 ($g'_{21}(x) = Ga(\alpha'_{21}, \beta)$). Then m'_{21} can be obtained by integrating the expected PDF times the corresponding POD on all possible values of maximum pit depth (x), multiplied by the number of pits that have been initiated before time t_1 (M_1) (Equation 5.12).

Based on the assumption of NHGP as the underlying stochastic process of pitting corrosion process, the expected PDF of the actual depth of the pits that have been initiated before ILL_1 , follows a gamma distribution ($g'_{21}(x)$) at time t_2 with a shape parameter equal to $\alpha'_{21} = k(t_2 - 0)^\nu$ and a scale parameter equal to β (Equation 5.8).

$$m'_{21} = M_1 \int g'_{21}(x)POD(x)d(x) \quad (5.12)$$

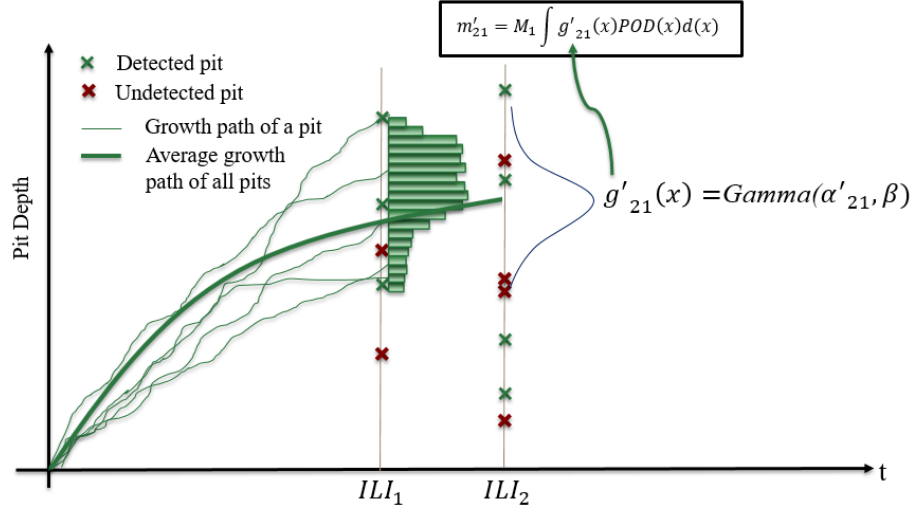


Figure 5.5: Estimating number of the pits that were initiated before ILL_1 that are expected to have been detected at ILL_2

And m'_{22} can be calculated by subtracting m'_{21} from the total number of truly detected pits (m_2) at t_2 by using Equation 5.13.

$$m'_{22} = m_2 - m'_{21} \quad (5.13)$$

- Step II-3: Assign each truly detected pit to a cluster:

At this step m'_{21} number of truly detected pits at t_2 are assigned to one cluster and m'_{22} of them are assigned to another cluster. To do so:

- Generate m'_{21} random number from $g'_{21}(x)$ and use Equation 5.1 to find the PMF of Y'_{21} .
- Generate m'_{22} random number from $g'_{22}(x) = Ga(\alpha'_{21} = k(t_2 - t_1)^\nu, \beta)$ and use Equation 5.1 to find the PMF of Y'_{22} .
- Discretize PMF of Y_2 and PMF of Y'_{21} with the same bins intervals.
- Use the following pseudo code to assign each truly detected pits to a

cluster:

Set $\text{PMF}(Y_{21}[\text{all bins}]).\text{freq} = 0$

Set $\text{PMF}(Y_{22}[\text{all bins}]).\text{freq} = 0$

For $i = 1$ to m_2

$BI_i =$ corresponding bin to pit i (find out each pit belongs to which bin).

If $\text{PMF}(Y_{21}[BI_i]).\text{freq} < \text{PMF}(Y'_{21}[BI_i]).\text{freq}$:

$\text{ClusterIndex}_i = 1.$

$\text{PMF}(Y_{21}[BI_i]).\text{freq} = \text{PMF}(Y'_{21}[BI_i]).\text{freq} + 1.$

else:

$\text{ClusterIndex}_i = 2.$

$\text{PMF}(Y_{22}[BI_i]).\text{freq} = \text{PMF}(Y'_{22}[BI_i]).\text{freq} + 1.$

End

In this pseudo code, BI_i stands for the bin index of pit i and .freq stands for the frequency of bin BI_i .

- Step II-4: Update the hyper-parameters and estimate the actual depth of the detected pits at ILL_2 :

Use the clustered measurement data in ILL_2 in the HB model that is shown in Figure 5.6 to update the estimation of the hyper-parameters and also to estimate the actual depth of the truly detected pits. It is worth noting that in this HB model, the prior values for the hyper-parameters are their estimated values in Phase I.

- Step II-5: Estimate the number of actual pits (M_2) given the number of truly

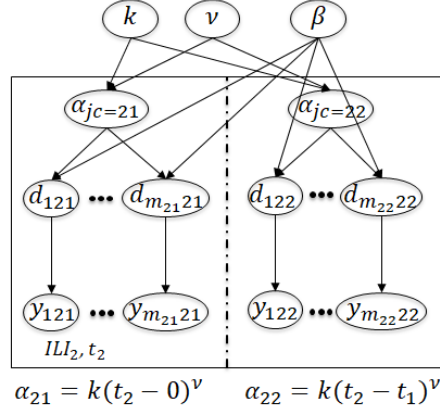


Figure 5.6: Modified HB model for ILL_2

detected pits (m_2) at ILL_2 :

Follow the same approach that has been used in Phase I to estimate M_2 according to Equation 5.14.

$$M_2 = \sum_{h=1}^H n_h(PMF(X_2)) = \sum_{h=1}^H n_h(PMF(D_2))/POD_h \quad (5.14)$$

- Step II-6: Estimate the PMF of the actual depth of the existing pits at ILL_2 :
For those bins that the frequency of $PMF(X_2)$ is higher than the frequency of $PMF(D_2)$, generate $n_h(PMF(X_2)) - n_h(PMF(D_2))$ number of random uniform values between the start and end depth of that bin.

For $ILL_j, j > 2$, the same steps should be followed. To shorten the paper, the algorithm is not demonstrated for those $ILLs$ in details and the related equations are generalized as follows:

$$\alpha'_{jc} = k(t_j - t_{c-1})^\nu \quad (5.15)$$

$$m'_{jc} = (M_c - M_{c-1}) \int g'_{jc}(x)POD(x)d(x), c = 1, \dots, j - 1 \quad (5.16)$$

$$m'_{jj} = m_j - \sum_{c=1}^{j-1} m'_{jc} \quad (5.17)$$

$$M_j = \sum_{h=1}^H n_h(PMF(X_j)) = \sum_{h=1}^H n_h(PMF(D_j))/POD_h \quad (5.18)$$

The output of phase II are the updated hyper-parameters, the number of the existing pits, and the probability mass function (PMF) of their actual depth at times $t_j, j=2, \dots, n$.

5.4.4 Phase III: Prognostics

In phase III the rate parameter of the HPP is estimated and the PMF of the actual depth of the existing pits at any time after the last ILI can be predicted. This phase includes the following steps:

- Step III-1: Estimate the rate of HPP:

As it was mentioned before, we assumed that the actual number of pits at each time interval follows a homogeneous Poisson process. By having the estimated number of existing pits at each ILI ($M_1, M_2 - M_1, M_3 - M_2, \dots$) a point estimate of the rate parameter of that Poisson process can be estimated by using the

maximum likelihood estimation:

$$\hat{\lambda} = \frac{\sum_{j=1}^n (M_j - M_{j-1})}{\sum_{j=1}^n (t_j - t_{j-1})} = \frac{M_j}{t_j} \quad (5.19)$$

- Step III-2: Estimate the number of new pits between the last ILI and the prediction time (t_{n+1}):

The mean value of the number of initiated pits between the last ILI and t_{n+1} is calculated by using Equation 5.20 which is the mean value of a Poisson distribution.

$$M_{n+1} - M_n = \hat{\lambda} \times (t_{n+1} - t_n) \quad (5.20)$$

- Step III-3: Estimate the PMF of the actual depth of the existing pits at t_{n+1} :

The final step is to predict the PMF of the existing pits at time t_{n+1} . To do so, for each cluster of pits, pit initiation times are randomly generated from the corresponding uniform distribution (since the number of pits follows a HPP, the pit initiation times follows a uniform distribution and the times between initiations follow an exponential distribution). The lower and upper bound of each uniform distribution is equal to the start and end point of each inspection interval and the number of random number at each time interval is equal to the numbers that are estimated previously (i.e., M_1, M_2, \dots, M_{n+1}). Those generated initiation times in conjunction with the updated hyper-parameters are used in the corresponding NHGP for each cluster according to Equation

5.21 to estimate the PMF of the existing pits at t_{n+1} .

$$\begin{aligned}
 x_{i(n+1)c} &= \text{random.gamma}(k[t_{n+1}- \\
 &\quad \text{random.uniform}(t_c, t_{c-1})]^\nu, \beta), \\
 &\quad i = 1, \dots, M_{n+1}
 \end{aligned} \tag{5.21}$$

The output of phase III are an estimation for the HPP rate parameter, the number of pits that will initiate between the last ILI and the prediction time and the PMF of actual depth of existing pits at the prediction time.

The application of the developed population-based algorithm is demonstrated in the next section by applying that on three sets of simulated ILI data and the estimated results are compared with the actual assumed values.

5.5 Demonstration of the developed algorithm

In this section the developed algorithm is demonstrated in a case study. Consider a pipeline that has been inspected three times ($n = 3$) by ILI, after $t_1 = 30, t_2 = 37, t_3 = 42$ years of operation. ILI data sets (i.e., reported number of pits and their measured depth (a combination of false calls and true calls)) for a segment of the pipeline are available. The ILI data sets are not matched because of the high density of the existing pits. The goal is to estimate the number of the new pits that are expected to be initiated between the time of the last ILI and 50 years (t_4 , prediction time) of operation and then using this result, estimating the distribution of the actual depth of the existing pits at prediction time to be used in pipeline

Parameters	Units	Description
T	C	Temperature
Pc	MPa	CO_2 partial pressure
pH	-	pH
S	MgL^{-1}	Sulphate ion
C	MgL^{-1}	Chloride ion
W	-	Water cut
r	Pa	Wall shear stress
Gs	m^3day^{-1}	Gas production rate
OL	m^3day^{-1}	Oil production rate
Wt	m^3day^{-1}	Water production rate
Pt	MPa	Operating pressure

Table 5.3: Operational parameters considered in the underlying generic model for data simulation [14]

reliability estimation and consequently condition-based maintenance optimization.

5.5.1 Case study data

Since the real field ILI data for a population of pits, are not available in the literature, we simulate three sets of ILI data by using a generic internal pitting corrosion degradation model that has been developed by Ossai et al. [14] to demonstrate the application of the developed algorithm and validate the results. Ossai's model was developed by using ten years (from 1999 to 2008) measurement of pit depth (using UT) and operating parameters for sixty X52 non-piggable oil and gas pipelines in Nigeria. To the best of authors' knowledge, this model is the most comprehensive generic population based model that has been developed based on field data (rather than experimental data). This model correlates eleven operational parameters (Table 5.3) with the average of the maximum depth of a population of pits.

The simulated data are generated by using the parameters that are given in

Table 5.4. In this table the hyper-parameters are based on Ossai’s model [14]. The characteristics of the sizing error of inspection tools (a, b, ϵ in Equation 5.1) are the characteristics of an UT tool that has been used at 2004 in Alberta, Canada [13]). The HPP rate is selected in a way to have the same order of magnitude of number of pits as is given in [18] and d_d and y_c are selected according to [24].

Given the assumed value in Table 5.4, following approach is used to generate simulated ILI data. The numbers of initiated pits at each time interval is calculated by generating a random number from the corresponding Poisson distribution with the rate parameter equal to $\lambda\Delta t$ (Table 5.5). The actual depth of each initiated pit, at each evaluation time (inspection times and prediction time), is calculated by generating a random number from the corresponding gamma distribution . The shape parameter of the gamma distribution corresponding to each pit is equal to $k(t_j - t_0)^\nu$. Where t_j is the evaluation time, and t_0 is the initiation time of that pit which is a uniformly distributed (i.e., HPP) random number between the start and end point of the time interval in which that specific pit is initiated in. The scale parameter of the gamma process is β . In order to consider POD in simulated data, a uniform random number is generated for each initiated pit and if that random number is less than the POD of that pit (Equation 5.2), it is considered as a detected pit, otherwise it is considered as an undetected one (hit-miss POD model[111]). For each detected pit, the measurement error is added by using Equation 5.1. At this stage the PMF of the detected pits at each evaluation time is available. In order to add the false call error to the simulated dataset, the PMF of the detected pits is discretized to a number of bins. Then the frequency of each bin is divided by (1-

Param.	value	Param.	value
k (mm)	0.12	a (% PWT)	2.04
ν	0.771	b	0.97
β	3.5	ϵ (% PWT)	5.97
λ	80	d_d (% PWT)	10
PWT (mm)	8.41	y_c (% PWT)	20

Table 5.4: Assumed values for input data simulation

Time (yr)	Exist. pits No.	Repor. pits No.
t_1 : 30	2374	2516
t_2 : 37	2955	3484
t_3 : 42	3336	3781
t_4 : 50	3967	—

Table 5.5: Number of existing and reported pits at each time interval

POFC) of the mean value of that bin (using Equation 5.3) to find the frequency of the corresponding bin in the PMF of reported pits (r_{ij} in Figure 5.1). For those bins that the frequency of the PMF of the reported pits is higher than the frequency of the PMF of the detected pits, uniformly distributed random measurements, between the lower and upper bound of each bin, are added to the reported dataset as false calls reported measurements. The number of those false called measurement for each bin is equal to the difference between the frequency of the PMF of the reported pits and the frequency of the PMF of the detected pits. The PMF of the reported pits are assumed as the reported data from the ILI service companies. Implementation of the algorithm on these data sets is explained as following.

5.5.2 Phases of the algorithm for the case study

5.5.2.1 Phase I for the case study

- Filter the truly detected pits from the reported pits of ILL_1 :

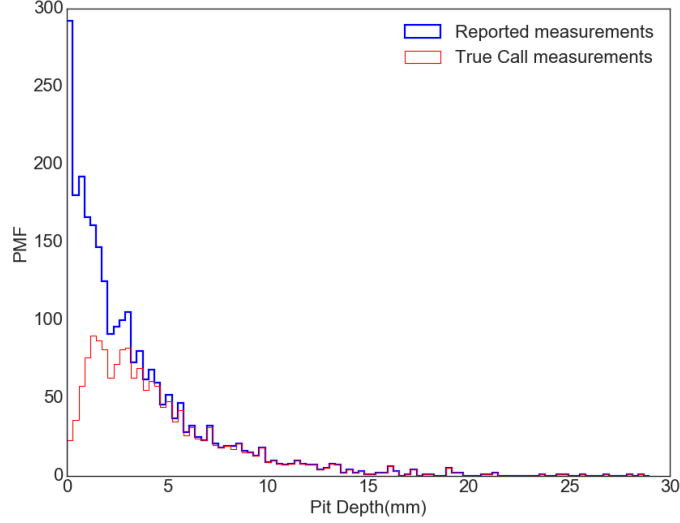


Figure 5.7: PMF of the reported and true calls measurements at LL_1

	Mean	std.	2.5%Qt.	97.5%Qt.
k	0.51	0.29	0.11	1.04
ν	0.37	0.20	0.11	0.75
β	3.07	0.13	2.83	3.33

Table 5.6: Estimated hyper-parameters at t_1

Following the procedure that is explained in Step I-1 the PMF of the truly detected pits is extracted from the PMF of the reported measurements as shown in Figure 5.7. According to this figure, the number of false measurement for pits with smaller depths is higher than the one for the deeper ones. Hence, the number of the filtered measurements is higher for smaller pits.

- Estimate d_{i11} and first estimate of the hyper-parameters:

The marginal distribution of the actual depth of the truly detected pits (d_{i11}) and the hyper-parameters are obtained by using HB model in Figure 5.4. The estimated hyper-parameters with 95% confidence level are given in Table 5.6.

- Estimate M_1 and PMF of existing pits at t_1 :

By discretizing the PMF of d_{i11} to $H = 100$ bins and using Equation 5.10 and

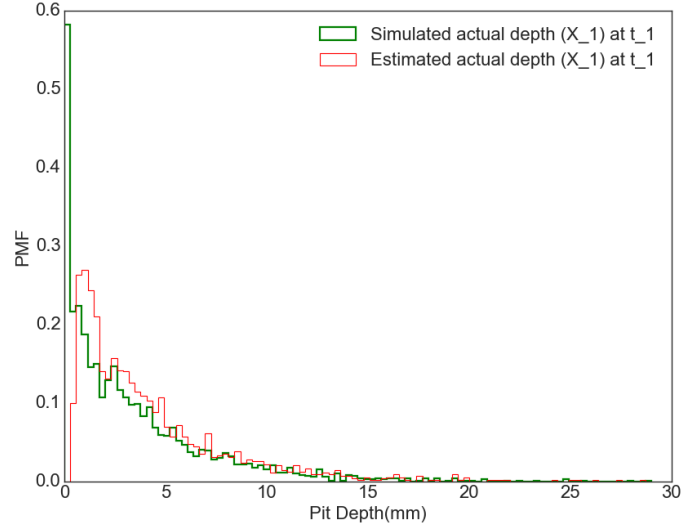


Figure 5.8: Simulated and estimated PMF of pits' actual depth at $t_1(X_1)$

5.11, the estimated number of existing pits at t_1 is obtained as $M_1 = 1816$. Then the PMF of the existing pits at t_1 is estimated by following the procedure that is explained in Section 5.4.2. Figure 5.8 shows a visual comparison between the assumed and estimated PMF of the existing pits at t_1 . This figure shows that for the first set of ILI dataset, the performance of the developed algorithm is visually acceptable. A quantified comparison between these two PMFs is given in the Discussion section.

5.5.2.2 Phase II for the case study

- Estimate m_{21} and m_{22} :

The first step in phase II is to filter the truly detected pits from reported pits by following the procedure that explained in Step II-1. Then it is desirable to estimate the number of pits that have been initiated before t_1 and are expected to have been detected at t_2 (m_{21}). In this way α'_{21} is equal to 1.97 by using

	Mean	std.	2.5%Qt.	97.5%Qt.
k	0.13	0.01	0.11	0.16
ν	0.72	0.03	0.66	0.76
β	3.02	0.08	2.88	3.19

Table 5.7: Updated hyper-parameters at t_2

the estimated k and ν in Phase I, $t_j = t_2$, and $t_{c-1} = t_0 = 0$ in Equation 5.15. Consequently, m_{21} is calculated as 1708 by using this shape parameter and the scale parameter that is estimated at t_1 in Equation 5.12. Accordingly, based on Equation 5.13, $m_{22} = m_2 - m_{21} = 528$. By having α'_{21} , β , m_{21} , m_{22} , and following the procedure that is given in Step II-3, the PMF of Y'_{21} and Y'_{22} are obtained. Then, by using the given pseudo code, the detected pits at t_2 are clustered.

- Update the hyper-parameters and estimate the actual depth of the detected pits at ILL_2 :

The next step in Phase II is to use the clustered measurements in the HB model that is shown in Figure 5.6. It is worth noting that the posterior distributions at Phase I are the prior distributions of this HB model. The updated hyper-parameters are shown in Table 5.7.

- Estimate the number of existing pits (M_2) and the PMF of their actual depth at t_2 :

By following Step II-5 and II-6, the number of existing pits at t_2 is obtained as 2541. The PMF of the simulated and estimated actual depth of the existing pits at t_2 are depicted in Figure 5.9.

To shorten the paper, the steps are not discussed in detail for ILL_3 . The

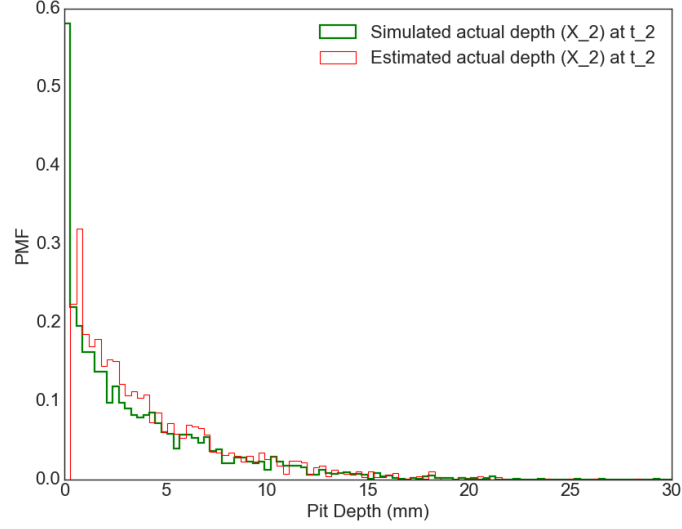


Figure 5.9: Simulated and estimated PMF of pits' actual depth at $t_2(X_2)$

updated hyper-parameters are given in Table 5.8 and the other results are presented briefly as following.

$$\alpha'_{31} = k(t_3 - t_0)^\nu = 1.93 \quad (5.22)$$

$$\alpha'_{32} = k(t_3 - t_1)^\nu = 0.78 \quad (5.23)$$

$$\alpha'_{33} = k(t_3 - t_2)^\nu = 0.41 \quad (5.24)$$

$$m'_{31} = (M_1) \int g'_{31}(x)POD(x)d(x) = 1704 \quad (5.25)$$

$$m'_{32} = (M_2 - M_1) \int g'_{32}(x)POD(x)d(x) = 425 \quad (5.26)$$

	Mean	std.	2.5%Qt.	97.5%Qt.
k	0.16	0.001	0.158	0.162
ν	0.67	0.004	0.66	0.68
β	3.17	0.013	3.14	3.19

Table 5.8: Updated hyper-parameters at t_3

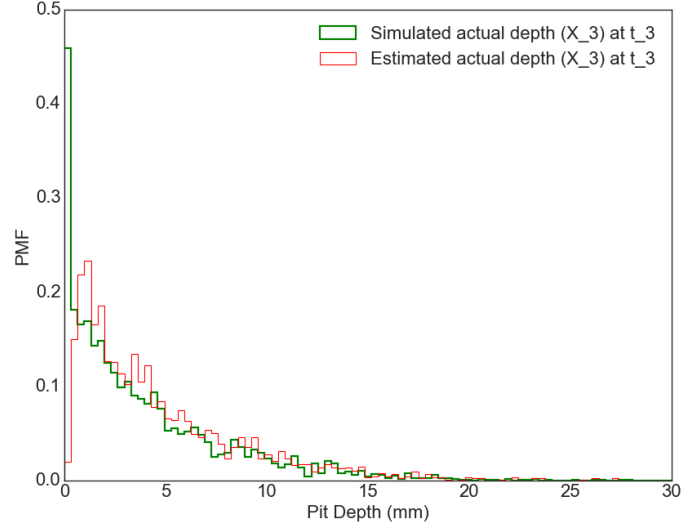


Figure 5.10: Simulated and estimated PMF of pits' actual depth at $t_3(X_3)$

$$m'_{33} = m_3 - \sum_{c=1}^2 m'_{3c} = 502 \quad (5.27)$$

$$M_3 = \sum_{h=1}^H n_h(PMF(X_3)) = \sum_{h=1}^H n_h(PMF(D_3))/POD_h = 2870 \quad (5.28)$$

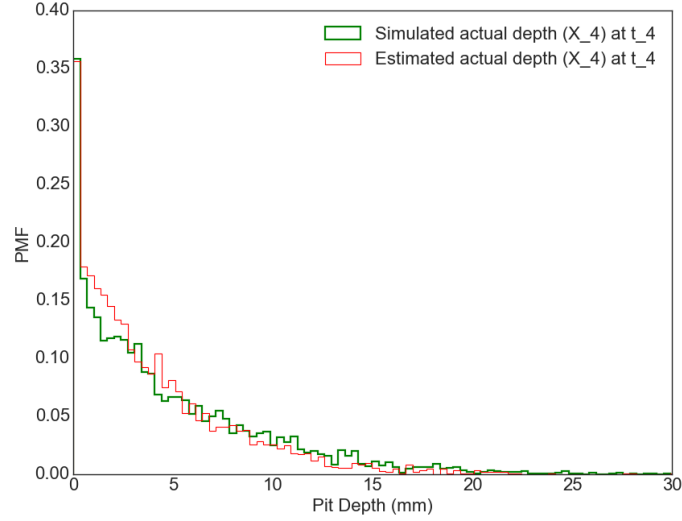


Figure 5.11: Simulated and estimated PMF of pits' actual depth at $t_4(X_4)$

5.5.2.3 Prognostics phase for the case study

Having those three sets of ILI data at 30, 37, and 42 years after pipeline operation, the goal is to estimate the actual depth of the existing pits at $t_4 = 50$. To do so, by using maximum likelihood estimation (5.19), the rate parameter of the assumed underlying HPP (λ) is obtained as 68. Consequently the expected number of new pits is equal to $M_4 = \lambda(t_4 - t_3) = 68 \times (50 - 42) = 544$. By using the updated hyper-parameters at t_3 (Table 5.8) and the number of initiated pits at each time interval, Equation 5.21 is used to find the actual depth of the existing pits at t_4 . The PMF of simulated and estimated actual depth of existing pits at t_4 are shown in Figure 5.11

	Assumed	ILL_1	ILL_2	ILL_3
k	0.12	0.51	0.13	0.16
ν	0.771	0.37	0.72	0.67
β	3.5	3.07	3.03	3.17
α_{11}	1.65	1.50	—	—
α_{21}	1.94	—	1.75	—
α_{22}	0.54	—	0.53	—
α_{31}	2.14	—	—	1.97
α_{32}	0.81	—	—	0.85
α_{33}	0.41	—	—	0.47

Table 5.9: Comparing hyper-parameters

5.5.2.4 Discussion

For the sake of comparison, the mean value of the hyper-parameters and the shape parameters of the gamma process at evaluation times are given in Table 5.9. According to this table, although the estimated hyper-parameters k and ν are not so close to the assumed ones, the absolute error of the estimated β and shape parameters (α_{jc}) are less than 10%.

The assumed and estimated number of exiting pits at each time interval is given in Table 5.10.

The next comparison is on the rate parameter of the HPP. As mentioned in phase III of the case study, the estimated rate for the underlying HPP is 72 which is in the $\pm 10\%$ boundary of the assumed value (80). This $\pm 10\%$ criteria is selected

	Assumed Pit.No.	Estimated Pit.No.
0- ILL_1	2374	1816
ILL_1 - ILL_2	577	725
ILL_2 - ILL_3	381	329
ILL_3 -Prediction	631	544

Table 5.10: Comparing No. of pits

based on the $\pm 10\%$ boundary that is accepted for depth estimation in the oil and gas industry [13].

In order to quantify the difference between simulated and estimated distribution of the actual depth of the existing pits at each evaluation time, Kullback Leibler divergence (KLD) [118] measure is used. KLD is a measure to find the relative entropy between two probability distribution on a random variable. Equation 5.29 shows this measure between two probability distribution functions ($P(x)$ and $Q(x)$).

$$KLD(P||Q) = \sum_{x \in X} P(x) \log \frac{P(x)}{Q(x)} \quad (5.29)$$

In this equation, usually P considered as the true distribution of data (in this case simulated actual depth of the existing pits) and Q comes from the proposed model that used to approximate the true distribution (in this paper estimated actual depth of the existing pits(X_j)) [119]. Larger KLD indicates less similarity between two distributions. Since KLD is not a symmetric distance, we used symmetric KLD (SKLD) to compare similarity between two distributions [120, 121] according to Equation 5.30.

$$SKLD(P||Q) = 1/2[KLD(P||Q) + KLD(Q||P)] \quad (5.30)$$

In case of having two distributions that are the exactly the same, the KLD and SKLD are equal to zero. In other words, the smaller value for KLD or SKLD the two distributions are more similar. SKLDs for the normalized PMF of the simulated

and estimated actual depth of existing pits at evaluations times are shown in Table 5.11. According to this results, the developed population-based algorithm has an acceptable performance (relatively small values for SKLD) and its performance is improved by arriving new ILI data (i.e., values for X_3 and X_4 in comparison to the values for X_1 and X_2).

In addition to SKLD measure, we compared the results with χ^2 distance measure (Equation 5.31).

$$\chi^2 = \sum_h \frac{(P_h - Q_h)^2}{(P_h + Q_h)} \quad (5.31)$$

where P and Q are the normalized histograms to be compared and index h refers to h_{th} bin.

This distance measure for different evaluation times are given in Table 5.11. Analogous to KLD measure, the smaller χ^2 shows that two compared distributions are more similar. In order to have a criteria to compare the calculated χ^2 distance, this measure is also calculated for the case when there is no overlap between the distributions of simulated and estimated actual depth (by shifting the simulated distributions from the estimated distribution in a way to have no overlap). According to Table 5.11, the χ^2 measures results also show that the developed algorithm have a good performance in terms of predicting the PMF of the actual depth of the existing pits at inspections times and also at prediction time after the last ILI.

	X_1	X_2	X_3	X_4
SKLD	0.187	0.226	0.112	0.030
χ^2	0.233	0.075	0.397	0.033
χ^2 (Shifted distributions)	1.994	1.999	1.990	1.984

Table 5.11: SKLD and χ^2 measures

5.6 Conclusion

The paper presents a novel algorithm to evaluate pipeline degradation due to pitting corrosion when the pit density is high. The algorithm employs the NHGP to address the temporal uncertainty and the POF knowledge about pitting corrosion process and homogeneous Poisson process to model the variation in pits' initiation time. This algorithm incorporates the sequential ILI data in degradation analysis by using the HB method and Markov Chain Monte Carlo simulation. A clustering algorithm is developed to cluster the detected pits based on their initiation times to be used in the corresponding HB model. Different types of measurement uncertainty (measurement error, POD, and POFC) are taken into account in this algorithm.

An example involving simulated ILI data used to illustrate the developed algorithm. We assumed that three ILI data sets are available for a pipeline segment. In addition to the degradation model's hyper-parameters, we estimated the number of existing pits and the distribution of their actual depth at each ILI time. In prognostic phase, the rate parameter of the underlying HPP is estimated by using maximum likelihood estimation and subsequently the number of new initiated pits in the future. Finally we estimated the PMF of the actual depth of the existing pits in the future which is the main input in pipeline reliability analysis and condition-base

maintenance optimization.

We verified the result of this algorithm by comparing the assumed and estimated hyper-parameters, number of initiated pits, and rate parameter of the HPP. In addition we compared the PMF of the simulated and estimated actual depth of exiting pits at each evaluation time by using the SKLD and Chi-Square methods.

In the next step of this research we will use the estimated degradation level to evaluate the reliability of the pipeline (i.e., the probability of different failure modes (small leak, large leak, and rupture)) to be used in maintenance optimization. The recommendation for future work of this study is to use non-homogeneous Poisson process to model the variation in pits' initiation times. Considering different inspection tools with different characteristic will be investigated as well. Another potential area to extend this study is to find an optimal number of bins in discretizing the PMFs, since this algorithm is sensitive to this number.

Finally it is worth noting that lack of the real ILI data is a big challenge in PHM of the oil and gas pipelines. Hence, it is highly recommended that oil and gas pipelines' owners and pipeline operating companies collect the operational conditions and inspection data and make them available in the public domain to make it possible for the researchers to validate their new corrosion degradation models that finally leads to the decrease in the number of unexpected failures and unnecessary maintenance.

Chapter 6: Development of a methodology to estimate the reliability and RUL of a pipeline with multiple segments of varying pit density

6.1 Introduction

In risk analysis and maintenance optimization of a pipeline, it is necessary to convert the estimation of maximum pit depth from the models in Chapters 4 and 5 into a reliability metric (e.g., probability of failure, mean time to failure, remaining useful life). In other words, it is necessary to evaluate if the estimated degradation level causes a failure mode or not. This section is dedicated to reliability analysis of a pipeline degraded due to internal pitting corrosion when in some segments of the pipeline have low pit density and other segments have pit density.

Since failure at any location of the pipeline will result in the failure of the whole pipeline, the pipeline is modeled as a series system. Eq. 6.1 shows the relationship between reliability of the whole pipeline and the reliability of each segment.

$$R_{sys}(t) = \prod_1^S R_s(t) \quad (6.1)$$

where $R_{sys}(t)$ is the reliability of the whole pipeline, at time t , S represents

the number of the segments, and $R_S(t)$ stands for the reliability of segment s at time t . It is worth noting that in this evaluation, a segment is a portion of the pipeline with an individual pit or a population of pits that are evaluated as a single unit. For the case of low density pits the developed defect-based degradation model (Ch. 4) is used, and for the case of high density pits the developed population-based degradation model (Ch. 5) is used to evaluate the degradation level of the pipeline.

The remainder of this chapter is organized as follows. Section 6.2 presents three potential failure modes and reliability analysis of oil and gas pipelines due to internal pitting corrosion. In Section 6.4 a case study is presented to demonstrate the application of the proposed methodology. And Section 6.5 is dedicated to the summary of this chapter.

6.2 Pipeline failure modes and reliability analysis

A pressurized pipeline can fail in one of these three failure modes: small leak, large leak, or rupture [13, 25]. A small leak occurs when a pit depth reaches the PWT. In practice, 80% of the PWT is considered as the threshold for assuming a small leak will occur. Using 80% PWT instead of PWT is consistent with the literature [13, 122]. In addition, industrial practice suggests that once the defect reaches 80% PWT, it is prone to develop cracks that can lead to a leak [13]. The other two failure modes occur because of the plastic breakdown of the pipe wall due to internal pressure, which can occur when the pit depth is less than the small leak threshold. These two failure modes together are referred to as pipe burst. The

difference between a large leak and a rupture is in the occurrence (or not) of an unstable axial propagation of the defect resulting from the burst. In the case of having an unstable axial propagation, the failure mode is considered as a rupture, otherwise, it is categorized as a large leak [25].

In order to calculate the probability of occurrence of each of those failure modes, proper limit state functions (LSF) must be defined and analyzed for each failure mode. Generally, a limit state function ($f(x)$) for estimating the failure probability can be defined as

$$f(x) = R - L(x) \quad (6.2)$$

Where R is the resistance and L indicated the load. The LSF $f(x)$ defines a failure criterion as a function of x . Based on this LSF, failure occurs when $f(x) < 0$ or $L(x) > R$ [123]. The three LSF for pitting corrosion in oil and gas pipelines are as follows.

The limit state function for the small leak is given in Equation 6.3.

$$f_1 = 0.8PWT - d \quad (6.3)$$

where d is the maximum pit depth at each point in time. Based on this LSF, small leak happens when $f_1 < 0$, i.e., if maximum pit depth is higher than 80%PWT.

The limit state function to calculate the probability of occurrence of burst (due to due to internal pressure) in a pipeline segment, containing a pit with the

maximum depth of d , is given in Equation 6.4.

$$f_2 = P_b - P_{op} \quad (6.4)$$

where P_b stands for the burst pressure and P_{op} stands for the operational pressure of the pipeline. Based on this equation when $P_{op} > P_b$ burst (i.e., large leak or rupture) happens in the pipeline. Several models are available in the literature to calculate a pipeline's burst pressure given pit depth and length, pipeline material properties, and the geometry of the pipeline. In this study the PCORRC (Pipeline CORROsion Criterion) model [27] is used which is given in Equation 6.5.

$$P_b = \zeta \frac{2\sigma_u PWT}{D} \left[1 - \frac{d}{PWT} \left(1 - \exp\left(\frac{-0.157l}{\sqrt{\frac{D(PWT-d)}{2}}} \right) \right) \right] \quad (6.5)$$

where σ_u is the ultimate tensile strength of the pipe material, D is the pipe diameter, l is the defect length, and ζ is the model error. This model is applicable for $d/PWT \leq 0.8$ and $l \leq 2D$ [13, 26].

The limit state function for rupture is given in Equation 6.6.

$$f_3 = P_{rp} - P_{op} \quad (6.6)$$

where P_{rp} stands for the rupture pressure and P_{op} stands for the operational pressure of the pipeline.

Calculation of rupture pressure can be implemented by using the model that

has been developed by Kiefner and Vieth [26] as follows.

$$P_{rp} = \frac{2\sigma_f PWT}{MD} \quad (6.7)$$

$$M = \begin{cases} \sqrt{1 + 0.6275 \frac{l^2}{D \cdot PWT} - 0.003375 \frac{l^4}{D^2 PWT^2}}, \frac{l^2}{D \cdot PWT} \leq 50 \\ 0.032 \frac{l^2}{D \cdot PWT} + 3.293, \frac{l^2}{D \cdot PWT} > 50 \end{cases} \quad (6.8)$$

where σ_f is the flow stress which is defined as $0.9\sigma_u$. Equation 6.4 in conjunction with Equation 6.6 are used to calculate the probability of occurrence of large leak or rupture. If $P_b < P_{rp} < P_{op}$ rupture happens and if $P_b < P_{op} < P_{rp}$ then large leak happens. A summary of different conditions that lead to these failure modes is given in Table 6.1.

	Pipeline health state
$f_1 \leq 0, f_2 > 0$	Small leak
$f_1 > 0, f_2 \leq 0, f_3 > 0$	Large leak
$f_1 > 0, f_2 \leq 0, f_3 \leq 0$	Rupture
Otherwise	Safe (No failure)

Table 6.1: Criteria for occurrence of different health states (failure modes or safe operation). f_1, f_2, f_3 refer to limit state functions defined in Equations 6.3-6.6.

Given the distributions of the pipeline material properties, pipeline geometry, and also the operational pressure, Monte Carlo simulation can be used to sample from their distributions, to be used in the above mentioned LSFs. The pseudo code given in Table 6.2 can be used to find the point estimate for the reliability of a pipeline at each point in time. In addition Equation (6.9) is used to find the confidence interval of the estimated reliability at each time given the confidence level

[124].

$$\text{Lower, Upper bound of } \hat{R}(t) = \hat{R}(t) \pm z(\alpha/2) \sqrt{\text{Var}(R(t))/\text{sample size}} \quad (6.9)$$

where z stands for the standard normal distribution, α is the 1- confidence level, $\hat{R}(t)$ represents the point estimate of the pipeline reliability at time t , n_f is the number of failure in the Monte Carlo simulation and n_{it} is the number of iterations.

```

 $R_{sys} = 1$ 
For  $t = 1:T$  (number of time steps):
  For  $s = 1:S$  (number of segments):
    For  $n = 1:N$  (number of iteration at each time step):
       $n_{sm} = \text{number of small leaks} = 0$ 
       $n_l = \text{number of large leaks} = 0$ 
       $n_r = \text{number of ruptures} = 0$ 
       $n_s = \text{number of safe operations} = 0$ 
      For  $i = 1: n_{it}$  (number of degradation iterations at each time step iteration):
        Sample a random number from the distributions of  $D, PWT, \sigma_u, P_{op}, l, \zeta$  (Table 6.3).
        Sample a random number from the estimated maximum pit depth distribution (use the
        defect-based (Ch.4), and population-based (Ch.5) model).
        Calculate  $f_1, f_2$ , and  $f_3$  according to Eqs. 6.3, 6.4, 6.6.
        If  $f_1 \leq 0, f_2 > 0$  then  $n_{sm} = n_{sm} + 1$ 
        Else If  $f_1 > 0, f_2 \leq 0, f_3 > 0$  then  $n_l = n_l + 1$ 
        Else If  $f_1 > 0, f_2 \leq 0, f_3 \leq 0$  then  $n_r = n_r + 1$ 
        Else  $n_s = n_s + 1$ 
      End
       $Pr(n, Smallleak) = n_{sm}/n_{it}$ 
       $Pr(n, Largeleak) = n_l/n_{it}$ 
       $Pr(n, Rupture) = n_r/n_{it}$ 
       $Pr(n, Safe) = n_s/n_{it}$ 
    End
     $\hat{R}_{s,t} = \sum_{n=1}^N Pr(n, Safe)/N$ 
    Lower  $\hat{R}_{s,t} = \hat{R}_{s,t} - z(\alpha/2)\sqrt{Var(R_{s,t})/N}$ 
    Upper  $\hat{R}_{s,t} = \hat{R}_{s,t} + z(\alpha/2)\sqrt{Var(R_{s,t})/N}$ 
  End
   $R_{t,sys} = R_{t,sys} \times \hat{R}_{s,t}$  (Eq. 6.1).
End

```

Table 6.2: Pseudo code to calculate the reliability of a pipeline

6.3 RUL estimation

Another useful reliability metric that can be extracted from calculated maximum pit depth distribution is the RUL of a pipeline segment. The RUL of each segment is estimated based on the allocated reliability of each segment, expressed as a tolerable probability of failure, T_{pf} . The reliability allocation is based on the risk analysis of the pipeline. (e.g., when the pipeline segment is in a high risk area

and the consequence of a failure is severe, the allocated reliability would be higher than the case when the pipeline is located in a low risk area where a lower level of reliability is acceptable). For example if (T_{pf} of small leak is 50% (i.e., the allocated reliability is 50%), the RUL will be $t_{50} - t_c$. Where t_c is the current time and t_{50} is the model-projected time when the probability of occurrence of small leak is 50%. And if the allocated reliability is 90% then the RUL is equal to $t_{10} - t_c$, where t_{10} is the model-projected time when the probability of small leak is 10%. This example is illustrated schematically in Figure 6.1. In this figure, the green line indicates the mean value of the estimated maximum depth of an individual pit in the defect-based model and the mean value of the maximum depth of the pits' population in the population-based model. The brown lines are the realizations of the estimated maximum pit depth for an individual pit or the pit population for the defect or population-based model respectively.

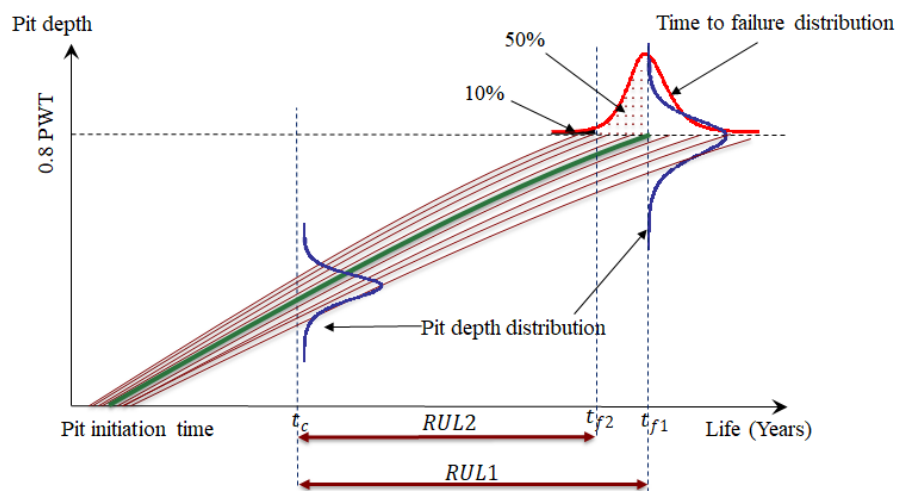


Figure 6.1: RUL estimation for small leak failure mode

6.4 Case study

In order to demonstrate the above-mentioned reliability analysis, it is applied on a case study in this section. Consider a piggable pipeline that is in service since 1970. This pipeline has been inspected at 2000, 2005, 2010 by ILI companies and the ILI data are available. These datasets include the number of reported pits (both true and false calls) and the noisy measurement of maximum depth of those pits. For simplicity we assume that this pipeline just has two segments, S1 and S2. The pit density of Segment S1 is low¹, hence the developed defect-based approach (Ch. 4) can be used to estimate the degradation level of this segment. The pit density of Segment S2 is high and therefore the developed population-based approach can be used to estimate the distribution of the maximum depth of the pit population (Ch. 5). The goal is to calculate the reliability of this pipeline at 2020, given the variation in its material properties and geometry and also the operating pressure (Table 6.3). In this case study, it is assumed that the distribution of the pit length does not change between each two ILIs, and it is equal to the probability distribution that is reported by the most recent ILI [68]. The reason behind this assumption is that changes in pit length have little or no influence on the estimation of the probability of failure associated with the individual pits [66, 122]. Since the developed population-based model does not cover the case of change in operational condition, in this case study, it is assumed that the operational condition does not change over time.

¹We assumed there is just one pit; the same procedure can be used for more than one pit

Variable	Mean	Standard deviation	Unit
Diameter (D)	508	0.3	mm
PWT	8.41	0.13	mm
Ultimate strength (σ_u)	455	14	MPa
Operating pressure (P_{op})	6.66	0.13	MPa
Pit length (l)	18	4.52	mm
ζ	1	0.26	mm

Table 6.3: Probabilistic characteristics of the random variables

By following the pseudo code (using 10000 iterations by Monte Carlo simulation) given in Table 6.2, and using the developed defect-based model, the probability of occurrence of small leak, large leak, and rupture are calculated for Segment S1 at each point in time. To do so, at each point in time, the distribution of the maximum depth of the pit on Segment S1 is obtained by using APF (Ch. 4). Since, the state of each particle in APF resembles a realization of the distribution of the maximum depth of that pit, that state is used as a sample to be used in the Monte Carlo simulation given in the pseudo code. In addition by sampling from the distributions given in Table 6.3, they are used to estimate the distributions of P_b and P_{rp} at each time. Accordingly f_1 , f_2 , and f_3 are estimated for each iteration and the health state for that iteration is obtained based on Table 6.1. Figure 6.2 shows the temporal change in probability of occurrence of each health state (6.1) for Segment S1.

According to this figure, Segment S1 will not face rupture based on the given pipeline properties and operating pressure. However, operating pressure can cause large leak in this segment because of the pipeline degradation, even when the maximum pit depth is much less than the small leak threshold (e.g., at $t=2020$ when the probability of small leak is zero). Figure 6.3 shows the application of stress-strength

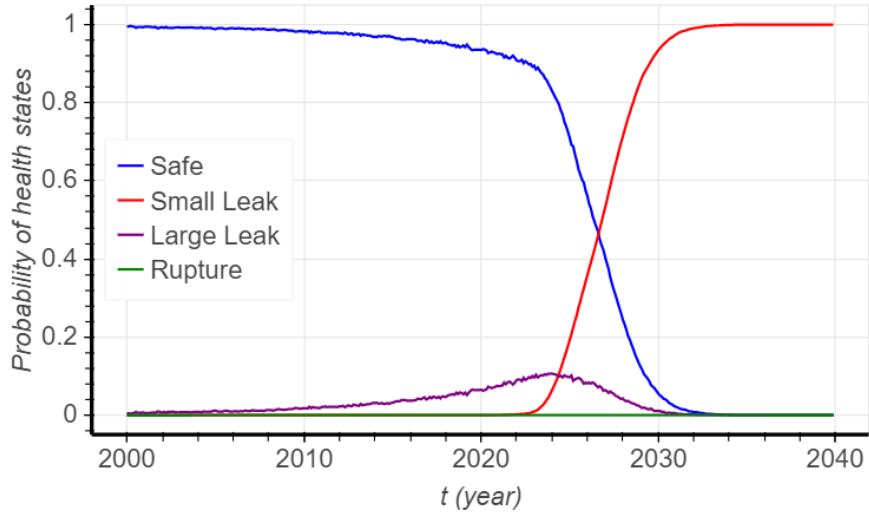


Figure 6.2: Probability of occurrence of each health state for Segment S1

interference theory in calculation of probability of failure at 2020. Since the distribution of operating pressure has overlap with the burst pressure distribution, while it does not have overlap with the rupture pressure distribution, this segment faces large leak at 2020 and it does not face rupture.

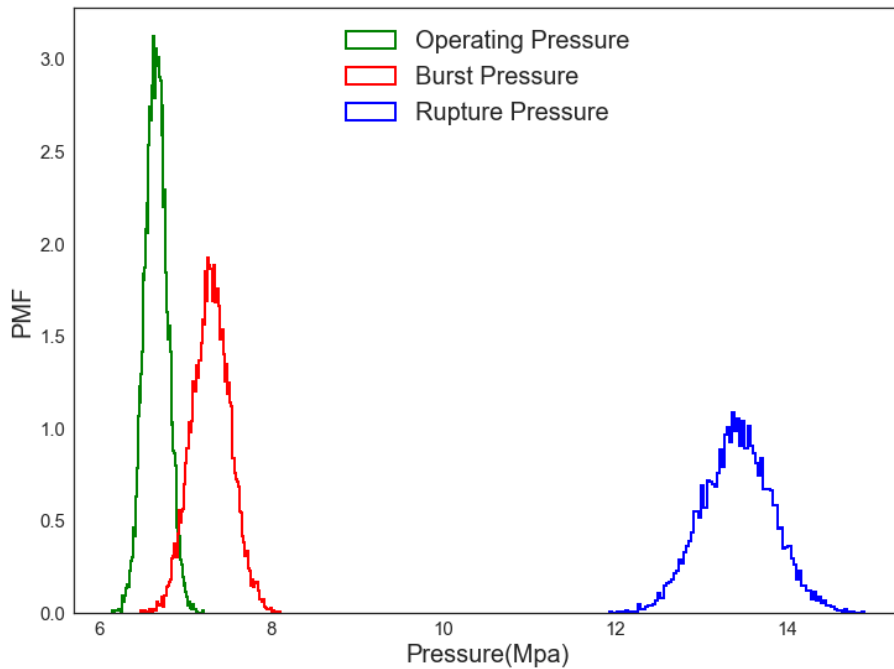


Figure 6.3: PMF of operating, burst, and rupture pressure for Segment S1, 50 years after operation

	Safe Operation	Small Leak	Large Leak	Rupture
S1	0.935	0.000	0.065	0.000
S2	0.803	0.190	0.007	0.000

Table 6.4: Probability of occurrence of different health states for Segment S1 and S2, 50 years after operation

For segment S2, we used Monte Carlo simulation to sample from the estimated PMF of maximum depth of the pit population to be used in the pseudo code that is given in Table 6.2. By following the same procedure that was explained for Segment S1, the obtained probability density functions for operating, burst, and rupture pressure, for segment S2 at 2020 is given in Figure 6.4. By using the criteria defined in Table 6.1, probability of small leak is 0.19, large leak is 0.007, and the reliability is equal to 0.803 fifty years after operation assuming no maintenance activity has been done on this period of time 6.4.

It is worth noting that for Segment S1, for which online inspection is available, the time dependent function of probability of occurrence of each health state is available and plotted in Figure 6.2. However, for Segment S2, since just ILI datasets are available, those probabilities can be calculated just at the ILI times and the prediction time as given in Table 6.4

The final step is to calculate the reliability of the whole pipeline (in this case two segments). By using Eq. 6.1 the reliability of this pipeline with two segment at 2020 is equal to $0.935 \times 0.803 = 0.751$.

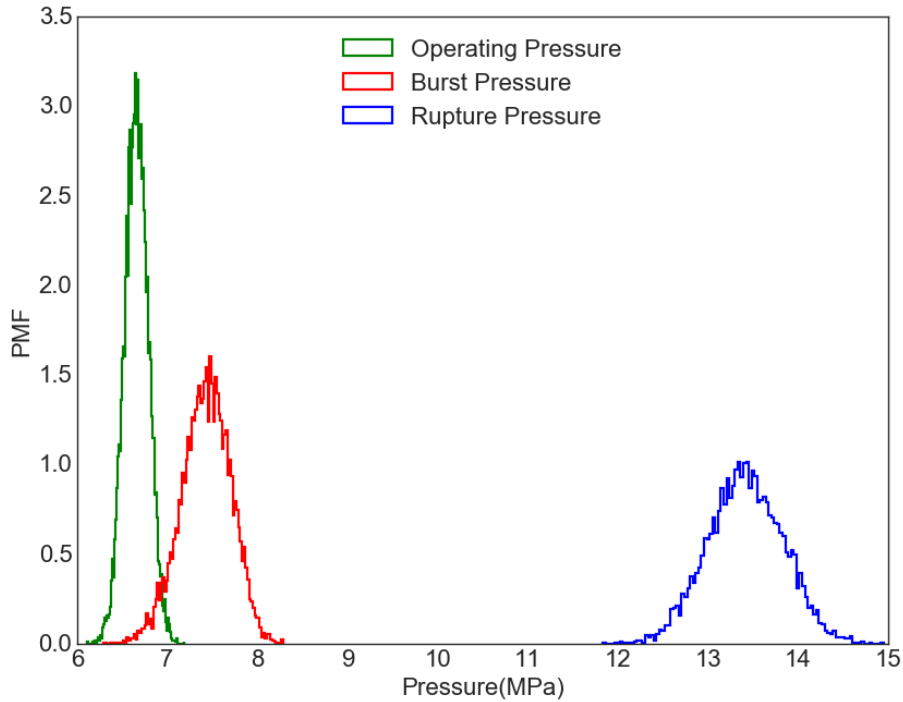


Figure 6.4: PMF of operating, burst, and rupture pressure for Segment S2, 50 years after operation

6.5 Summary

In this section the reliability of a piggable pipeline is modeled as a series system, since failure at any location of the pipeline results in the failure of the whole pipeline. We considered this practical case, and it enables modeling the system as a series of segments, some with low pit density and some with high pit density. For those segments with low pit density, the developed hybrid defect-based PHM model has been used to estimate the degradation level of that segment. For those segments with high pit density, the developed population-based PHM model has been used for this purpose. We defined four pipeline health states (small leak, large leak, rupture, safe). In order to find the probability of occurrence of the health

states, three limit state functions are defined. Based on those limit state functions, small leak happens when the maximum pit depth exceed 80% of PWT. Large leak and rupture happen because of the plastic collapse of the pipeline material, which occurs when the burst pressure of that segment decreases because of degradation due to internal pitting corrosion and become less than the operating pressure. If that plastic collapse causes stable crack propagation, then the burst is considered as a large leak and the consequences is less severe than the consequences of an unstable crack propagation which is considered as a rupture.

In order to demonstrate the application of this methodology, a simple case study was presented in this chapter. In this case study, given the distributions of pipeline material properties, pipeline geometry, and operating pressure, the burst and rupture pressure of a segment with a low pit density and a segment with a high pit density are calculated. The degradation level of the first pipeline segment was calculated by using the developed defect-based model and for the second segment, the developed population-based model was used. Finally the reliability of each of those segments was calculated and were used to calculate the reliability of the whole pipeline as a series system. According to the results of this case study, for both segments with a low and high pit density, even before having small leak, large leak can happen because of the plastic collapse in the pipeline due to operating pressure and degradation of the pipeline.

The predicted probability of occurrence of different failure modes can be used in pipelines optimal maintenance optimization to find the optimal maintenance activity and time for each segment and the optimal next ILI time for the whole pipeline.

Chapter 7: Summary, contributions, and suggested future work

7.1 Summary

This dissertation presents a new framework and algorithms for PHM of pig-gable oil and gas pipelines degraded due to internal pitting corrosion. The algorithms estimate pit depth and pit density in a pipeline segment based on multiple types of data, and predict RUL of that segment (i.e., the useful life left on a pipeline segment at a particular time of operation given the probability distribution of maximum pit depth on that segment). This framework covers both potential cases of low and high density of pit population in different segments of the pipeline. A defect-based algorithm has been developed for those segments with sparse pits and a population-based algorithm for those with a high density of pits population. Both algorithms are hybrid PHM models that consider both POF knowledge of internal pitting corrosion process (IPC) together with inspection data. In addition, in the algorithms, four types of uncertainty have been addressed including epistemic, spatial, temporal and measurement uncertainty.

In the case of sparse pits, temporal change in the operational conditions has been addressed in IPC degradation modeling for the first time. In this dissertation, a novel similarity-based IPC degradation model has been developed. It can be used

to infer the maximum pit depth of those pits that have not been inspected after the change in operational condition, given the uncertain online measurement data of an active reference pit that has been monitored continuously.

In the case of a high density population of pits, a novel population-based algorithm has been developed to estimate the distribution of maximum depth of the population. This algorithm eliminates the need of matching procedure that is computationally expensive and prone to error in the case of having a high pit density. This algorithm has covered several aspects of measurement uncertainty including uncertainty in maximum pit depth measurement and uncertainty in the number of detected pits (i.e., POD and POFC). In addition, it has taken into account the non-linearity of the pitting corrosion process, and the initiation of new pits between the last ILI and the prediction time.

The application of both defect-based and population-based algorithms have been demonstrated by applying them on two case studies and their performance has been compared with simulated data. Those case studies and simulated data are based on a comprehensive generic pitting corrosion degradation model that is available in the literature, which has been developed by using field data. It has been shown that in both cases the developed algorithms decrease the uncertainty in estimated pipeline's degradation level due to IPC.

The resulting models can be used to support condition-based maintenance activities for oil and gas pipelines. And since in the condition-based maintenance optimization of oil and gas pipelines, estimated degradation level is a main input for condition-based maintenance, and also the most challenging one to obtain, the

results of this study will decrease the probability of having unpredicted failures, enhance reliability, and eliminate unnecessary costly maintenance activities.

7.2 Technical contributions

In Chapter 3, an extensive review on the different stochastic processes applicable to corrosion modeling was carried out. Six characteristics were defined to drive selection of the most appropriate stochastic process to fuse IPC POF knowledge and inspection data. Those characteristics include addressing four types of uncertainty (i.e., epistemic, temporal, spatial, and measurement) and addressing the time and depth dependency of IPC. Results from Chapter 3 suggest the family of gamma process models as the most appropriate one to model IPC process in oil and gas pipelines.

In Chapter 4, a novel hybrid (POF and inspection data) defect-based PHM model has been developed. The model can be used to estimate maximum depth of a number of pits when the pit density is low. The model matches the sequential ILI data with respect to the location of the pits, which is feasible for low pit density segments. This research expanded beyond the assumption of constant operational conditions, creating the first model to include conditions which change over time. The change in operational conditions is reflected in the online inspection data of a reference active pit.

The defect-based corrosion PHM model also has linked this change to the growing behavior of the other pits (for which there are no new ILI data available

after change in operational conditions) by developing a similarity-based degradation model. In the available similarity-based RUL estimation models in the PHM literature, the inspection frequency of the test components and the reference component are the same. In contrast, in this research, the similarity-based pitting corrosion degradation model has been developed for the data where the inspection frequency of the test components (i.e., in-line inspected pits) and the reference components (i.e., an online inspected pits) are different. This was implemented in Chapter 4 in a hierarchical dynamic Bayesian model which fuses ILI data of the sparse pits and POF knowledge of IPC. An augmented particle filtering has been used to fuse the online inspection data of the active reference pit and POF knowledge of IPC.

The POF aspect of the hybrid defect-based model is enhanced by incorporating the variation of the operational parameters in IPC degradation modeling. In the available defect-based models in the literature, the POF of IPC process has been considered by assuming a power law model, with a positive exponent less than one, as the general form of the degradation model. In the new model, in addition to using the known power law form, it incorporates the operational parameters (e.g., pressure, temperature, pH, Sulphate ion, Chloride ion) in the development of the hybrid model. Monte Carlo simulation and non-linear regression analysis are used to estimate the standard deviation of the white noise of the process model in augmented particle filtering, based on the variation in operational parameters.

In Chapter 5, a novel hybrid population-based degradation model has been developed. This model estimates the distribution of the maximum depth of a population of pits when mass ILI data are available for that population. In this case,

using a pit matching procedure is expensive and prone to error. In the new model, the need for matching the sequential ILI data to specific pit locations has been eliminated. In comparison to the state of the art population-based model that is available in the literature, this model is able to take into account the non-linearity of the growing behavior of the maximum pit depth by using non-homogeneous gamma process as the underlying stochastic process. Variation in pits' initiation times has been also considered by using a homogeneous Poisson process. Based on this HPP assumption, this model is able to consider initiation of the new pits between the last ILI and the prediction time. Moreover, this model is applicable for two or more sets of ILI data which is the common practice in the industry and has not been addressed in the literature. In this way, a new clustering algorithm has been developed to cluster the detected pits at each ILI based on their initiation time. Moreover, this population-based model, has taken into account the probability of not detecting some of the existing pits and also the POFC of some measurements.

In Chapter 6, these two (defect-based and population-based) hybrid models, are combined in a series system to create an approach to calculate the reliability of a pipeline with multiple segments with both low and high density pit regions. The probability of occurrence of different failure modes (small leak, large leak, rupture) can be calculated with a high confidence level by using the developed hybrid defect-based and population-based pitting corrosion degradation models together.

The application of the developed degradation model is not limited to pipeline pitting corrosion process and it can be used to model degradation due to a wide range of failures mechanism where the general form of the degradation behavior is

known and the inspection data are available to update the hyper-parameters of that degradation model.

7.3 Work Products

Journal papers

- Roohollah Heidary, Steven A. Gabriel, Mohammad Modarres, et al. “A Review of Data-Driven Oil and Gas Pipeline Pitting Corrosion Growth Models Applicable for Prognostic and Health Management”. In: *International Journal of Prognostics and Health Management* 9.1 (2018)
- Roohollah Heidary and Katrina M. Groth. “A hybrid model of internal pitting corrosion degradation under changing operational conditions for pipeline integrity management”. In: *Structural Health Monitoring* (2019). DOI: 10.1177/1475921719877656

Conference papers

- Roohollah Heidary, Katrina M. Groth, and Mohammad Modarres. “Fusing More Frequent and Accurate Structural Damage Information from One Location to Assess Damage at another Location with Less Information”. In: *Proceedings of the 14th Probabilistic Safety Assessment and Management Conference (PSAM 14)* (Sept. 16, 2018–Sept. 21, 2019). Los Angeles, CA, 2018
- Roohollah Heidary, Katrina M. Groth, Mohammad Modarres, et al. “Finding optimal maintenance policy for pipeline corrosion using data fusion”. In: *RDPETRO 2018: Research and Development Petroleum Conference and Ex-*

hibition (May 9–10, 2018). Abu Dhabi, UAE, 2018, pp. 232–233. DOI: 10.1190/RDP2018-50000066.1

Source code

- <https://github.com/SyRRA/Hybrid-PHM-Algorithms-Corrosion>

7.4 Limitations

As mentioned in Section 1.3, this research is founded on some assumptions. Since pitting corrosion is a highly stochastic process, making some assumptions is inevitable to enable degradation modeling due to process complexity. However, those assumptions limit the use of the developed models beyond the scope of the data types for which the models were developed.

For the defect-based PHM model, the application is limited to this assumption that the reference pit is in the stable phase (i.e., it is always growing). In reality, a pit can stop growing at various times. To address this limitation, using multiple OLI pits is recommended in the future work.

For both the defect-based and population-based model, it has been assumed that the pits are not interacting with each other. In reality, when two pits are close to each other, they can coalesce and make a bigger pit which grows faster. Studying the coalesce of pits is another area that is under investigation in the literature.

Another assumption was that the maximum pit depth growing behavior follows a power law function with a less than one positive exponent. Although this is a well-accepted assumption in the literature, more physics and material science studies are

required to have a better understanding of the physics behind the pitting corrosion process.

7.5 Future work

This study can be extended in the following directions:

- The developed defect-based model could be extended by several research directions. One option is considering data from more than one online inspected pits and developing an algorithm to, e.g., investigate the most similar one for each ILI pit or creating an average of similarity index between each ILI pit and multiple online inspected pits. Another aspect that can be improved in this model is to consider the variation in pits' initiation times in degradation modeling.
- The developed population-based model can be extended through future research. Exploring the use of the non-homogeneous Poisson process for the number of initiated pits at each time interval would enable the model to address cases where the initiation times of different pits are not uniformly distributed. In addition, considering change in operational condition in this model would extend the range of application of this model as well. Optimizing the number of bins in discretizing the probability mass functions is another potential research area since the developed algorithm is sensitive to this number. Moreover, considering different ILI tools with different characteristics makes this model more practical.

- There are several research paths which could enhance both the defect-based and population-based models. Using raw MFL or UT signals (instead of measured depth that are reported by ILI companies) as the input of these models and using machine learning techniques to estimate the maximum pit depth could decrease the uncertainty in IPC degradation modeling.
- Although the performance of these models has been checked by using some simulated data, it is also necessary to validate them by using field ILI and online inspection data.
- During this research, one of the main challenges was to find real field inspection data and operation parameters measurements. The lack of field data is a big challenge in PHM of the oil and gas pipelines. Therefore, it is highly recommended to make an international repository and collaborate with oil and gas pipelines' owners, pipeline operating companies, and research institutes to collect the operational conditions and inspection data and make them available in the public domain to make it possible for the researchers to validate their new pitting corrosion degradation models.

Bibliography

- [1] Hossam A. Kishawy and Hossam A. Gabbar. “Review of pipeline integrity management practices”. In: *International Journal of Pressure Vessels and Piping* 87.7 (2010), pp. 373–380.
- [2] J. C. Velazquez, F. Caleyó, A. Valor, and J. M. Hallen. “Predictive model for pitting corrosion in buried oil and gas pipelines”. In: *Corrosion* 65.5 (2009), pp. 332–342.
- [3] J. M. Van Noordwijk. “A survey of the application of gamma processes in maintenance”. In: *Reliability Engineering & System Safety* 94.1 (2009), pp. 2–21.
- [4] Sankara Papavinasam. *Corrosion control in the oil and gas industry*. Elsevier, 2013.
- [5] Kwok L. Tsui, Nan Chen, Qiang Zhou, Yizhen Hai, and Wenbin Wang. “Prognostics and health management: A review on data driven approaches”. In: *Mathematical Problems in Engineering* 2015 (2015).
- [6] Vepa Atamuradov, Kamal Medjaher, Pierre Dersin, Benjamin Lamoureux, and Noureddine Zerhouni. “Prognostics and health management for maintenance practitioners-Review, implementation and tools evaluation”. In: *International Journal of Prognostics and Health Management* 8.060 (2017), pp. 1–31.
- [7] Anahita Imanian and Mohammad Modarres. “A thermodynamic entropy-based damage assessment with applications to prognostics and health management”. In: *Structural Health Monitoring* 17.2 (2018), pp. 240–254.
- [8] Dawn An, Nam H. Kim, and Joo-Ho Choi. “Practical options for selecting data-driven or physics-based prognostics algorithms with reviews”. In: *Reliability Engineering & System Safety* 133 (2015), pp. 223–236.
- [9] Srdjan Nešić. “Key issues related to modelling of internal corrosion of oil and gas pipelines-A review”. In: *Corrosion Science* 49.12 (2007), pp. 4308–4338.
- [10] Frédéric Vitse, S. Nešić, Yves Gunaltun, D. Larrey de Torreben, and Pierre Duchet-Suchaux. “Mechanistic model for the prediction of top-of-the-line corrosion risk”. In: *Corrosion* 59.12 (2003), pp. 1075–1084.
- [11] David V. Svintradze and Ramana M. Pidaparti. “A theoretical model for metal corrosion degradation”. In: *International Journal of Corrosion* 2010 (2010).

- [12] Rolf Nyborg. “Co2 corrosion models for oil and gas production systems”. In: *Corrosion 2010* (2010).
- [13] Shenwei Zhang and Wenxing Zhou. “System reliability of corroding pipelines considering stochastic process-based models for defect growth and internal pressure”. In: *International Journal of Pressure Vessels and Piping* 111 (2013), pp. 120–130.
- [14] Chinedu I. Ossai, Brian Boswell, and Ian J. Davies. “Modelling the effects of production rates and physico-chemical parameters on pitting rate and pit depth growth of onshore oil and gas pipelines”. In: *Corrosion Engineering, Science and Technology* 51.5 (2016), pp. 342–351.
- [15] Roohollah Heidary, Steven A. Gabriel, Mohammad Modarres, Katrina M. Groth, and Nader Vahdati. “A Review of Data-Driven Oil and Gas Pipeline Pitting Corrosion Growth Models Applicable for Prognostic and Health Management”. In: *International Journal of Prognostics and Health Management* 9.1 (2018).
- [16] Marc A. Maes, Michael H. Faber, and Markus R. Dann. “Hierarchical modeling of pipeline defect growth subject to ILI uncertainty”. In: *ASME 2009 28th International Conference on Ocean, Offshore and Arctic Engineering*. American Society of Mechanical Engineers. 2009, pp. 375–384.
- [17] Chinedu I. Ossai, Brian Boswell, and Ian J. Davies. “Predictive modelling of internal pitting corrosion of aged non-piggable pipelines”. In: *Journal of The Electrochemical Society* 162.6 (2015), pp. C251–C259.
- [18] Markus R. Dann and Marc A. Maes. “Stochastic corrosion growth modeling for pipelines using mass inspection data”. In: *Reliability Engineering & System Safety* 180 (2018), pp. 245–254.
- [19] H. Duckworth and R. Eiber. “Assessment of Pipeline Integrity of Kinder-Morgan Conversion of the Rancho Pipeline”. In: *City of Austin, Austin, TX* (2004).
- [20] Rolf Nyborg. “Controlling internal corrosion in oil and gas pipelines”. In: *Business Briefing: Exploration & Production: The Oil & Gas Review* 2 (2005), pp. 70–74.
- [21] Paul E. Dodds and Stephanie Demoullin. “Conversion of the UK gas system to transport hydrogen”. In: *International Journal of Hydrogen Energy* 38.18 (2013), pp. 7189–7200.
- [22] Martin Klann and Thomas Beuker. “Pipeline inspection with the high resolution EMAT ILI-tool: Report on field experience”. In: *Proceedings of IPC 2006*. 2006.
- [23] Yaman Hamed, A’fza Shafie, Zahiraniza Mustaffa, and Naila Rusma. “Error-reduction approach for corrosion measurements of pipeline inline inspection tools”. In: *Measurement and Control* 52.1-2 (2019), pp. 28–36.

- [24] Markus R. Dann and Christoph Dann. “Automated matching of pipeline corrosion features from in-line inspection data”. In: *Reliability Engineering & System Safety* 162 (2017), pp. 40–50.
- [25] Alma Valor, Francisco Caleyó, Lester Alfonso, Julio Vidal, and José M Hallen. “Statistical analysis of pitting corrosion field data and their use for realistic reliability estimations in non-piggable pipeline systems”. In: *Corrosion* 70.11 (2014), pp. 1090–1100.
- [26] John F. Kiefner and Patrick H. Vieth. “Evaluating pipe-1. new method corrects criterion for evaluating corroded pipe”. In: *Oil and Gas Journal* 88.32 (1990).
- [27] Gery Wilkowski, Denny Stephens, Prabhat Krishnaswamy, Brian Leis, and David Rudland. “Progress in development of acceptance criteria for local thinned areas in pipe and piping components”. In: *Nuclear Engineering and Design* 195.2 (2000), pp. 149–169.
- [28] Guian Qian, Markus Niffenegger, and Shuxin Li. “Probabilistic analysis of pipelines with corrosion defects by using FITNET FFS procedure”. In: *Corrosion Science* 53.3 (2011), pp. 855–861.
- [29] Madesh D. Pandey. “Probabilistic models for condition assessment of oil and gas pipelines”. In: *NDT & E International* 31.5 (1998), pp. 349–358.
- [30] Felipe Alexander Vargas Bazán and André Teófilo Beck. “Stochastic process corrosion growth models for pipeline reliability”. In: *Corrosion Science* 74 (2013), pp. 50–58.
- [31] Pe Paris and Fazil Erdogan. “A critical analysis of crack propagation laws”. In: *Journal of Basic Engineering* 85.4 (1963), pp. 528–533.
- [32] Yongzhi Zhang, Rui Xiong, Hongwen He, and Michael G. Pecht. “Long short-term memory recurrent neural network for remaining useful life prediction of lithium-ion batteries”. In: *IEEE Transactions on Vehicular Technology* 67.7 (2018), pp. 5695–5705.
- [33] Linxia Liao and Felix Köttig. “Review of hybrid prognostics approaches for remaining useful life prediction of engineered systems, and an application to battery life prediction”. In: *IEEE Transactions on Reliability* 63.1 (2014), pp. 191–207.
- [34] Ratna Babu Chinnam and Pundarikaksha Baruah. “A neuro-fuzzy approach for estimating mean residual life in condition-based maintenance systems”. In: *International Journal of Materials and Product Technology* 20.1-3 (2004), pp. 166–179.
- [35] David C. Swanson. “A general prognostic tracking algorithm for predictive maintenance”. In: *2001 IEEE Aerospace Conference Proceedings (Cat. No. 01TH8542)*. Vol. 6. IEEE. 2001, pp. 2971–2977.

- [36] Jihong Yan and Jay Lee. “A hybrid method for on-line performance assessment and life prediction in drilling operations”. In: *2007 IEEE International Conference on Automation and Logistics*. IEEE. 2007, pp. 2500–2505.
- [37] Elaheh Rabiei, Enrique Lopez Droguett, and Mohammad Modarres. “A prognostics approach based on the evolution of damage precursors using dynamic Bayesian networks”. In: *Advances in Mechanical Engineering* 8.9 (2016).
- [38] Giulio Gola and Bent Helge Nystad. “From measurement collection to remaining useful life estimation: Defining a diagnostic-prognostic frame for optimal maintenance scheduling of choke valves undergoing erosion”. In: *Annual Conference of the Prognostics and Health Management Society*. 2011, pp. 26–29.
- [39] Wilfried Elmenreich. “An introduction to sensor fusion”. In: *Vienna University of Technology, Austria* 502 (2002).
- [40] David L. Hall and James Llinas. “An introduction to multisensor data fusion”. In: *Proceedings of the IEEE* 85.1 (1997), pp. 6–23.
- [41] Bahador Khaleghi, Alaa Khamis, Fakhreddine O. Karray, and Saiedeh N. Razavi. “Multisensor data fusion: A review of the state-of-the-art”. In: *Information Fusion* 14.1 (2013), pp. 28–44.
- [42] Hugh F. Durrant-Whyte. “Sensor models and multisensor integration”. In: *Autonomous Robot Vehicles*. Springer, 1990, pp. 73–89.
- [43] Belur V. Dasarthy. “Sensor fusion potential exploitation-innovative architectures and illustrative applications”. In: *Proceedings of the IEEE* 85.1 (1997), pp. 24–38.
- [44] Franklin E. White. *Data fusion lexicon*. Tech. rep. Joint Directors of Labs Washington DC, 1991.
- [45] Federico Castanedo. “A review of data fusion techniques”. In: *The Scientific World Journal* 2013 (2013).
- [46] Rachel C. King, Emma Villeneuve, Ruth J. White, R. Simon Sherratt, William Holderbaum, and William S. Harwin. “Application of data fusion techniques and technologies for wearable health monitoring”. In: *Medical Engineering & Physics* 42 (2017), pp. 1–12.
- [47] Lawrence A. Klein. *Sensor and data fusion: A tool for information assessment and decision making*. Vol. 324. SPIE Press Bellingham, WA, 2004.
- [48] M. I. Mazhar, S. Kara, and H. Kaebernick. “Remaining life estimation of used components in consumer products: Life cycle data analysis by Weibull and artificial neural networks”. In: *Journal of Operations Management* 25.6 (2007), pp. 1184–1193.
- [49] Gérard Dreyfus. *Neural networks: Methodology and applications*. Springer Science & Business Media, 2005.

- [50] Shuai Zheng, Kosta Ristovski, Ahmed Farahat, and Chetan Gupta. “Long short-term memory network for remaining useful life estimation”. In: *2017 IEEE International Conference on Prognostics and Health Management (ICPHM)*. IEEE. 2017, pp. 88–95.
- [51] Yaguo Lei, Naipeng Li, Liang Guo, Ningbo Li, Tao Yan, and Jing Lin. “Machinery health prognostics: A systematic review from data acquisition to RUL prediction”. In: *Mechanical Systems and Signal Processing* 104 (2018), pp. 799–834.
- [52] Sunil K. Sinha and Mahesh D. Pandey. “Probabilistic neural network for reliability assessment of oil and gas pipelines”. In: *Computer-Aided Civil and Infrastructure Engineering* 17.5 (2002), pp. 320–329.
- [53] A. A. Carvalho, J. M. A. Rebello, L. V. S. Sagrilo, C. S. Camerini, and I. V. J. Miranda. “MFL signals and artificial neural networks applied to detection and classification of pipe weld defects”. In: *NDT&E International* 39.8 (2006), pp. 661–667.
- [54] Piero Baraldi, Michele Compare, Sergio Saucó, and Enrico Zio. “Ensemble neural network-based particle filtering for prognostics”. In: *Mechanical Systems and Signal Processing* 41.1-2 (2013), pp. 288–300.
- [55] Jui-Sheng Chou, Ngoc-Tri Ngo, and Wai K Chong. “The use of artificial intelligence combiners for modeling steel pitting risk and corrosion rate”. In: *Engineering Applications of Artificial Intelligence* 65 (2017), pp. 471–483.
- [56] Khanh Le Son, Mitra Fouladirad, Anne Barros, Eric Levrat, and Benoît Iung. “Remaining useful life estimation based on stochastic deterioration models: A comparative study”. In: *Reliability Engineering & System Safety* 112 (2013), pp. 165–175.
- [57] Tianyi Wang, Jianbo Yu, David Siegel, and Jay Lee. “A similarity-based prognostics approach for remaining useful life estimation of engineered systems”. In: *International Conference on Prognostics and Health Management, 2008. PHM 2008*. IEEE. 2008, pp. 1–6.
- [58] Ömer Faruk Eker, Faith Camci, and Ian K. Jennions. “A similarity-based prognostics approach for remaining useful life prediction”. In: *Second European Conference of the Prognostics and Health Management Society 2014*. PHM Society, 2014.
- [59] Enrico Zio and Francesco Di Maio. “A data-driven fuzzy approach for predicting the remaining useful life in dynamic failure scenarios of a nuclear system”. In: *Reliability Engineering & System Safety* 95.1 (2010), pp. 49–57.
- [60] Sankara Papavinasam, R. Winston Revie, Waldemar I. Friesen, Alex Doiron, and Tharani Panneerselvan. “Review of models to predict internal pitting corrosion of oil and gas pipelines”. In: *Corrosion Reviews* 24.3-4 (2006), pp. 173–230.

- [61] K. R. Tarantseva. “Models and methods of forecasting pitting corrosion”. In: *Protection of Metals and Physical Chemistry of Surfaces* 46.1 (2010), pp. 139–147.
- [62] F. Caleyo, J. C. Velázquez, J. M. Hallen, A. Valor, and A. Esquivel-Amezcuca. “Markov chain model helps predict pitting corrosion depth and rate in underground pipelines”. In: *2010 8th International Pipeline Conference*. American Society of Mechanical Engineers. 2010, pp. 573–581.
- [63] M. Nuhi, T. Abu Seer, A. M. Al Tamimi, M. Modarres, and A. Seibi. “Reliability analysis for degradation effects of pitting corrosion in carbon steel pipes”. In: *Procedia Engineering* 10 (2011), pp. 1930–1935.
- [64] T. Shibata. “1996 WR Whitney Award lecture: Statistical and stochastic approaches to localized corrosion”. In: *Corrosion* 52.11 (1996), pp. 813–830.
- [65] A. Valor, F. Caleyo, L. Alfonso, D. Rivas, and J.M. Hallen. “Stochastic modeling of pitting corrosion: a new model for initiation and growth of multiple corrosion pits”. In: *Corrosion Science* 49.2 (2007), pp. 559–579.
- [66] A. Valor, F. Caleyo, .L Alfonso, J. C. Velázquez, and J. M. Hallen. “Markov chain models for the stochastic modeling of pitting corrosion”. In: *Mathematical Problems in Engineering* 2013 (2013).
- [67] Melvin Romanoff. *Underground corrosion*. US Government Printing Office Washington, DC, 1957.
- [68] Shenwei Zhang, Wenxing Zhou, and Hao Qin. “Inverse Gaussian process-based corrosion growth model for energy pipelines considering the sizing error in inspection data”. In: *Corrosion Science* 73 (2013), pp. 309–320.
- [69] Shenwei Zhang and Wenxing Zhou. “Bayesian dynamic linear model for growth of corrosion defects on energy pipelines”. In: *Reliability Engineering & System Safety* 128 (2014), pp. 24–31.
- [70] Sheldon M. Ross, John J. Kelly, Roger J. Sullivan, William James Perry, Donald Mercer, Ruth M. Davis, Thomas Dell Washburn, Earl V. Sager, Joseph B. Boyce, and Vincent L. Bristow. *Stochastic processes*. Vol. 2. Wiley New York, 1996.
- [71] Rabi N. Bhattacharya and Edward C. Waymire. *Stochastic processes with applications*. Vol. 61. Society for Industrial and Applied Mathematics, 2009.
- [72] J. W. Provan and E. S. Rodriguez III. “Part I: Development of a Markov description of pitting corrosion”. In: *Corrosion* 45.3 (1989), pp. 178–192.
- [73] P. M. Aziz. “Application of the statistical theory of extreme values to the analysis of maximum pit depth data for aluminum”. In: *Corrosion* 12.10 (1956), pp. 35–46.
- [74] Han-Ping Hong. “Application of the stochastic process to pitting corrosion”. In: *Corrosion* 55.1 (1999), pp. 10–16.

- [75] J. L. Bogdanoff and F. Kozin. *Probabilistic models of cumulative damage*. Wiley, New York, 1985.
- [76] F. Caleyo, J. C. Velázquez, A. Valor, and J. M. Hallen. “Markov chain modelling of pitting corrosion in underground pipelines”. In: *Corrosion Science* 51.9 (2009), pp. 2197–2207.
- [77] Harold Ascher and Harry Feingold. *Repairable systems reliability: modeling, inference, misconceptions and their causes*. M. Dekker New York, 1984.
- [78] D. R. Cox and H. D. Miller. “The theory of stochastic processes, Methuen & Co”. In: *Ltd, London, UK* (1965).
- [79] R. E. Melchers. “Pitting corrosion of mild steel in marine immersion environment—Part 2: Variability of maximum pit depth”. In: *Corrosion* 60.10 (2004), pp. 937–944.
- [80] J. E. Strutt, J. R. Nicholls, and B. Barbier. “The prediction of corrosion by statistical analysis of corrosion profiles”. In: *Corrosion Science* 25.5 (1985), pp. 305–315.
- [81] I. T. Castro, Nuria C. Caballé, and C. J. Pérez. “A condition-based maintenance for a system subject to multiple degradation processes and external shocks”. In: *International Journal of Systems Science* 46.9 (2015), pp. 1692–1704.
- [82] Dan M. Frangopol, Maarten-Jan Kallen, and Jan M. van Noortwijk. “Probabilistic models for life-cycle performance of deteriorating structures: Review and future directions”. In: *Progress in Structural Engineering and Materials* 6.4 (2004), pp. 197–212.
- [83] Marc A. Maes, Markus R. Dann, Karl W. Breitung, and Eric Brehm. “Hierarchical modeling of stochastic deterioration”. In: *Proceedings of the 6th International Probabilistic Workshop, C. A. Graubner, H. Schmidt, D. Proske, T. U. Darmstadt, eds.* 2008, pp. 111–124.
- [84] Roohollah Heidary and Katrina M. Groth. “A hybrid model of internal pitting corrosion degradation under changing operational conditions for pipeline integrity management”. In: *Structural Health Monitoring* (2019). DOI: 10.1177/1475921719877656.
- [85] Roohollah Heidary, Katrina M. Groth, and Mohammad Modarres. “Fusing More Frequent and Accurate Structural Damage Information from One Location to Assess Damage at another Location with Less Information”. In: *Proceedings of the 14th Probabilistic Safety Assessment and Management Conference (PSAM 14)* (Sept. 16, 2018–Sept. 21, 2019). Los Angeles, CA, 2018.
- [86] Ramin Moradi and Katrina M. Groth. “Hydrogen storage and delivery: Review of the state of the art technologies and risk and reliability analysis”. In: *International Journal of Hydrogen Energy* (2019).

- [87] Marc W. Melaina, Olga Antonia, and Mike Penev. *Blending hydrogen into natural gas pipeline networks. A review of key issues*. Tech. rep. National Renewable Energy Laboratory, 2013.
- [88] Keo Yuan Wu and Ali Mosleh. “Effect of Temporal Variability of Operating Parameters in Corrosion Modelling for Natural Gas Pipelines Subjected to Uniform Corrosion”. In: *Journal of Natural Gas Science and Engineering* (2019), p. 102930.
- [89] Pipeline and Hazardous Materials Safety Administration. *Guidance for Pipeline Flow Reversals, Product Changes, and Conversion to Service*. Tech. rep. 2014.
- [90] J. C. Velázquez, J. A. M. Van Der Weide, Enrique Hernández, and Héctor Herrera Hernández. “Statistical modelling of pitting corrosion: extrapolation of the maximum pit depth-growth”. In: *International Journal of Electrochemical Science* 9.8 (2014), pp. 4129–4143.
- [91] Antoine Grall and Mitra Fouladirad. “Maintenance decision rule with embedded online Bayesian change detection for gradually non-stationary deteriorating systems”. In: *Proceedings of the Institution of Mechanical Engineers, Part O: Journal of Risk and Reliability* 222.3 (2008), pp. 359–369.
- [92] M. Sanjeev Arulampalam, Simon Maskell, Neil Gordon, and Tim Clapp. “A tutorial on particle filters for online nonlinear/non-Gaussian Bayesian tracking”. In: *IEEE Transactions on Signal Processing* 50.2 (2002), pp. 174–188.
- [93] Niclas Bergman. “Recursive Bayesian estimation: Navigation and tracking applications”. PhD thesis. Linköping University, 1999.
- [94] Arnaud Doucet, Nando De Freitas, and Neil Gordon. “An introduction to sequential Monte Carlo methods”. In: *Sequential Monte Carlo methods in practice*. Springer, 2001, pp. 3–14.
- [95] Genshiro Kitagawa. “A self-organizing state-space model”. In: *Journal of the American Statistical Association* (1998), pp. 1203–1215.
- [96] Jane Liu and Mike West. “Combined parameter and state estimation in simulation-based filtering”. In: *Sequential Monte Carlo Methods in Practice*. Springer, 2001, pp. 197–223.
- [97] Arnaud Doucet and Vladislav B. Tadić. “Parameter estimation in general state-space models using particle methods”. In: *Annals of the Institute of Statistical Mathematics* 55.2 (2003), pp. 409–422.
- [98] Tao Chen, Julian Morris, and Elaine Martin. “Particle filters for state and parameter estimation in batch processes”. In: *Journal of Process Control* 15.6 (2005), pp. 665–673.
- [99] Dana Kelly and Curtis Smith. *Bayesian inference for probabilistic risk assessment: A practitioner’s guidebook*. Springer Science & Business Media, 2011.
- [100] Mohamed Abdel-Hameed. “A gamma wear process”. In: *IEEE Transactions on Reliability* 24.2 (1975), pp. 152–153.

- [101] Ronald E. Walpole, Raymond H. Myers, Sharon L. Myers, and Keying Ye. *Probability and statistics for engineers and scientists*. Vol. 5. Macmillan New York, 1993.
- [102] Z. Mustafa, P. V. Gelder, A. W. Dawotola, S. Y. Yu, and D. K. Kim. “Reliability assessment for corroded pipelines in series considering length-scale effects”. In: *International Journal of Automotive and Mechanical Engineering* 15.3 (2018), pp. 5607–5624.
- [103] Det Norske Veritas. “Recommended practice DNV-RP-F101 corroded pipelines”. In: *Hovik, Norway* 11 (2004), pp. 135–138.
- [104] W. Zhou, H.P. Hong, and S. Zhang. “Impact of dependent stochastic defect growth on system reliability of corroding pipelines”. In: *International Journal of Pressure Vessels and Piping* 96 (2012), pp. 68–77.
- [105] Wenxing Zhou. “System reliability of corroding pipelines”. In: *International Journal of Pressure Vessels and Piping* 87.10 (2010), pp. 587–595.
- [106] Markus R Dann, Marc A Maes, and Mamdouh M Salama. “Pipeline corrosion growth modeling for in-line inspection data using a population-based approach”. In: *ASME 2015 34th International Conference on Ocean, Offshore and Arctic Engineering*. American Society of Mechanical Engineers Digital Collection. 2015.
- [107] API. “A new Kullback-Leibler VAD for speech recognition in noise”. In: *IEEE signal processing letters* 1163 (2010).
- [108] Dongliang Lu. “Estimation of stochastic degradation models using uncertain inspection data”. In: (2012).
- [109] HR Vanaei, A Eslami, and A Egbewande. “A review on pipeline corrosion, in-line inspection (ILI), and corrosion growth rate models”. In: *International Journal of Pressure Vessels and Piping* 149 (2017), pp. 43–54.
- [110] Y Tsukaue, G Nakao, Y Takimoto, and K Yoshida. “Initiation behavior of pitting in stainless steels by accumulation of triiodide ions in water droplets”. In: *Corrosion* 50.10 (1994), pp. 755–760.
- [111] Kaushik Chatterjee and Mohammad Modarres. “A probabilistic approach for estimating defect size and density considering detection uncertainties and measurement errors”. In: *Proceedings of the Institution of Mechanical Engineers, Part O: Journal of Risk and Reliability* 227.1 (2013), pp. 28–40.
- [112] B Baroux. “The kinetics of pit generation on stainless steels”. In: *Corrosion science* 28.10 (1988), pp. 969–986.
- [113] Shenwei Zhang. “Development of probabilistic corrosion growth models with applications in integrity management of pipelines”. In: (2014).
- [114] Chinedu Ishiodu Ossai. “Predictive modelling and reliability analysis of aged, corroded pipelines”. PhD thesis. Curtin University, 2016.

- [115] F. Hunkeler and H. Bohni. “Mechanism of pit growth on aluminum under open circuit conditions”. In: *Corrosion* 40.10 (1984), pp. 534–540.
- [116] Weilong Zhang and GS Frankel. “Localized corrosion growth kinetics in AA2024 alloys”. In: *Journal of the Electrochemical Society* 149.11 (2002), B510–B519.
- [117] Armen Der Kiureghian and Ove Ditlevsen. “Aleatory or epistemic? Does it matter?” In: *Structural Safety* 31.2 (2009), pp. 105–112.
- [118] Solomon Kullback and Richard A Leibler. “On information and sufficiency”. In: *The annals of mathematical statistics* 22.1 (1951), pp. 79–86.
- [119] Elaheh Rabiei, Enrique Droguett, and Mohammad Modarres. “Fully adaptive particle filtering algorithm for damage diagnosis and prognosis”. In: *Entropy* 20.2 (2018), p. 100.
- [120] Shima Tabibian, Ahmad Akbari, and Babak Nasersharif. “A new wavelet thresholding method for speech enhancement based on symmetric Kullback-Leibler divergence”. In: *2009 14th International CSI Computer Conference*. IEEE. 2009, pp. 495–500.
- [121] Javier Ramírez, Jaime C Segura, Carmen Benítez, Angel De La Torre, and Antonio J Rubio. “A new Kullback-Leibler VAD for speech recognition in noise”. In: *IEEE signal processing letters* 11.2 (2004), pp. 266–269.
- [122] F. Caleyó, J. L. Gonzalez, and J. M. Hallen. “A study on the reliability assessment methodology for pipelines with active corrosion defects”. In: *International Journal of Pressure Vessels and Piping* 79.1 (2002), pp. 77–86.
- [123] Mohamed A. El-Reedy. *Offshore structures: Design, construction and maintenance*. Gulf Professional Publishing, 2012.
- [124] Mohammad Modarres, Mark P Kaminskiy, and Vasilii Krivtsov. *Reliability engineering and risk analysis: a practical guide*. CRC press, 2016.
- [125] Roohollah Heidary, Katrina M. Groth, Mohammad Modarres, and Nader Vahdati. “Finding optimal maintenance policy for pipeline corrosion using data fusion”. In: *RD PETRO 2018: Research and Development Petroleum Conference and Exhibition* (May 9–10, 2018). Abu Dhabi, UAE, 2018, pp. 232–233. DOI: 10.1190/RDP2018-50000066.1.